

University of Alberta

Recent glacier retreat within the southern Canadian Cordillera

^{by}
Christopher Michael DeBeer
Christopher Michael DeBeer



A thesis submitted to the Faculty of Graduate Studies and Research in partial fulfillment
of the requirements for the degree of Master of Science

Department of Earth and Atmospheric Sciences

Edmonton, Alberta

Fall 2006



Library and
Archives Canada

Bibliothèque et
Archives Canada

Published Heritage
Branch

Direction du
Patrimoine de l'édition

395 Wellington Street
Ottawa ON K1A 0N4
Canada

395, rue Wellington
Ottawa ON K1A 0N4
Canada

Your file *Votre référence*
ISBN: 978-0-494-22248-5
Our file *Notre référence*
ISBN: 978-0-494-22248-5

NOTICE:

The author has granted a non-exclusive license allowing Library and Archives Canada to reproduce, publish, archive, preserve, conserve, communicate to the public by telecommunication or on the Internet, loan, distribute and sell theses worldwide, for commercial or non-commercial purposes, in microform, paper, electronic and/or any other formats.

The author retains copyright ownership and moral rights in this thesis. Neither the thesis nor substantial extracts from it may be printed or otherwise reproduced without the author's permission.

AVIS:

L'auteur a accordé une licence non exclusive permettant à la Bibliothèque et Archives Canada de reproduire, publier, archiver, sauvegarder, conserver, transmettre au public par télécommunication ou par l'Internet, prêter, distribuer et vendre des thèses partout dans le monde, à des fins commerciales ou autres, sur support microforme, papier, électronique et/ou autres formats.

L'auteur conserve la propriété du droit d'auteur et des droits moraux qui protègent cette thèse. Ni la thèse ni des extraits substantiels de celle-ci ne doivent être imprimés ou autrement reproduits sans son autorisation.

In compliance with the Canadian Privacy Act some supporting forms may have been removed from this thesis.

Conformément à la loi canadienne sur la protection de la vie privée, quelques formulaires secondaires ont été enlevés de cette thèse.

While these forms may be included in the document page count, their removal does not represent any loss of content from the thesis.

Bien que ces formulaires aient inclus dans la pagination, il n'y aura aucun contenu manquant.


Canada

ABSTRACT

Net changes in glacier area in the region 50–51° N and 116–125° W, which includes the Columbia and Rocky Mountains (1951/52–2001), and the Coast Mountains (1964/65–2002), were determined from a comparison of historic aerial photography and recent Landsat 7 ETM+ imagery. Estimates of ice volume for both time periods were made using an empirical volume-area scaling relationship. There is a high degree of spatial variability in the magnitude of observed changes across the study area. This may be due to gradients in the nature of climate forcing over the study area, and to differences in the intrinsic sensitivity of individual glaciers to climate forcing. Over the ~38 year time period, glaciers within the Coast Mountains experienced a net area change of -120 ± 10 km², corresponding to a loss of 5% from the initial ice covered area of ~2400 km². Glaciers within this region typically lost between -2 and -10% of their initial area and volume, representing wastage of ~0.2–2 km² of ice depending on their size. Over the ~50 year period, glaciers within the Columbia and Rocky Mountains underwent a net change of -20 and -6 km² from initial areas of ~400 and ~40 km² respectively, corresponding to relative changes in total area of -5 and -15%. Individual glaciers within these regions underwent area changes between +25 and -75% in some extreme cases, which suggests that the intrinsic sensitivity of glaciers is important in explaining the pattern of retreat here. These glaciers are generally much smaller than those of the Coast Mountains however, and total ice loss from individual glaciers was on the order of 0.01–0.1 km².

TABLE OF CONTENTS

1. Introduction	1
2. Study Area	5
2.1 Location and Distribution of Ice	5
2.2 Regional Physiography	6
2.3 Regional Climate	8
3. Methods	9
3.1 Sources of Data	9
3.2 Image Preparation and Geometric Correction	10
3.3 Ice Margin Delineation	11
3.4 Area and Volume Calculations	12
3.5 Error Estimation	13
4. Results	16
4.1 Net Changes in Glacier Area and Volume	16
4.2 Local Variability of Glacier Changes	17
4.2.1 Rocky Mountains	18
4.2.2 Columbia Mountains	20
4.2.3 Coast Mountains	25
5. Analysis and Discussion	29
5.1 Recent Climate Trends	29
5.1.1 Recent Temperature Trends	29
5.1.2 Recent Precipitation Trends	34
5.1.3 Glacier – Climate Interactions	41
5.2 Response Time	43
5.3 Glacier Geometry and Response	49
5.3.1 Glacier Shape	49
5.3.2 Area and Elevation	55
5.3.3 Glacier Slope	58
5.3.4 Dynamic Sensitivity	62
5.4 Glacier Hypsometry	65
5.4.1 Geometric Balance Ratios	66
5.4.2 Basin Sensitivity	76
5.5 Sensitivity to Further Climatic Change	79
5.5.1 Coast Mountains	80
5.5.2 Other Regions	83
6. Summary and Conclusions	86
References	90
Appendix A (Field Measurement of Glacier Volume Changes)	93
Appendix B (Summary of Morphologic and Glaciological Parameters)	96

LIST OF TABLES

<i>TABLE 4.1. Summary of area measurements and volume estimates (using values of 28.5 and 1.36 for c_0 and c_1 respectively), and net changes in these variables over the study period for all mountain ranges. Measurements of the initial conditions in the Coast Mountains are relative to the period 1964/65.</i>	17
<i>TABLE 4.2. Summary of net changes in area and volume (using values of 28.5 and 1.36 for c_0 and c_1 respectively) over the period 1951/52–2001 for the largest glaciers in the southern Rocky Mountain region (accounting for ~65% of the total ice loss here).</i>	19
<i>TABLE 4.3. Summary of net changes in area and volume (using values of 28.5 and 1.36 for c_0 and c_1 respectively) over the period 1951/52–2001 for large glaciers, or glaciers which have undergone substantial retreat in the southern Purcell Mountain region.</i>	22
<i>TABLE 4.4. Summary of net changes in area and volume (using values of 28.5 and 1.36 for c_0 and c_1 respectively) over the period 1965/65–2002 of the 10 largest glaciers in the Coast Mountain region (accounting for 48% of the total ice loss here).</i>	27
<i>TABLE 5.1. Annual and seasonal temperature warming rates over the period 1950–2000 at individual stations. Significant trends (i.e., those that are significantly different from zero at the 95% confidence level) are shown in bold.</i>	33
<i>TABLE 5.2. Matrix of loadings for the three extracted components of the standardized annual precipitation series.</i>	37
<i>TABLE 5.3. Matrix of loadings for the two extracted components of the standardized winter precipitation series.</i>	39
<i>TABLE 5.4. Changes in winter precipitation associated with the 1976–77 PDO regime shift. All the changes, with the exception of that at Summerland, are significant at the 95% confidence level.</i>	40
<i>TABLE 5.5. Changes in spring snowpack depth measured at snow survey locations across the region associated with the 1976–77 PDO regime shift. All changes are significant at the 95% confidence level. SOURCE: Alberta Environment Water Supply Outlook: http://www3.gov.ab.ca/env/water/WS/WaterSupply/Index.html; and B.C. Ministry of Environment River Forecast Center: http://www.env.gov.bc.ca/rfc/river_forecast/data.htm.</i>	40
<i>TABLE 5.6. Summary of the five basic (idealized) glacier shapes considered by Furbish and Andrews (1984). Ice flow direction is to the left in the diagrams.</i>	50
<i>TABLE 5.7. Comparison of the balance ratio calculated from both mass balance data and ice surface topography.</i>	69
<i>TABLE 5.8. Variability of the balance ratio with different choices of ELA for several different glaciers of the Bridge Icefield.</i>	76
<i>TABLE A.1. Summary and comparison of volume loss measured from glacier surface reconstructions and estimated with different variations of the scaling parameters of Equation (1). The various coefficients are taken from Chen and Ohmura (1990).</i>	94
<i>TABLE B.1. Summary of parameters derived for selected glaciers in the southern Rocky Mountains region. Glaciological parameters were derived only for glaciers with an initial area >1 km².</i>	96
<i>TABLE B.2. Summary of parameters derived for selected glaciers in the southern Purcell Mountains region. *denotes unofficial names.</i>	97
<i>TABLE B.3. Summary of parameters derived for selected glaciers in the southern Selkirk Mountains region.</i>	98
<i>TABLE B.4. Summary of parameters derived for selected glaciers in the southern Monashee Mountains region. The reference numbers refer to the figures in section 5.4. *denotes unofficial names.</i>	98
<i>TABLE B.5. Summary of parameters derived for the outlet glaciers of the Bridge Icefield in the southern Coast Mountains. The reference numbers refer to the figures in section 5.4. *denotes unofficial names.</i>	99

LIST OF FIGURES

FIGURE 2.1. Distribution of the glaciers and ice fields analyzed in this study.	6
FIGURE 4.1. Net changes in extent of glaciers in the southern Rocky Mountains over the period 1951/52–2001 shown over the ETM+ false color imagery. 1: Tipperary; 2: Robertson; 3: French; 4: Smith-Dorrien; 5: Haig; 6: Mangin; 7: Marlborough; 8: Pétain; 9: Castelnau; 10: Elk; 11: Nivelles; 12: Rae; 13: Abruzzi; 14: King; 15: Northover; and 16: Lyautey Glaciers.	18
FIGURE 4.2. Plot of percentage area change of individual glaciers of the southern Rocky Mountains against their initial size.	19
FIGURE 4.3. Net changes in extent of glaciers in the southern Purcell Mountains over the period 1951/52–2001 shown over the false color ETM+ imagery. 1: Conrad; 2: MacCarthy; 3: Vowell; 4: Bugaboo; 5: Catamount; 6: North Star; 7: Delphine; 8: Jumbo; 9: Commander; 10: Stockdale; 11: Starbird; 12: Toby; 13: Hamill; 14: Horseshoe; 15: Macbeth Icefield; and 16: The Four Squatters Glaciers.	21
FIGURE 4.4. Net changes in extent of glaciers in the southern Selkirk Mountains over the period 1951/52–2001 shown over the false color ETM+ imagery. 1: Wrong; 2: Nemo; 3: Hatteras; 4: Spokane; and 5: Tenderfoot Glaciers.	22
FIGURE 4.5. Net changes in extent of glaciers in the southern Monashee Mountains over the period 1951/52–2001 shown over the false color ETM+ imagery. 1: Cranberry; 2: Blanket Icefield; 3: Gates; and 4: Frigg Glaciers.	23
FIGURE 4.6. Plot of percentage area change of individual glaciers of the Columbia Mountains against their initial area.	24
FIGURE 4.7. Histograms showing the size distribution of glaciers in individual sub-regions of the Columbia Mountains for 6 distinct size classes (<0.1, 0.1–0.5, 0.5–1.0, 1.0–5, 5–10, and 10–20 km ²). The mean percentage area change over the study period (for those glaciers that have undergone a non-zero net change) is given in bold together with the standard deviation (in italics) for each class.	24
FIGURE 4.8. Net changes in extent of glaciers in the southern Coast Mountains over the period 1964/65–2002 shown over the false color ETM+ imagery. 1: Tavistock; 2: Filer; 3: Gilbert; 4: Falcon; 5: Compton; 6: Toba; 9: Bishop; 8: Lillooet; 9: Stanley Smith; 10: Bridge; 11: Place; 12: Weart; 13: Squamish; 14: Clendenning; 15: Elaho; 16: Meager Glaciers; and 17: Tahumming Glaciers.	26
FIGURE 4.9. Plot of percentage area change of individual glaciers of the Coast Mountains against their initial area.	27
FIGURE 4.10. Histograms showing the size distribution of glaciers in individual drainage basins of the Coast Mountains for 7 distinct size classes (<0.1, 0.1–0.5, 0.5–1.0, 1.0–5, 5–10, 10–20, and >20 km ²). The mean percentage area change over the study period (for those glaciers that have undergone a non-zero net change) is given in bold together with the standard deviation (in italics) for each class.	28
FIGURE 5.1. Local anomalies of mean annual temperature over the period 1900–2000. The anomalies are calculated with reference to the 1950–2000 mean, and are shown together with a 5-year filter. SOURCE: Historical Canadian Climate Dataset (HCCD); (http://www.cccma.bc.ec.gc.ca/hccd/index.shtml).	30
FIGURE 5.2. Local anomalies of mean winter (Dec 21–Mar 21) temperature over the period 1900–2000, shown together with a 5-year filter.	31
FIGURE 5.3. Local anomalies of mean spring (Mar 21–Jun 21) temperature over the period 1900–2000, shown together with a 5-year filter.	32
FIGURE 5.4. Local anomalies of mean summer (Jun 21–Sep 21) temperature over the period 1900–2000, shown together with a 5-year filter.	33
FIGURE 5.5. Regional anomalies of a: annual, b: winter, c: spring, and d: summer temperature over the period 1950–2000, shown together with a 5-year filter. The regional series were determined as the average of all the individual stations. Rates of warming are also shown together with their respective P-values (italics), and significant trends (at the 95% confidence level) are shown in bold.	34

FIGURE 5.6. Annual precipitation records shown together with the mean over the period of record (horizontal dashed line) and a 3 rd order polynomial trend line (solid curve). SOURCE: (HCCD).	35
FIGURE 5.7. Time series of the component scores derived from the principal component analysis of the standardized annual precipitation series.	37
FIGURE 5.8. Winter (Dec 21–Mar 21) precipitation records shown together with the means over each of the periods 1947–1976 and 1977–2001 (horizontal dashed lines).	38
FIGURE 5.9. Time series of the component scores derived from the principal component analysis of the standardized winter precipitation series.	39
FIGURE 5.10. Relative changes in glacier area plotted against the calculated response times. Values of response time are derived using an estimate of H that is based on the lower slope of the individual glaciers.	46
FIGURE 5.11. Terminus positions at different times for the Covenant and Banquo Glaciers (unofficial names) in the central Purcell Mountains. The surface of the Covenant Glacier is very steep and heavily crevassed (top right), while the recent formation of a large proglacial lake below the terminus of the Banquo Glacier (bottom right) attests to the very low initial bed slope in this region. The 1984–87 glacier margins are represented by the Terrain Resource Information Mapping (TRIM) digital maps of the Ministry of Sustainable Resource Management, Government of British Columbia.	48
FIGURE 5.12. General relation between terminus altitude (TA) and ELA for the five idealized glaciers in Table 5.3. FROM: Furbish and Andrews (1984).	50
FIGURE 5.13. Changes in surface extent of 2 glaciers in the Purcell Mountains with differing planimetric shapes.	52
FIGURE 5.14. Retreat of the Tenderfoot Glacier (1) and neighboring glaciers in the Slocan Ranges of the central Selkirk Mountains.	53
FIGURE 5.15. Relative (a) and absolute (b) changes in area of individual glaciers of the Bridge Icefield plotted against their initial area. Mean values of relative glacier area change (horizontal bars) are given together with \pm one standard deviation for seven distinct area classes (<0.5, 0.5–1.0, 1.0–2.0, 2.0–5.0, 5.0–10, 10–25, and >25 km ²).	56
FIGURE 5.16. Plot of relative change in area against mean elevation of glaciers situated within different parts of the study area. The area-weighted mean elevation was determined as: $\bar{z} = \sum z_i (S_i / S_{tot})$, where z_i and S_i are the median elevation and surface area respectively of individual hypsometric bins, and S_{tot} is the total glacier area.	57
FIGURE 5.17. Plot of the relative change in area against the slope at the terminus for major glaciers of the Rocky, Purcell, Selkirk, and Monashee Mountains.	59
FIGURE 5.18. Plot of the relative change in area against the slope at the terminus for outlet glaciers of the Bridge Icefield.	59
FIGURE 5.19. Surface topography and glacier margins of glaciers with unique surface slope characteristics in the Purcell Mountains (contour interval is 40 m).	61
FIGURE 5.20. Plot of the median elevation of individual small glaciers (in the central Purcells) that underwent no net change in area against the fraction of their surface area shaded by the surrounding topography during times of peak ablation. The regional ELA is based on the surrounding larger glaciers, none of which were included in this analysis.	63
FIGURE 5.21. Average median elevation of glaciers with differing aspect shown together with the percentage of the sample these glaciers represent.	64
FIGURE 5.22. Distribution and elevational characteristics of small glaciers in the central Purcell Mountains that underwent no net change in area, shown over shaded relief map. 1: Macbeth Icefield; 2: Horseshoe Glacier; 3: Starbird Glacier; 4: Commander Glacier; 5: Delphine Glacier.	65
FIGURE 5.23. Hypsometric distribution of planimetric area in relation to elevation, and hypsometric curve relating the cumulative area to elevation for the Pétain Glacier in the southern Rocky Mountains. The steady-state ELA is selected based on the change in contour curvature, which occurs at an elevation of 2700 m on this glacier (contour interval is 30 m).	67
FIGURE 5.24. Net changes in surface extent of outlet glaciers of the Bridge Icefield over the period 1964/65–2002.	70

<i>FIGURE 5.25. Plot of the relationship between calculated balance ratios and relative area change for outlet glaciers of the Bridge Icefield. The glaciers are separated based on the side of the icefield on which they are situated.</i>	70
<i>FIGURE 5.26. Sample hypsometric curves for selected outlet glaciers of the Bridge Icefield in relation to elevational distance from the estimated ELA. The distribution of geometric moments calculated from (8) is also shown (dashed lines).</i>	71
<i>FIGURE 5.27. Net changes in surface extent of major glaciers of the southern Monashee Mountains over the period 1951–2001. The solid bars indicate a distance of 1 km.</i>	73
<i>FIGURE 5.28. Plot of the relationship between calculated balance ratios and relative area change for major glaciers of the Monashee Mountains.</i>	73
<i>FIGURE 5.29. Hypsometric distribution of area and distribution of geometric moments calculated from (10) for glacier # 2 in the Monashee Mountains (contour interval is 20 m).</i>	74
<i>FIGURE 5.30. Plot of the relationship between calculated basin sensitivity index values and relative area change for outlet glaciers of the Bridge Icefield.</i>	77
<i>FIGURE 5.31. Hypsometric curves of selected outlet glaciers of the Bridge Icefield with a: low basin sensitivity values, and b: high basin sensitivity values.</i>	77
<i>FIGURE 5.32. Dependence of basin sensitivity index on area of individual outlet glaciers of the Bridge Icefield.</i>	78
<i>FIGURE 5.33. Hypsometry of the Bridge Glacier; (a) ice margin and surface topography of the Bridge Glacier in 1965 shown over the 2002 ETM+ image; (b) distribution of geometric moments calculated from (10) for different ELAs and surface extents. The distribution for the 2002 surface does not take into account changes in ice surface elevation that have occurred over the ablation zone.</i>	81
<i>FIGURE 5.34. Surface topography (ca. 1950) and margins of the Conrad (left) and Starbird (right) Glaciers in the Purcell Mountains (contour interval is 40 m).</i>	84
<i>FIGURE 5.35. Surface topography (ca. 1950) and margins of the Wrong (left) and Nemo (right) Glaciers in the Selkirk Mountains (contour interval is 30 m).</i>	85

LIST OF SYMBOLS AND ABBREVIATIONS

Symbol	Meaning	Abbreviation	Meaning
$\bar{\alpha}$	Average slope over the glacier	AAR	Accumulation Area Ratio
$\bar{\alpha}_t$	Average slope near the terminus	BR	Balance Ratio
α	Surface slope	BS	Basin Sensitivity
b_0	Reference elevation for bed	DDF	Degree-Day Factor
b_{nb}	Gradient of mass balance with elevation in the ablation zone	DEM	Digital Elevation Model
b_{nc}	Gradient of mass balance with elevation in the accumulation zone	ELA	Equilibrium Line Altitude
b_t	Mass balance rate at the terminus	ETM+	Enhanced Thematic Mapper
c_0	Volume – area scaling coefficients	GCP	Ground Control Point
c_1		GIS	Geographic Information Systems
g	Acceleration due to gravity	GLIMS	Global Land Ice Measurements from Space
G_e	Gradient of specific balance with elevation	GPS	Global Positioning System
H	Ice thickness	HCCD	Historical Canadian Climate Dataset
L	Equilibrium length	IPCC	Intergovernmental Panel on Climate Change
M	Amount of melt	LIA	Little Ice Age
m_b	Geometric moment of area in the accumulation zone	NAD83	North American Datum 1983
m_c	Geometric moment of area in the ablation zone	NTDB	National Topographic Database
p	Precipitation value	NTS	National Topographic Series
S	Glacier surface area	NHRI	National Hydrology Research Institute
s	Standardized precipitation	PC	Principal Component
T^+	Positive daily air temperatures	PDO	Pacific Decadal Oscillation
t_v	Response time	SST	Sea Surface Temperature
V	Glacier volume	TA	Terminus Altitude
z	Elevation	TIN	Triangulated Irregular Network
γ	Slope of bed	TRIM	Terrain Resource Information Mapping
δQ	Total uncertainty	UTM	Universal Transverse Mercator
δq	Individual uncertainties		
Δt	Time interval		
Λ	Product of thickness and surface slope		
ρ	Ice density		
σ	Standard deviation		
τ	Basal shear stress		
τ_v	Response time (including mass balance gradient)		

1. INTRODUCTION

In recent decades the net mass balance of most alpine glaciers has been markedly negative, and mass loss and terminal retreat of these glaciers has accelerated since the mid-1980s (Cogley and Adams, 1998; Dyurgerov, 2001; Dyurgerov and Meier, 1997, 2000, 2005; Haeberli et al., 1999; McCabe et al., 2000; Meier et al., 2003; Oerlemans, 2000; Paul et al., 2004a). This trend has also been reported in the Canadian Cordillera, where a recent period of sustained negative mass balance and terminal retreat corresponds to unusually warm mean annual air temperatures and to a reduction in winter snowfall. For example, Moore and Demuth (2001) found that the summer balance of Place Glacier in coastal British Columbia is negatively correlated with summer temperature, and that a significant and persistent period of more negative mass balance was initiated by reduction in winter snowfall after 1976. The ensuing more rapid rise of the transient snowline resulted in greater summer ablation because of the earlier exposure of lower-albedo glacier ice. The dominance of negative net balance caused significant terminal retreat, and since 1965 the glacier has lost roughly 15% of its surface area, with most of this loss occurring since 1981 (Moore and Demuth, 2001). Mass balance data for Peyto Glacier (1965–1995) in the Canadian Rockies also indicate that a shift to strongly negative balance after 1976 resulted primarily from reduced winter accumulation (Demuth and Keller, 2005), and a similar linkage between winter balance, snowline elevation, and summer ablation has been identified for this glacier (Young, 1981). It too has undergone significant terminal recession (~1 km) and long-term net mass loss since the start of formal observations in 1965 (Demuth and Keller, 2005; Luckman, 2005).

Observations of glacier frontal variations in the Rocky and Columbia Mountains show a sharp decline in rates of terminal recession at different times between 1950 and 1980. In Peter Lougheed Provincial Park, southern Canadian Rockies, McCarthy and Smith (1994) found that a period of cooler than average summer temperatures during the 1940s and 50s resulted in reduced or negligible rates of retreat at 13 glaciers (~70% of those examined), and a subsequent cooler period in the 1960s had a similar effect. This second period of wet/cool conditions immediately preceded a minor advance of several glaciers in the region, including the Elk and Sir Douglas Glaciers. In the Premier Ranges

of the Columbia Mountains, Luckman et al. (1987) identified a minor advance of 14 glaciers between 1970 and 1985. At the same time, several glaciers in the Columbia Icefield area of the Canadian Rockies also advanced (Luckman, 1998). These changes in terminus behavior have been attributed to inferred mass balance changes (higher winter precipitation, lower summer temperatures) during the previous decades (Luckman et al., 1987). Renewed frontal recession has been observed at all sites through the 1980s and 1990s.

The strong spatial and temporal coherence of these fluctuations in mass balance and terminal response across the southern Canadian Cordillera indicates that mass balance variations are strongly related to large-scale climatic variability. Bitz and Battisti (1999) found that the mass balances of several glaciers in Washington and British Columbia were negatively correlated with the PDO (Pacific Decadal Oscillation) index, which accounted for up to 56% of the variance in net winter balance. The PDO index is computed as the time history of the leading principal component of sea surface temperature (SST) in the northern Pacific Ocean (Mantua et al., 1997). Positive values of the PDO indicate a 'warm phase', which is characterized by warmer than average SST in the nearshore waters along the west coast of North America, colder than average SST in the central North Pacific, and negative sea level pressure anomalies that represent an intensification of the climatological mean Aleutian low. Negative values indicate a 'cool phase', which has the opposite pattern. During a positive PDO anomaly, storm tracks are shifted further north and there is a reduction of onshore flow and moisture flux into the Pacific Northwestern U.S. and southern British Columbia (Hodge et al., 1998; Bitz and Battisti, 1999). As a result, there is a reduction in winter snowfall, and the mass balance of most glaciers in this region decreases as a result of reduced snow accumulation.

Over the past century there have been several statistically significant reversals in the polarity of the PDO index with predominantly warm or cool phase conditions persisting between these reversals (Mantua et al., 1997; Zhang et al., 1997). From 1925 until 1947 warm phase conditions prevailed, resulting in a period of rapid retreat of most glaciers in the southern Cordillera (Luckman, 1998). Cool phase conditions followed until 1976. This period of increased winter snowfall and cooler than usual air temperature is responsible for the decline in recession rates and the minor advance of

some glaciers during this time. The most recent decades have been dominated by warm phase PDO conditions and more rapid rates of recession have been resumed. In addition to glacier mass balance and terminus position, these variations in the PDO are strongly reflected in other environmental data such as winter snowpack and regional streamflow (Moore, 1996; Moore and McKendry, 1996), which further emphasizes the importance of Pacific hemisphere climate variations for local climate and glacier variability.

Glacier recession in the Canadian Cordillera is expected to continue in the foreseeable future as current global warming is predicted to result in sustained retreat of mountain glaciers worldwide (IPCC, 2001). Concern exists over the loss of glacier ice in this region because of the potential impacts on regional water resources. It is expected that declining glacier extent will eventually lead to a reduction in glacial meltwater runoff in headwater catchments, even with sustained high specific melt rates (Jansson et al., 2003). In the Coast Mountains, Moore and Demuth (2001) found a significant negative trend in mean August streamflow for Place Creek below Place Glacier, which they attributed in part to the declining glacier surface area available for melt. Although only a minor fraction of the total annual runoff of higher order streams and rivers in the Cordillera is contributed by glacial melt, mountain glaciers tend to moderate interannual variability in streamflow and help to maintain higher runoff volume during extreme warm and dry periods (Fountain and Tangborn, 1985). For example, Hopkinson and Young (1998) found that the average contribution of glacial meltwater to the annual discharge (1951–1993) of the upper Bow River in the Rocky Mountains was only ~2%, but that the contribution increased to 13% during a low flow year. During the driest month of that year glacial melt contributed 54% of the total basin runoff. Evidence is already emerging for a decline in the regulatory effects of glacier cover in the headwaters of the North Saskatchewan River, Rocky Mountains, where reduced low and mean flows in the August – October period have been observed together with an increase in flow variability and slightly higher maximum flows (Demuth and Pietroniro, 2002). A decrease in late summer flow of glacially-fed rivers throughout British Columbia has also been observed, and it has been suggested that most glaciers in B.C. may have already passed the phase of warming-induced increased runoff (Stahl and Moore, 2006).

Glaciological research in the Canadian Cordillera has primarily focused on a few selected glaciers such as the Peyto, Athabasca, and Place Glaciers. Inventory and glacier mapping efforts have been carried out for parts of the Coast Mountains (Evans, 2004), the Columbia Mountains (Sidjak and Wheate, 1999), and the Rocky Mountains (Hopkinson and Young, 1998; McCarthy and Smith, 1994), but these studies have either examined only a limited region, or do not account for very recent terminus fluctuations (i.e., during the previous 1–2 decades). Periodic glacier inventories and measurements of changes in glacier area and volume are useful as an index of climate change, and provide information necessary for regional water management. A primary objective of the international GLIMS (Global Land Ice Measurements from Space) project is the repeated acquisition of glacier inventories from remotely sensed imagery at time intervals of a few decades (Bishop et al., 2004). In a global context, accurate regional inventories of the distribution and geometric characteristics of individual glaciers permit validation of climate and mass balance models and are important for projecting the glacial contribution to sea level rise in future years as glaciers are reduced in size (Dyurgerov and Meier, 2005). There is, therefore, currently a need for an inventory of glacier area and volume in the Canadian Cordillera, and for a summary of recent changes in these parameters.

The principal objective of this work is to quantify the total glacier area and volume at a regional scale across a section of the Canadian Cordillera that has received little previous study, and to measure the net change in these parameters over the past several decades. This is done by comparing remotely sensed imagery acquired at different times with the use of GIS (Geographic Information Systems) software. A secondary objective of this work is to identify patterns of spatial variability in these changes within the study area, and to investigate potential causes of the observed variability. This will help to identify specific regions or individual glaciers with a high sensitivity to climate change.

2. STUDY AREA

2.1 LOCATION AND DISTRIBUTION OF ICE

The study area comprises an east – west transect within the approximate region 50–51° N and 115–125° W, encompassing the Rocky, Columbia, and Coast Mountains of Alberta and B.C. (Fig. 2.1). The precise boundaries of the study area are defined by the divides of regional drainage basins within this approximate region. Icefields and glaciers cover an area of ~2690 km² within this region and volume – area scaling techniques (Chen and Ohmura, 1990; Bahr et al., 1997) indicate that the present ice volume is $\sim 164 \pm 33$ km³. Most of this ice is situated within the Coast Mountains, where several extensive (i.e., >150–200 km²) icefields, such as the Bridge – Lillooet, Elaho, and Pemberton Icefields, and many large valley glaciers account for ~90% of the total ice volume. The Purcell Mountains, located in the eastern Columbia Mountains, contain ~65% of the remaining ice volume in the region. Here there are several large icefields (e.g., Conrad and Macbeth Icefields) and many moderately sized valley and cirque glaciers, which together contain $\sim 11 \pm 4$ km³ of ice. The remaining mountain ranges within the study area contain $\sim 5 \pm 2$ km³ of ice in the form of small (i.e., <4 km²) cirque and hanging glaciers, with the exception of the ~ 7 km² Blanket Icefield in the central Monashee Mountains.

Ice cover in this region probably reached its most recent maximum extent during the mid-19th century when mountain glaciers in many parts of Europe and North America reached their maximum Holocene extents. Since this Little Ice Age (LIA) maximum ice extent, glaciers in the Rocky Mountains have lost ~25% or more of their area (Luckman, 2000). This can be seen by comparing the well-defined moraines that formed at this time to the current margins of individual glaciers. LIA moraines are clearly visible below most glaciers in the study area, and are located anywhere from several hundred meters to several kilometers downvalley from the present glacier termini. This indicates that similar losses of area have taken place in all parts of the study area since the time when the moraines were formed.

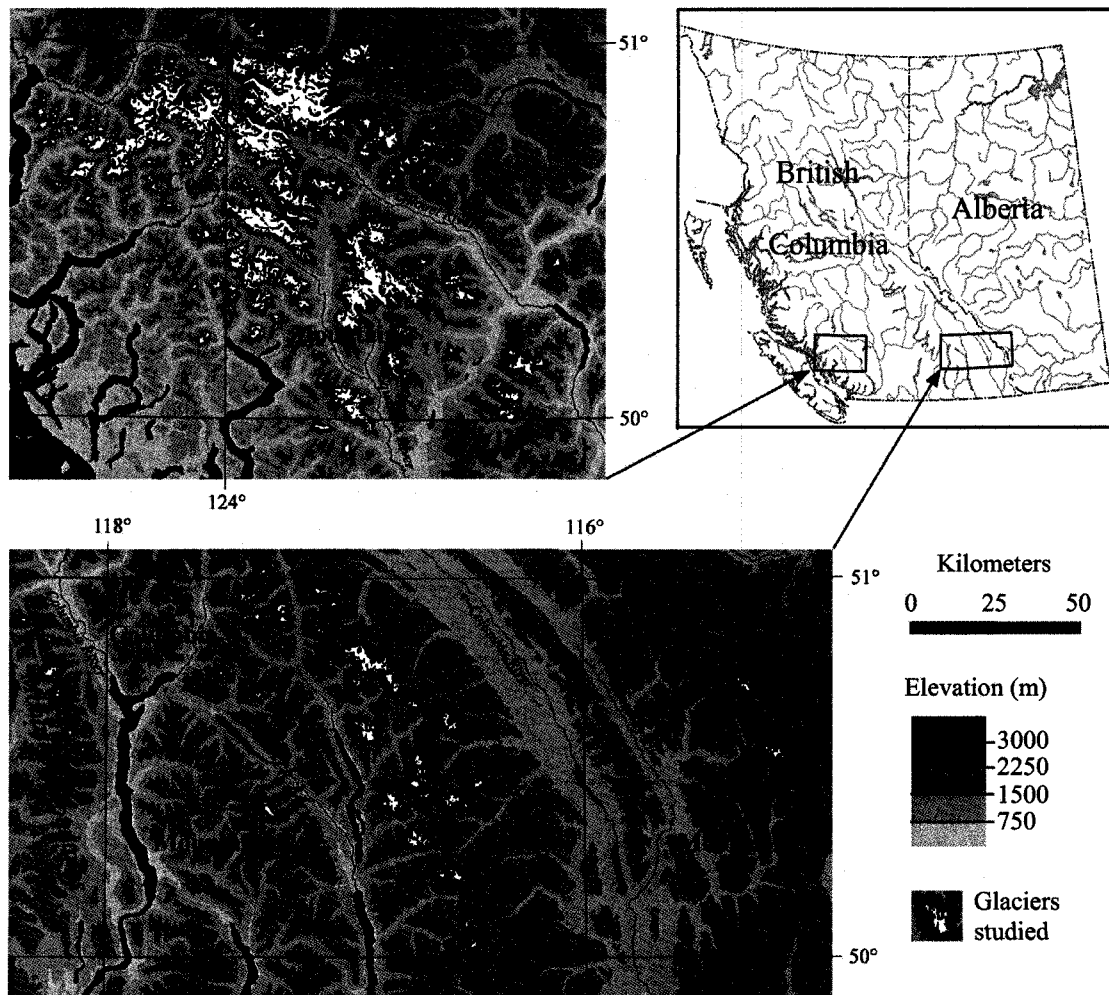


FIGURE 2.1. Distribution of the glaciers and ice fields analyzed in this study.

2.2 REGIONAL PHYSIOGRAPHY

The glaciers in the easternmost portion of the study area are situated within the Continental Ranges of the Rocky Mountains. Here, topography is extremely rugged, with steep slopes, narrow ridges, and high-level cirque basins (Holland, 1976). Relief ranges up to 1800 m around the Kananaskis and Elk Lakes, with the highest summits extending up to elevations of 3200–3450 m (e.g., Mt. Joffre, King George, Sir Douglas, and Abruzzi). These mountains are drained by the Kananaskis River in Alberta, which is a tributary to the Bow River, and the Elk and Palliser Rivers in British Columbia, which are both part of the Kootenay River system.

West of the Rocky Mountain Trench are the Purcell Mountains, which also have considerable relief (e.g., ~2500 and ~2900 m around Columbia and Kootenay Lakes respectively). Several peaks reach elevations of over 3400 m, including Mt. Farnham, Jumbo Mountain, and Hamill Peak, and the topography is similarly rugged as in the Rockies. These mountains are drained by eastward flowing tributaries of the Columbia River such as Bobbie Burns, Horsethief, and Toby Creeks, and westward flowing tributaries of the Kootenay River including the Duncan River, and Howser and Glacier Creeks.

Further west, the Selkirk Mountains are separated from the Purcells by the Duncan River valley. In the northern ranges of the Selkirks, mountains are topographically and geologically similar to those in the neighboring Purcells. The more southerly ranges (Slocan Ranges), where Kokanee Peak (2800 m) is the highest summit, are more subdued in relief. Drainage is into the Kootenay River system via the Lardeau and Duncan Rivers.

West of the Columbia River and the Upper Arrow Lake, the Monashee Mountains consist of sharp matterhorn-like peaks sculpted by cirque glaciers (Holland, 1976), with relief of ~2400 m between the highest summit (Mt. Odin; 2972 m) and the Columbia River valley. The eastern slopes of this range are drained by tributaries such as Blanket, Cranberry, and Pingston Creeks that flow directly into the Columbia River, and the western slopes drain into the Shuswap River, which is part of the upper Fraser River system.

All the glaciers in the Coast Mountains are situated within the Pacific Ranges, which extend over a width of ~150 km from the Coastal Trough to the Fraser and Thomson Plateaus in the Interior System. These mountains include some of the highest peaks in the Coast Mountains, with a number of summits over 3000 m in elevation. Relief in this area is immense, ranging from ~2700 m in Garibaldi Provincial Park between the summit of Wedge Mountain and Lillooet Lake, up to 3200 m between the highest peaks in the northwest part of the region (e.g., Mount Gilbert and Monmouth Mountain) and the Bute and Toba Inlets. These mountains drain to the coast by way of the Southgate, Squamish, and Toba Rivers, and into the Fraser River via the Bridge and Lillooet Rivers.

2.3 REGIONAL CLIMATE

Mean annual precipitation varies considerably across the study area, with a spatial pattern that is controlled primarily by topography and the direction of regional air flow. In general, precipitation declines from west to east across the region and similar, but less pronounced patterns occur at local scales between the windward and leeward slopes of individual ranges. The Coast Mountains receive an average precipitation of 150–250 cm/year in low valleys, and up to 350 cm or more per year at higher elevations. The Monashee Mountains receive 100–150 cm of precipitation annually, but this increases to 150–250 cm over the northern Selkirks and the Purcell Mountains which are higher in elevation. Further east, precipitation decreases to 100–150 cm/year in the Rockies despite the fact that these mountains are considerably higher than the Monashees.

Regional differences in the seasonal distribution of temperature and precipitation result from differences in the relative dominance of specific air mass types. The coastal region is dominated by westerly flow from the Pacific, and has a maritime climate with cooler summer temperature and milder winter temperature than the interior regions. Mean January temperature ranges between -10 and -15°C , and July temperature is typically between 10 and 15°C . Most of the precipitation is received during the winter due to the westerly movement of mid-latitude cyclones and strong onshore flow of air, which is forced over the north-west–south-east trending mountain ranges. During the summer, air pressure gradients are weaker, air flow is gentler, and there are fewer days with measurable precipitation. Most of the southern interior of B.C. is influenced by both continental and maritime air masses, and precipitation is distributed more uniformly throughout the year. Winter temperature is moderated by the influence of maritime air so that it is similar in magnitude to the coastal region, but July temperature ranges from 16°C up to 20°C due to reduced westerly air flow at this time. The eastern ranges of the Rocky Mountains are dominated by continental air masses. January temperature here is more extreme with an average of -15 to -20°C , while temperature during the summer is similar to that in the Columbia Mountains.

3. METHODS

Changes in glacier surface area were determined from comparisons of remotely sensed imagery acquired in 1951/52 over the Columbia and Rocky Mountains, in 1964/1965 over the Coast Mountains, and in 2001/02 over the entire study area. Ice margins were delineated for each time period using GIS software, and compared to obtain measurements of the net area change of individual glaciers. Estimates of ice volume for each time period were based on the measured glacier surface area, and net volume change was determined as the difference between estimates.

3.1 SOURCES OF DATA

Satellite imagery used in this study consists of 3 Landsat 7 ETM+ (Enhanced Thematic Mapper) scenes acquired on Sept 14, 2001 (path 44, row 25), Sept 23, 2001 (path 43, row 25), and Sept 13, 2002 (path 48, row 25). These scenes were obtained as Landsat 7 Orthorectified Imagery over Canada through the GeoGratis website of Natural Resources Canada (NRCan, 2006). The data set is derived from Landsat-7 raw image level L1G (i.e., radiometrically and systematically corrected) which has been processed using ground control points (GCPs) from provincial vectors and digital elevation models (DEMs), considered to be the most accurate control data available at the time of creation. The planimetric error associated with this imagery is estimated to be ± 30 meters or better with a 90% level of confidence, but well-defined features located in areas of greater than 25% slope may not meet this level of accuracy (NRCan, 2006).

The aerial photography consists of British Columbia Government aerial photos, archived as part of the Canadian Glacier Inventory at the National Hydrology Research Institute (NHRI) in Saskatoon, Saskatchewan. Photos over the Coastal Mountains were taken in late July 1964/65 (~1:30,000 scale), and those of the Columbia and Rocky Mountains were acquired from late July through September 1951/52 (~1:50,000 scale).

1:50,000 scale first edition National Topographic Series (NTS) map sheets, and the Glacier Map of Southern British Columbia and Alberta (1:1,000,000 scale) were obtained from the William C. Wonders Map Collection of the University of Alberta. The

1st edition NTS maps are based on aerial photography taken in 1951 and 1970 over the Coast Mountains, and in 1947, 1951, and 1953 over the Interior Ranges and Rocky Mountains. The Glacier Map of Southern B.C. and Alberta is based on glacier outlines reduced from the 1:250,000 scale NTS maps and other source maps available in 1965. All of the maps were scanned at 300–400 dpi using a Vidar 36” large format upright scanner to produce TIFF format image files. In addition to these maps, National Topographic Database (NTDB) vector files (derived from the 1:50,000 NTS map sheets) were obtained from the University of Alberta’s data library. The specific themes represented in these data were permanent snow and ice, lakes and rivers, roads, and topographic contours. These data are digitized from the 1st edition NTS maps over most of the Coast Mountains, and primarily from 2nd edition maps over the rest of the study area. However, in most cases the glacier outlines have not been updated from the first edition map, so the NTDB data effectively represent the earlier time period. Planimetric accuracy of these data, reported in the metadata files accompanying the data, varies between 50–100 m based on estimates of the degree of correspondence between the geometric data versus geodetic foundation (horizontal reference system). It is noted that this error is not very significant for the topographic contours.

The digital elevation model (DEM) used in this study is part of the DMTI Spatial Inc. dataset, which was created from interpolation of the NTDB 1:50,000 scale digital mapping (Standards and Specifications V3.0 and later) using contours, elevation points, and water bodies. The DEMs are projected at 30 meter resolution to the NAD83 UTM grid. Vertical accuracy is not reported within the metadata files of the NTDB from which the DEMs are derived, so the error associated with the DEMs is estimated to be one half the contour interval of the NTDB (i.e., ± 20 m).

3.2 IMAGE PREPARATION AND GEOMETRIC CORRECTION

The ETM+ Orthorectified Imagery was obtained with spatial reference to the Lambert Conformal Conic map projection with standard parallels of 49° and 77°N on the NAD83 datum and GRS 1980 ellipsoid, and subsequently projected in UTM coordinates. Individual scenes were clipped to the specific regions of interest using the software PCI

Imageworks™ in order to reduce file size as well as processing time in subsequent operations and analysis. Data fusion was performed to enhance the apparent resolution of the imagery using the FUSION function in the PCI Geomatica™ *Xpace* module. ETM+ bands 2, 3, and 4 [$\lambda = 0.53\text{--}0.61, 0.63\text{--}0.69, \text{ and } 0.78\text{--}0.90 \mu\text{m}$ (30m resolution)] were combined with the panchromatic band 8 [$\lambda = 0.52\text{--}0.90 \mu\text{m}$ (15m resolution)]. In this process, an input pseudocolour image is fused with a grayscale intensity image to produce an output RGB pseudocolour image with the same resolution as the original grayscale image.

Original aerial photo prints were scanned as TIFF image files using a Bell-Howell 500XF flatbed scanner at 300 dpi [~ 4 meter ground resolution (1:50,000 scale photos); ~ 2.5 meter resolution (1:30,000 scale photos)]. The digitized aerial photos were then spatially referenced to the fused ETM+ Orthorectified Imagery using the thin plate spline math model in PCI Orthoengine™. This model fits the GCPs exactly and warping is distributed throughout the image with minimum curvature between points becoming almost linear away from the GCPs. For this reason it is not suitable for the removal of terrain distortions or for images of rough terrain, but GCPs can be added in areas where the transformation is not satisfactory. Individual photographs were referenced to the Landsat 7 imagery by selecting between 15 and 20 GCPs that were clearly identifiable in both images, with most of the points chosen immediately adjacent to glacier termini and areas where obvious changes were observed on each glacier. Thus, although the geometric accuracy of the corrected image as a whole may have been poor, the localities with a high density of GCPs were accurately tied to the Landsat 7 imagery.

3.3 ICE MARGIN DELINEATION

Ice margins and interior bedrock outcrops for the 2001/02 time period were delineated using on-screen digitizing techniques in ArcMap 8.3™ GIS. Discrete ice masses and outcrops were defined by manually digitizing a series of points to construct polygon shapefiles, and the interior bedrock polygons were used to clip the ice extent to create an ‘ice surface only’ polygon. Most of the point collection was carried out while zoomed to a nominal scale of 1:10,000, which seemed to represent the best compromise between the

ability to clearly identify unobscured ice-rock boundaries, and the ability to place points to within \pm one image pixel of the boundary.

Separate polygons representing icefields and diverging glaciers were then clipped to allow area change measurements to be associated with individual drainage catchments. This was done by manually cutting the polygons along the ice flow divides, which were identified based on ice topography using topographic contours and defined drainage basins. The extent of the first order basins was identified using the map algebra syntax ‘BASIN(FLOWDIRECTION([elevation]))’ within the Spatial Analyst extension of ArcMap™. FLOWDIRECTION first creates a grid of flow direction from each cell to its steepest downslope neighbor, and BASIN then creates a grid delineating all drainage basins within the analysis extent. In cases where the position of ice divides was clearly misrepresented by the topographic information, it was defined by visual interpretation of the ETM+ imagery. For situations in which an icefall or a steep slope separates two or more distinct ice masses, the polygons were merged so that all upstream areas contributing ice to a particular glacier terminus were included within a single catchment.

In the lower portion of each individual glacier, ice margins were derived in a similar manner for the 1951/52 and 1964/65 time periods using the geometrically corrected aerial photos. For the accumulation zones of individual glaciers, margins were copied from the 2001/02 polygons. This was a reasonable approach as the change in width across this portion of most glaciers was negligible. Only where obvious changes had occurred was the margin adjusted in this region. Ice flow divides were held constant between both periods.

3.4 AREA AND VOLUME CALCULATIONS

Area measurements were made for individual glaciers by adding a field to the attribute table of each shapefile and updating the records for area using the field calculator in ArcMap™. Two additional fields were created and populated in a similar manner to represent the centroid x and y positions of individual polygons, given in units of meters, which were necessary in order to derive a unique ID for each glacier. The tables for the 2001/02 glacier shapefiles were then exported in .dbf format into Microsoft® Office

Excel and the centroid x and y coordinates were converted into values of latitude and longitude for deriving the GLIMS format glacier IDⁱ. The tables for the shapefiles of earlier periods were similarly exported, and corresponding rows were matched in the spreadsheet to compare the areas for different periods. In cases where a glacier had split into several distinct ice masses between subsequent periods, the net area change was computed using the total area of the individual glaciers in the 2001/02 period.

Measurements of area were used to estimate glacier volume with an empirically derived volume-area scaling relationship (Chen and Ohmura, 1990). The volume (V ; 10^6 m³) of an alpine valley glacier is related to its surface area (S ; 10^6 m²) as:

$$V = c_0 S^{c_1}. \quad (1)$$

Observations of a wide range of glaciers worldwide give values of 28.5 and 1.36 for c_0 and c_1 respectively. Volume changes were determined from comparison of the volume estimates for each period. Where a glacier had disintegrated, (1) was applied to the total area of all separate ice masses in order to avoid potentially large errors in the estimated volume change.

3.5 ERROR ESTIMATION

The potential error associated with the measurements of the 2001–02 glacier surface area depends upon the accuracy with which the ice margin of individual glaciers can be identified and digitized. This in turn depends upon both the image resolution and the level of contrast between the ice and the adjacent terrain. The uncertainty associated with the regional measurements of glacier area was estimated from a detailed analysis of small samples of regionally representative glaciers. For each sample, the fraction of the total perimeter affected by various types of obscurities was determined and a maximum offset distance between the digitized boundary and the true ice margin was assigned to each type of obscurity. The error was then scaled up to the entire set of glaciers by multiplying the fraction of the regional ice perimeter length by the estimated offset distance for the various types of obscurity.

ⁱ This ID is of the form GnnnnnnEmmmmm[N|S], where [N|S] means “either N or S”, nnnnnn has the range [000000,359999], and mmmmm has the range [00000,90000]. The numeric values are in decimal degrees multiplied by 1000.

For unobscured sections of ice margin, measurement uncertainty was judged to be no greater than the resolution of the fused ETM+ imagery (± 15 m) as there is significant spectral contrast between the ice and the surrounding rock and debris. Where continuous debris cover or shadows obscure ice margins, the error was estimated to be ± 45 m. For debris-covered sections, this estimate is based on a comparison between measurements derived from the ETM+ imagery and field observations at several sites within the Rocky and Purcell Mountains. In general, accurate manual delineation is possible for debris-covered termini because of the difference in illumination that results from the shape of the glacier boundary. Where the margin is obscured by shadow, a contrast stretching function was applied to the ETM+ imagery to improve the ability to detect the ice – rock boundary. The uncertainty is greatest where late-lying snow obscures the ice margin or could be misinterpreted as glacial ice. Measures taken to avoid misclassification in such cases included comparison with other remotely sensed imagery (e.g., the TRIM [Terrain Resource Information Mapping] ortho-photo mosaic available on the B.C. Integrated Land Management Bureau webpage: <http://ilmbwww.gov.bc.ca/bmgs/airphoto/IMF/Index.htm>) and detection of crevasses or emerging bare ice within the aerial photography. Here error was estimated to be ± 90 m for the ice margin, which seems to be an average potential offset distance observed in the ETM+ imagery throughout the study area.

Planimetric errors within the orthorectified ETM+ imagery are not considered to be of significance in this study because the positional error of this imagery is unlikely to be random, and correspondence between locations within the imagery and their true ground position is unimportant in terms of the measurement of surface area. Similarly, this error has no effect on the measurements of area change as the uncertainty in these measurements depends only on the accuracy of the co-registration between the aerial photography and the ETM+ imagery, and the ability to correctly identify the ice margins.

Repeated measurements of surface area change were made to estimate the uncertainty associated with these measurements. This was done for a range of different magnitudes of area change and for aerial photos with differing amounts of snow cover. Extreme potential positions of the ice margin were digitized to determine both the maximum and minimum change in area. A regression of the relative uncertainty against the magnitude of the absolute change in area was performed for three categories of aerial

photo quality (based on the amount of snow cover obscuring the glacier margin), and the equations were used to predict the relative uncertainty in these measurements for all glaciers.

In addition to the potential error resulting from the digitizing process, error may also arise due to imperfect co-registration between the aerial photography and the ETM+ imagery. This was accounted for by measuring the length of perimeter digitized from the aerial photography for the same test glaciers as above, and multiplying this length by the co-registration error. Because the mathematical model used in the geometric correction process fits the GCPs exactly, co-registration error near the control points is estimated to be equal to the fused ETM+ image resolution (i.e., ± 15 m) on average. However, since it is assumed to be independent and randomly distributed, 50% of this error was chosen as a more reasonable estimate. A regression was used to relate the relative error associated with image co-registration to the magnitude of the absolute area change, and the resulting equation was used to predict the uncertainty for all area change measurements.

The total error (δQ) related to the 2001/02 surface area and the measured change in area, was calculated as:

$$\delta Q = \sqrt{(\delta q_1)^2 + (\delta q_2)^2 + \dots + (\delta q_n)^2}, \quad (2)$$

where $\delta q_1, \dots, \delta q_n$ represent the individual uncertainties in surface area associated with each type of image problem. The actual error is likely overestimated as this assumes a maximum digitizing offset over all linework derived from the ETM+ imagery and the aerial photography. It is more likely that multiple random errors in the digitizing process roughly cancel, and that the majority of the error results from image registration problems and rare occurrences of major ice margin obstructions.

The estimates of glacier volume and net ice loss over the study period are also subject to uncertainty. This is a result of error in the measurements of area, from which ice volume is estimated, and the choice of parameters used in the volume – area scaling relationship. For glaciers that have experienced a significant loss of ice, uncertainty due to the choice of scaling parameters is typically an order of magnitude greater than that due to area measurement error. Since it is likely that this error is overestimated to begin with, uncertainty in the volume estimates as a result of the area measurements is considered to be negligible. To quantify the uncertainty in the estimates of volume, the

parameters c_0 and c_1 in (1) were varied to reflect the range of estimates of these parameters that have been derived empirically for different regions (e.g., Chen and Ohmura, 1990), and on the basis of physical considerations (e.g., Bahr et al., 1997). Combinations of these parameters that were found to be representative of the glaciers in this region (e.g., where volume change has been measured from comparison of multi-temporal DEMs in the Coast Mountains, and from field reconstruction of several LIA glacier surfaces in the Purcell and Rocky Mountains [see Appendix A]) were used to quantify the potential range of error in the volume estimates. Combinations of c_0 and c_1 that poorly represent the glaciers here were disregarded in this analysis. The maximum difference between the different estimates of volume obtained provides a measure of the uncertainty in these results (i.e., ± 36 , 33 , and 3 km^3 for the initial and final conditions, and the difference respectively).

4. RESULTS

4.1 NET CHANGE IN GLACIER AREA AND VOLUME

Ice coverage in the study area decreased by $146 \pm 10 \text{ km}^2$ ($\sim 5.2\%$) between image acquisition dates, corresponding to a net volume loss of $13 \pm 3 \text{ km}^3$. Table 4.1 compares regional measurements of area and volume for each time period, and shows how changes in these quantities vary in both relative and absolute magnitude at this scale. In general, the percentage of ice loss is greater in the eastern portion of the study area, excluding the central Columbia Mountains, and an eastward trend of increasing relative area change is evident. However, this general pattern may be due in part to the different length of comparison periods, as the initial observations over the Columbia and Rocky Mountains were obtained ~ 13 years prior to those in the coastal region. Despite the pattern of relative glacier changes, ice coverage in the Monashee and Rocky Mountains is far less extensive, so that absolute changes here are relatively insignificant in comparison to the Coast Mountains. The reduction of glacier area in the coastal region accounts for $\sim 80\%$ of the total surface area change and $\sim 90\%$ of the total ice volume change. The Purcell Mountains also contain a large amount of ice, and although the relative reduction in

TABLE 4.1. Summary of area measurements and volume estimates (using values of 28.5 and 1.36 for c_0 and c_1 respectively), and net changes in these variables over the study period for all mountain ranges. Measurements of the initial conditions in the Coast Mountains are relative to the period 1964/65.

Mountain Range	1951/52 Area (km ²)	2001/02 Area (km ²)	Δ Area (km ²)	Δ Area (%)	1951/52 Volume (km ³)	2001/02 Volume (km ³)	Δ Volume (km ³)
Rocky Mountains	40 ± 3	34 ± 3	-6.0 ± 0.7	-15.0	1.4 ± 0.7	1.1 ± 0.6	-0.3 ± 0.2
Purcell Mountains	257 ± 17	245 ± 17	-12 ± 2	-5.1	11.3 ± 3.7	10.5 ± 3.6	-0.8 ± 0.2
Selkirk Mountains	103 ± 11	100 ± 11	-3 ± 1	-3.2	3.4 ± 1.8	3.3 ± 1.8	-0.1 ± 0.05
Monashee Mountains	37 ± 3	32 ± 3	-4.9 ± 0.5	-13.4	1.2 ± 0.7	1.0 ± 0.6	-0.2 ± 0.08
Coast Mountains	2397 ± 113	2277 ± 113	-120 ± 10	-5.0	160 ± 36	148 ± 33	-12 ± 3
Study Area Total	2834 ± 115	2688 ± 115	-146 ± 10	-5.2	177 ± 36	164 ± 33	-13 ± 3

glacier area has been limited in this region, these mountains have still lost a considerable amount of ice. Nearly 60% of the ice loss that has occurred outside the coastal region is due to the retreat of glaciers within the Purcells. The least significant changes in glacier area and volume occurred in the Selkirk Mountains, where there is also a large amount of ice. The relative change in area here is very low, so that glacier loss is less than in either the Monashees or the southern Rockies, which each have an initial ice extent of only $\sim 1/3$ that of the Selkirks.

4.2 LOCAL VARIABILITY OF GLACIER CHANGES

The net area and volume changes observed in each mountain range are generally not representative of the changes of individual glaciers or even large groups of glaciers within individual ranges. This is because there is a high degree of local variability across the study area, with neighboring glaciers exhibiting a dissimilar response in many instances. Within most regions, the majority of the ice loss is due to the retreat of the largest glaciers, which comprise only a small percentage of the total number of glaciers, so the relative changes listed in Table 1 are generally representative of only this small group of glaciers. This of course depends on the glacier size distribution in each region and the variability of area changes in the individual glacier size classes. Such variations observed at the regional and local scale are described below.

4.2.1 Rocky Mountains

The glaciers in the southern Rocky Mountains display a large range in relative area loss, with changes in the area of individual glaciers varying from +2 to nearly -70% in extreme cases. No obvious spatial patterns of glacier area change were observed in this region (Fig 4.1). Most of the variation occurs between the glaciers with an initial area of 0.25–1.0 km² (Fig. 4.2), while the largest glaciers display a more consistent pattern. These larger glaciers have generally undergone area changes between -5 and -20%, and

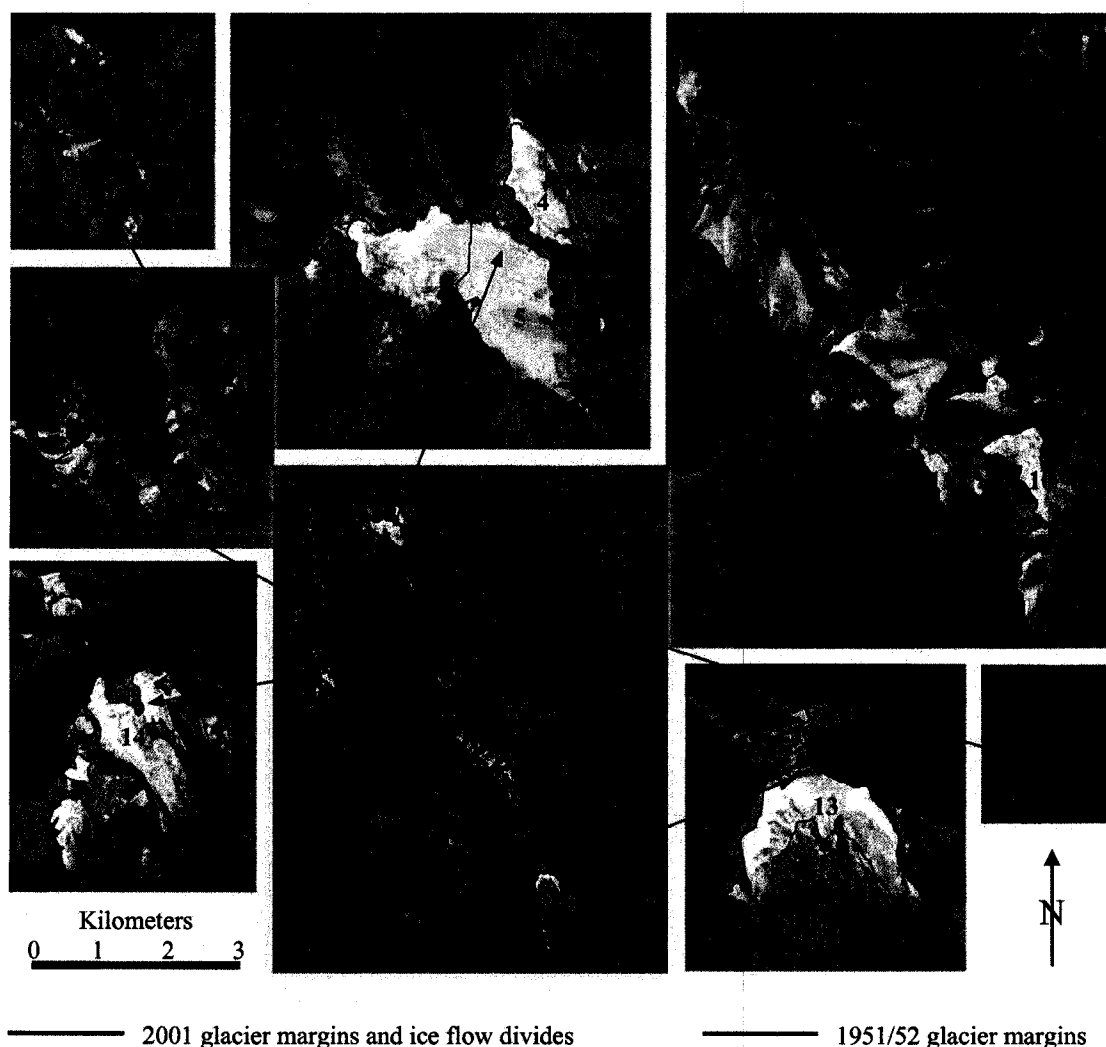


FIGURE 4.1. Net changes in extent of glaciers in the southern Rocky Mountains over the period 1951/52–2001 shown over the ETM+ false color imagery. 1: Tipperary; 2: Robertson; 3: French; 4: Smith-Dorrien; 5: Haig; 6: Mangin; 7: Marlborough; 8: Pétain; 9: Castelnau; 10: Elk; 11: Nivelle; 12: Rae; 13: Abruzzi; 14: King; 15: Northover; and 16: Lyautey Glaciers.

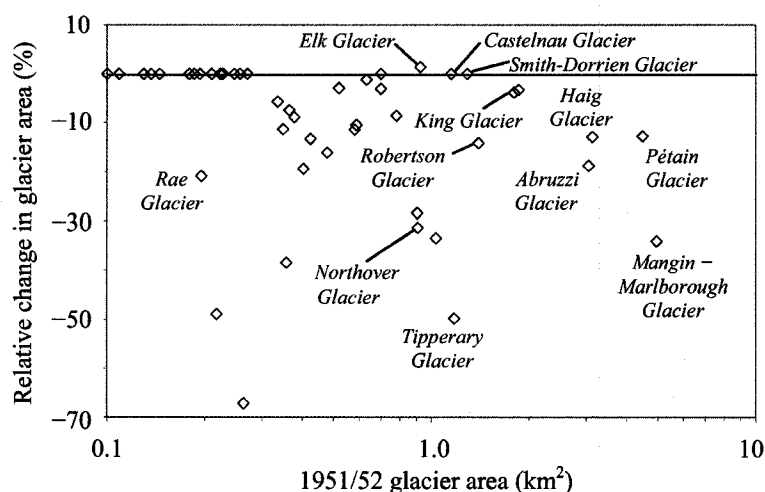


FIGURE 4.2. Plot of percentage area change of individual glaciers of the southern Rocky Mountains against their initial size.

TABLE 4.2. Summary of net changes in area and volume (using values of 28.5 and 1.36 for c_0 and c_1 respectively) over the period 1951/52–2001 for the largest glaciers in the southern Rocky Mountain region (accounting for ~65% of the total ice loss here).

Glacier Name	GLIMS ID	2001 Area (km ²)	1951/52 Area (km ²)	Δ Area (km ²)	Δ Area (%)	2001 Vol. (km ³)	1951/52 Vol. (km ³)	Δ Vol. (km ³)
Mangin	G295217E50543[N]	2.1	4.9	-1.7	-34	0.14	0.25	-0.11
Marlborough	G295199E50542[N]	1.1	4.9	-1.7	-34	0.14	0.25	-0.11
Pétain	G295180E50533[N]	3.9	4.5	-0.6	-13	0.18	0.22	-0.04
Haig	G295300E50710[N]	2.7	3.1	-0.4	-13	0.11	0.13	-0.02
Abruzzi	G295119E50426[N]	2.5	3.0	-0.5	-19	0.10	0.13	-0.03

up to -35% in the case of the Mangin – Marlborough Glacier. Also notable is the fact that all but two of the glaciers with an area of less than 0.25 km² have undergone no change in area over the study period.

The most significant loss of ice volume here is due to the retreat of the largest glaciers (Table 4.2). In comparison, ice loss from the relatively small glaciers (i.e., <1.0 km²) is insignificant despite the fact that there are far more glaciers in these classes, and many of these have undergone relative changes that are similar or greater in magnitude. Most of the wastage in the largest group is due to the substantial retreat and breakup of the Mangin – Marlborough Glacier, which retreated by over 2 km at its front. Its loss of over 0.1 km³ accounts for roughly 35% of the total ice loss of the region. The Pétain, Haig, and Abruzzi Glaciers also underwent a relatively large amount of terminal retreat

and lost a considerable volume of ice. Together, the loss from these glaciers accounts for a further 30% of the total ice wastage in the southern Rockies. Other glaciers that have undergone extensive terminal retreat include both the Robertson and Northover Glaciers, but because of their smaller size, their combined volume loss was only $\sim 4 \times 10^{-3} \text{ km}^3$.

4.2.2 Columbia Mountains

Relative changes in glacier area across the Columbia Mountains display a considerable amount of local variability, superimposed on a broad regional pattern. In general, the greatest relative changes and the highest local variability are observed in the Monashee Mountains, where changes range from +11 to -75% (Figs. 4.5, 4.6). Glaciers on the eastern slopes of the Purcell Mountains (Fig 4.3) and in the central Selkirk Mountains near Trout Lake (Fig. 4.4) also display a significant amount of variability. Changes here generally range from +3 to -30%, and up to -44% in the case of the Tenderfoot Glacier (Fig 4.6). In contrast, glaciers in the Duncan River Basin, which is situated in the northern Selkirk Mountains and the northwestern Purcells, display a more consistent pattern. Here the vast majority of glaciers have undergone little or no change in area, and only a small number have changed by more than -10%. As in the southern Rockies, nearly all of the smallest glaciers in the Columbia Mountains have not changed in area.

Nearly 90% of the ice volume loss from the Purcell Mountains is due to the retreat of only 15 of the more than 330 glaciers here. The retreat of 3 glaciers (e.g., Starbird, Stockdale, and Jumbo Glaciers) in the Horsethief Creek Basin accounts for nearly 30% of the total ice loss from this mountain range (Table 4.3). Several of the larger glaciers have also contributed significantly to this wastage, including the Toby, Vowell, and Conrad Glaciers, as well as 3 other unnamed outlet glaciers from the Conrad and Macbeth Icefields that each lost an estimated 0.04 km^3 of ice. Each of these glaciers has undergone a frontal retreat of 500–1000 m, and together their ice loss accounts for a further 45% of the total wastage in the southern Purcell Mountains.

Ice volume loss from the Selkirk Mountains is largely due to the retreat of the Tenderfoot Glacier in the Lardeau River Basin, which retreated by $\sim 1700 \text{ m}$ and separated to form 2 distinct termini, resulting in an estimated loss of 0.04 km^3 of ice. The

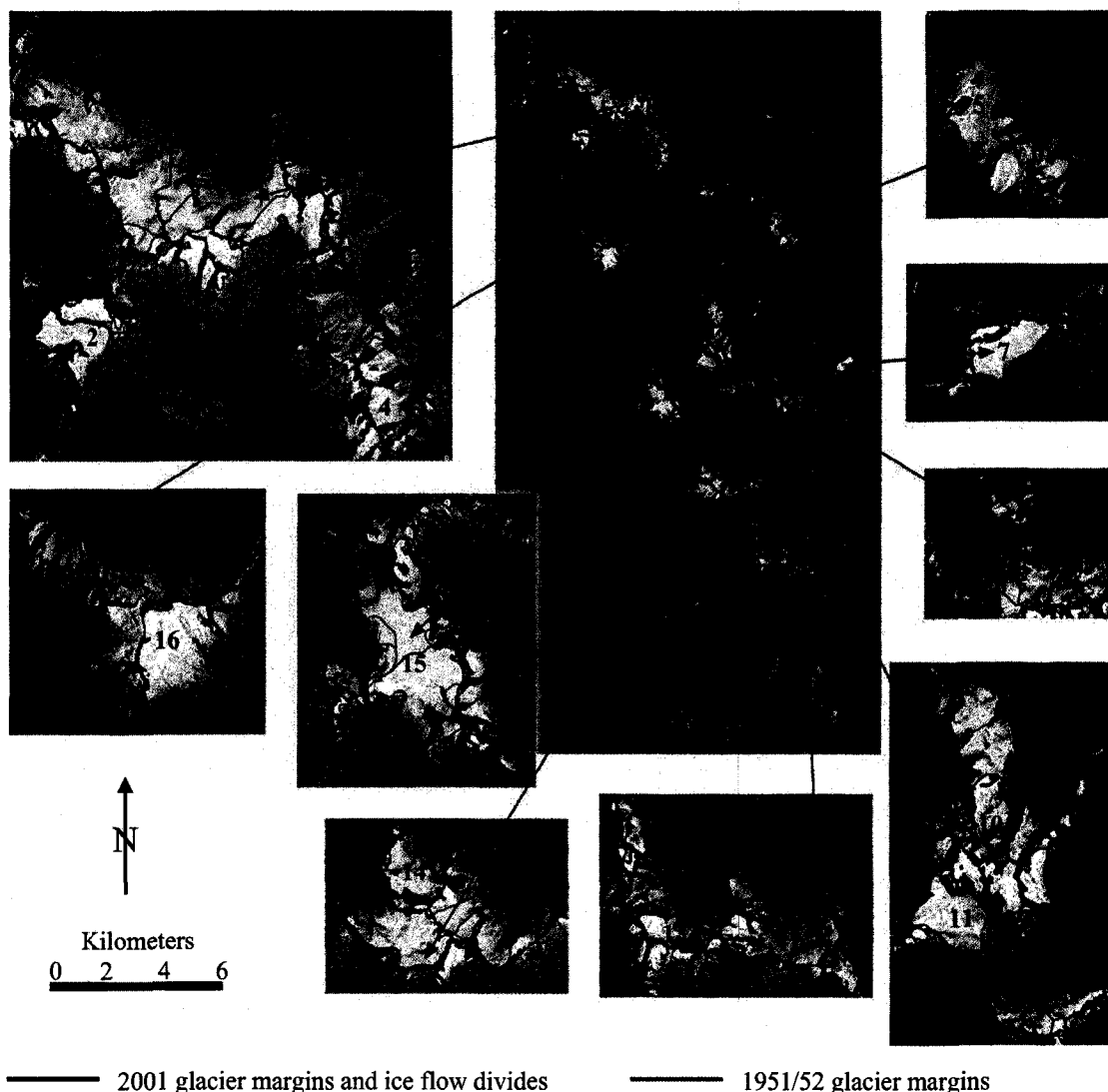


FIGURE 4.3. Net changes in extent of glaciers in the southern Purcell Mountains over the period 1951/52–2001 shown over the false color ETM+ imagery. 1: Conrad; 2: MacCarthy; 3: Vowell; 4: Bugaboo; 5: Catamount; 6: North Star; 7: Delphine; 8: Jumbo; 9: Commander; 10: Stockdale; 11: Starbird; 12: Toby; 13: Hamill; 14: Horseshoe; 15: Macbeth Icefield; and 16: The Four Squatters Glaciers.

remainder of the wastage here is due to the retreat of relatively small (i.e., $<2.0 \text{ km}^2$) glaciers in the Duncan River Basin that each lost between $2\text{--}10 \times 10^3 \text{ km}^3$ of ice. Due to the poor quality of the aerial photography covering these glaciers, however, the relative uncertainty of these estimates is high, and the values represent the loss associated with the maximum possible initial ice extent.

TABLE 4.3. Summary of net changes in area and volume (using values of 28.5 and 1.36 for c_0 and c_1 respectively) over the period 1951/52–2001 for large glaciers, or glaciers which have undergone substantial retreat in the southern Purcell Mountain region.

Glacier Name	GLIMS ID	2001 Area (km ²)	1951/52 Area (km ²)	Δ Area (km ²)	Δ Area (%)	2001 Vol. (km ³)	1951/52 Vol. (km ³)	Δ Vol. (km ³)
Conrad	G296930E50806[N]	18.6	18.9	-0.3	-1.8	1.52	1.55	-0.03
Starbird	G296698E50464[N]	10.0	11.7	-1.7	-14.6	0.65	0.81	-0.16
Vowell	G296802E50748[N]	7.5	8.4	-0.9	-11.1	0.44	0.52	-0.08
Toby	G296530E50216[N]	6.8	8.1	-1.3	-16.3	0.39	0.49	-0.10
Stockdale	G296681E50496[N]	5.5	6.3	-0.8	-12.4	0.29	0.35	-0.06
Jumbo	G296572E50421[N]	2.2	2.9	-0.7	-22.1	0.08	0.12	-0.04

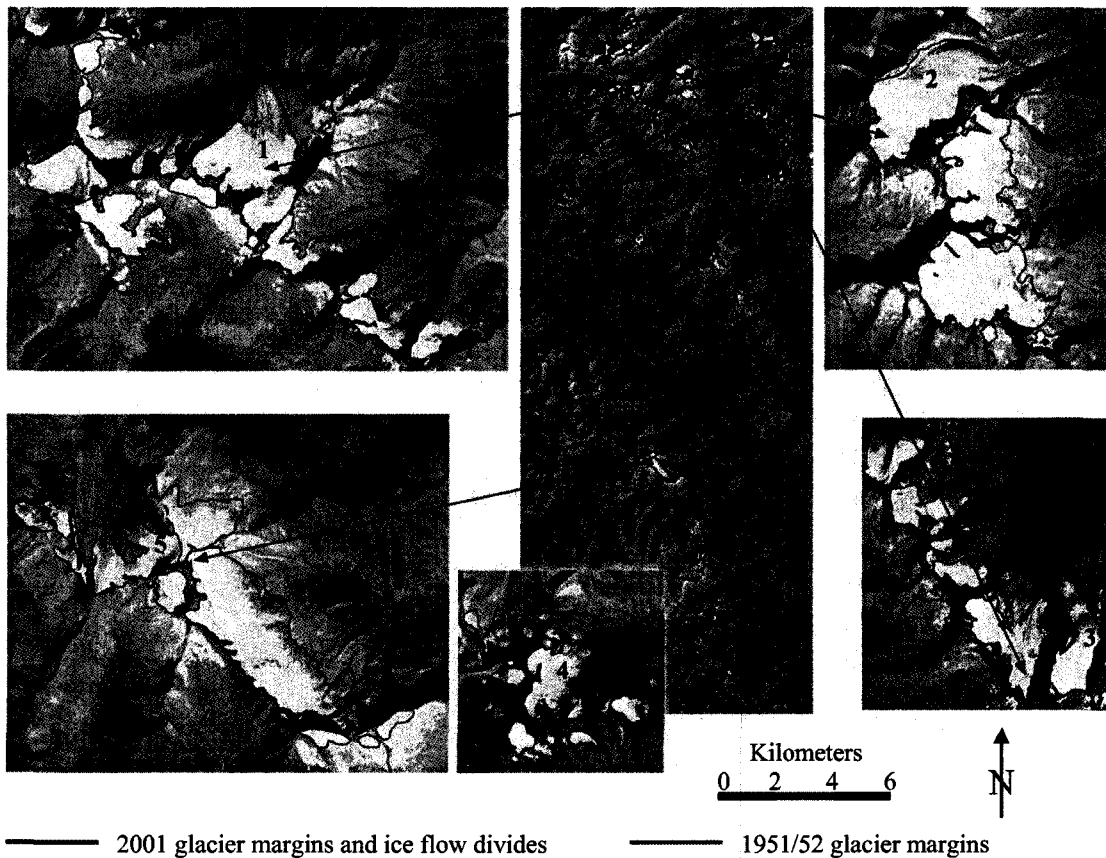
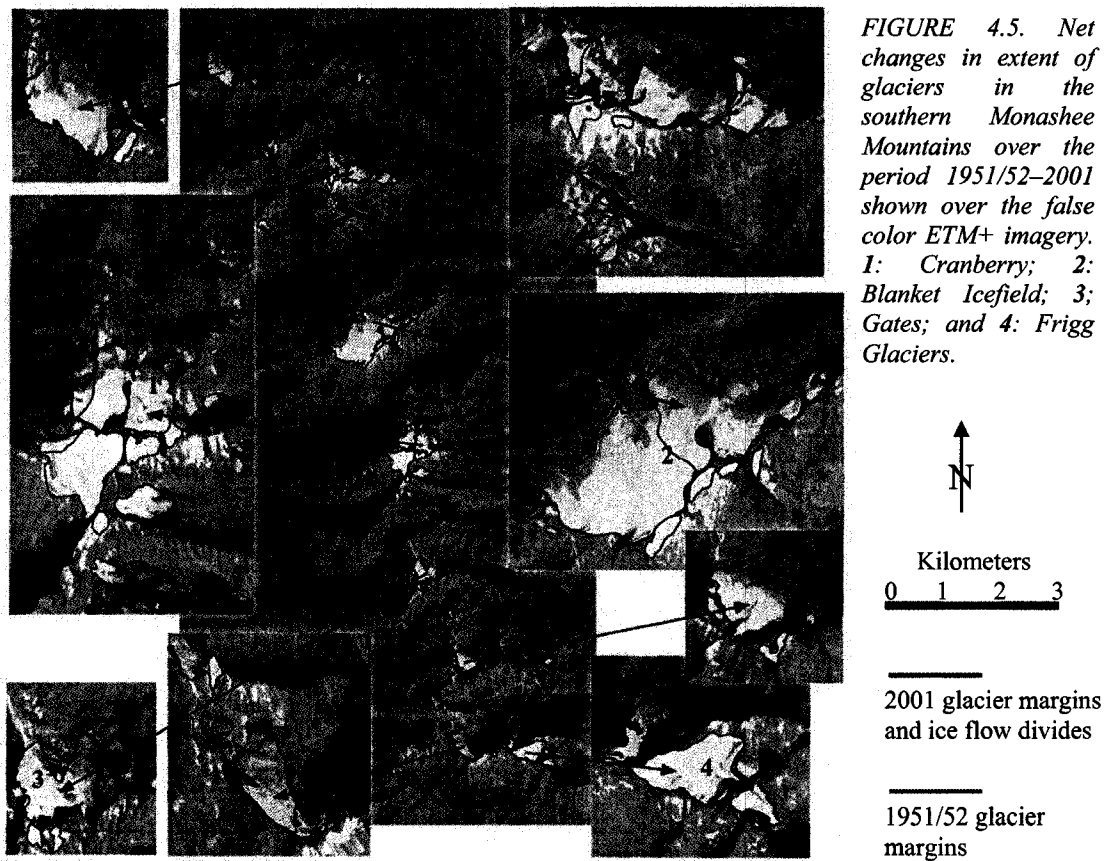


FIGURE 4.4. Net changes in extent of glaciers in the southern Selkirk Mountains over the period 1951/52–2001 shown over the false color ETM+ imagery. 1: Wrong; 2: Nemo; 3: Hatteras; 4: Spokane; and 5: Tenderfoot Glaciers.



The retreat of the Blanket Icefield in the Monashee Mountains resulted in an estimated ice volume loss of 0.06 km^3 , accounting for $\sim 25\%$ of the wastage in this mountain range. Significant losses were also estimated from the Cranberry and Gates Glaciers, and several other unnamed glaciers immediately north of the Blanket Icefield and west of the Frigg Glacier (Fig. 4.5). These glaciers all retreated substantially (i.e., from 500 m to over 1.5 km) and lost a significant portion of their ablation zone. The wastage of each of these glaciers was equal to $\sim 0.03 \text{ km}^3$ of ice, which taken together accounts for a further 40% of the ice loss here.

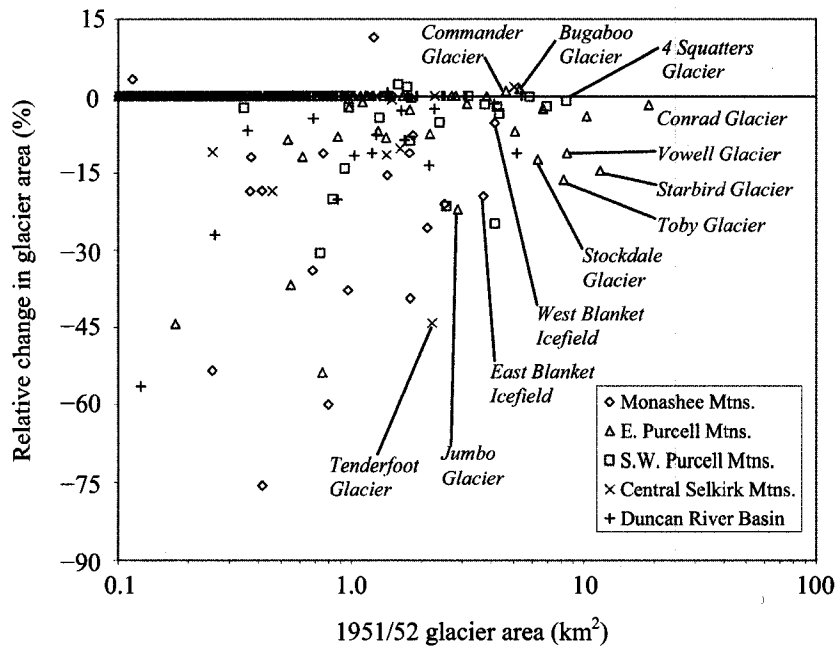


FIGURE 4.6. Plot of percentage area change of individual glaciers of the Columbia Mountains against their initial area.

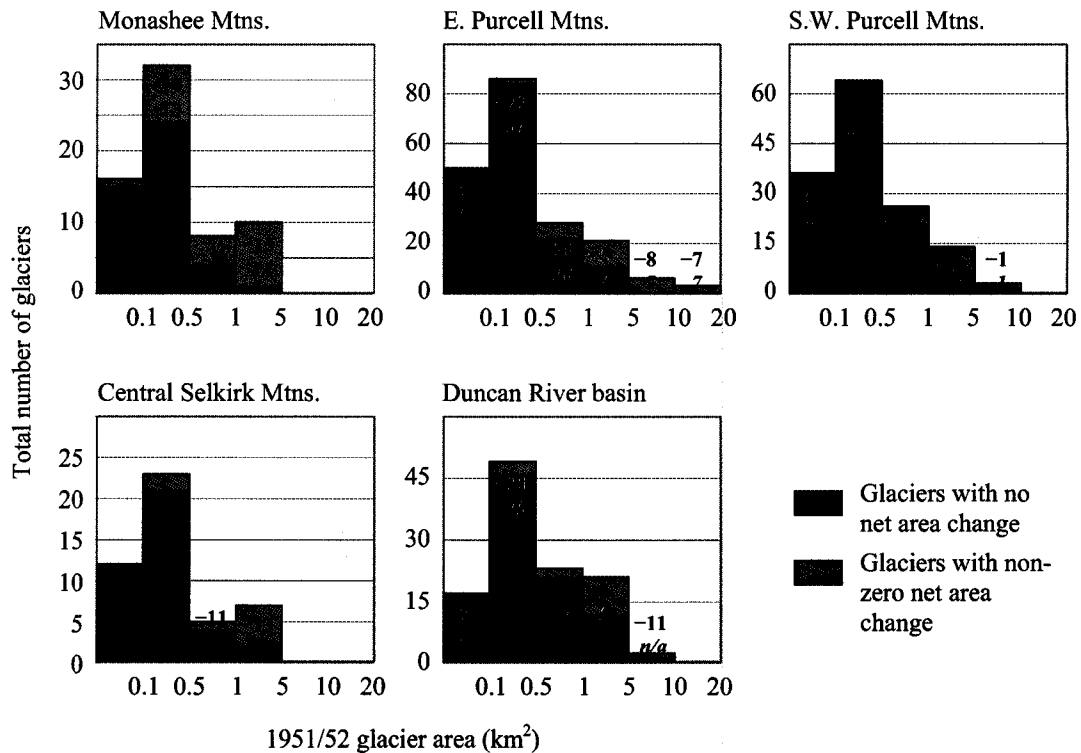


FIGURE 4.7. Histograms showing the size distribution of glaciers in individual sub-regions of the Columbia Mountains for 6 distinct size classes (<0.1, 0.1–0.5, 0.5–1.0, 1.0–5, 5–10, and 10–20 km²). The mean percentage area change over the study period (for those glaciers that have undergone a non-zero net change) is given in bold together with the standard deviation (in italics) for each class.

4.2.3 Coast Mountains

Within the Coast Mountains, there is a distinct regional pattern of variability in the changes of glacier area (Figs. 4.8, 4.9). Glaciers located furthest to the west have undergone little or no change, and the relative area change of glaciers becomes greater and progressively more variable towards the northeast. The glaciers within the Lower Southgate River basin, and the neighboring Orford and Tahumming River watersheds, provide a prime example of glaciers that are situated close to the coast and have undergone only very minor relative changes. Even large glaciers here, such as the Tahumming and Tavistock Glaciers, changed in area by less than -1% (Fig 4.9). Typical changes in area of -5 to -10% were observed for glaciers in the central ranges of the Coast Mountains, where many of the region's largest glaciers (i.e., $>20 \text{ km}^2$) are situated. Here even a very limited relative change in surface area may correspond to a substantial absolute change, ranging from -2 to greater than -7 km^2 for example. Further east, in watersheds such as the Bridge and Lillooet River basins, relative reductions in area range up to 40% or more in some cases. These glaciers are generally less than 5 km^2 in size, however, and for the most part, absolute changes are less significant than those of glaciers located further west. Very few glaciers in the Coast Mountains advanced over the study period, and as in other parts of the study area, most of the smallest glaciers have remained essentially unchanged.

The loss of ice volume in this region is primarily due to the substantial wastage of a very small proportion of the glaciers. Nearly 50% of the total ice volume loss is due to the retreat of the largest 1% of the glaciers in this region (Table 4.4). Most notable is the Bridge Glacier, which lost $\sim 1.4 \text{ km}^3$ of ice, and the Bishop and Elaho Glaciers, which both lost well over 0.5 km^3 during the study period. Other glaciers that underwent a considerable amount of retreat and volume loss include the Stanley Smith, Lillooet, and Squamish Glaciers. Unlike the other regions investigated in this study, the retreat of intermediate sized glaciers in the Coast Mountains has contributed significantly to the total ice wastage. Over 30% of the net ice loss here is from glaciers between 1 – 10 km^2 in initial size, which is due to the fact that 57 of the ~ 400 glaciers in this size class underwent a reduction in area of $>10\%$.

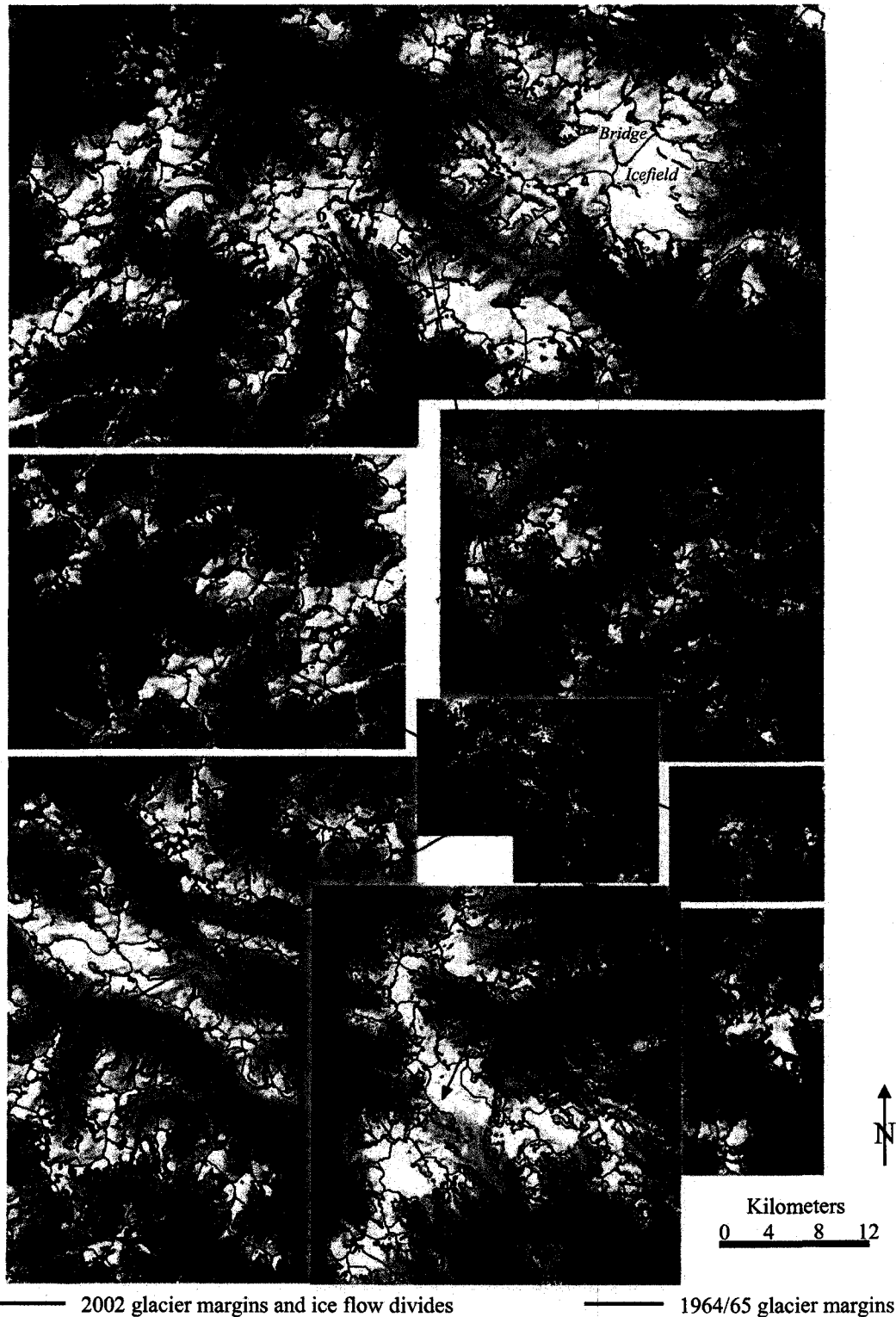


FIGURE 4.8. Net changes in extent of glaciers in the southern Coast Mountains over the period 1964/65–2002 shown over the false color ETM+ imagery. 1: Tavistock; 2: Filer; 3: Gilbert; 4: Falcon; 5: Compton; 6: Toba; 9: Bishop; 8: Lillooet; 9: Stanley Smith; 10: Bridge; 11: Place; 12: Weart; 13: Squamish; 14: Clendenning; 15: Elaho; 16: Meager Glaciers; and 17: Tahumming Glaciers.

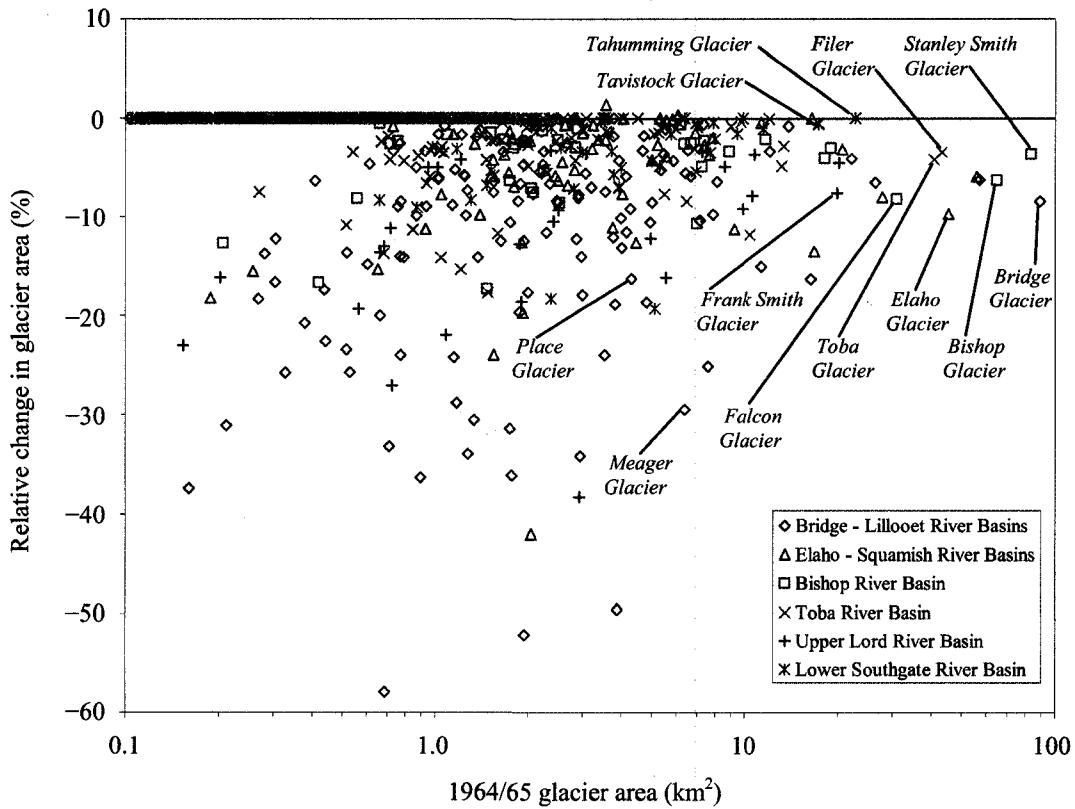


FIGURE 4.9. Plot of percentage area change of individual glaciers of the Coast Mountains against their initial area.

TABLE 4.4. Summary of net changes in area and volume (using values of 28.5 and 1.36 for c_0 and c_1 respectively) over the period 1965/65–2002 of the 10 largest glaciers in the Coast Mountain region (accounting for 48% of the total ice loss here).

Glacier Name	GLIMS ID	2002 Area (km ²)	1964/65 Area (km ²)	Δ Area (km ²)	Δ Area (%)	2002 Vol. (km ³)	1964/65 Vol. (km ³)	Δ Vol. (km ³)
Bridge	G303641E50822[N]	81.6	89.1	-7.5	-8.4	11.3	12.8	-1.4
Stanley Smith	G303798E50869[N]	80.3	83.3	-3.0	-3.6	11.1	11.7	-0.6
Bishop	G303876E50752[N]	60.5	64.6	-4.1	-6.3	7.6	8.3	-0.7
Lillooet	G303796E50746[N]	53.3	56.9	-3.5	-6.2	6.4	6.9	-0.6
Squamish	G303366E50356[N]	52.3	55.6	-3.3	-5.9	6.2	6.7	-0.5
Filer	G304316E50805[N]	41.6	43.0	-1.5	-3.4	4.5	4.7	-0.2
Elaho	G303773E50512[N]	40.8	45.2	-4.4	-9.7	4.4	5.1	-0.7
Toba	G304052E50798[N]	38.9	40.6	-1.7	-4.2	4.1	4.4	-0.2
Falcon	G304186E50821[N]	28.4	30.9	-2.5	-8.2	2.7	3.0	-0.3
Clendenning	G303889E50389[N]	25.4	27.6	-2.2	-8.0	2.3	2.6	-0.3

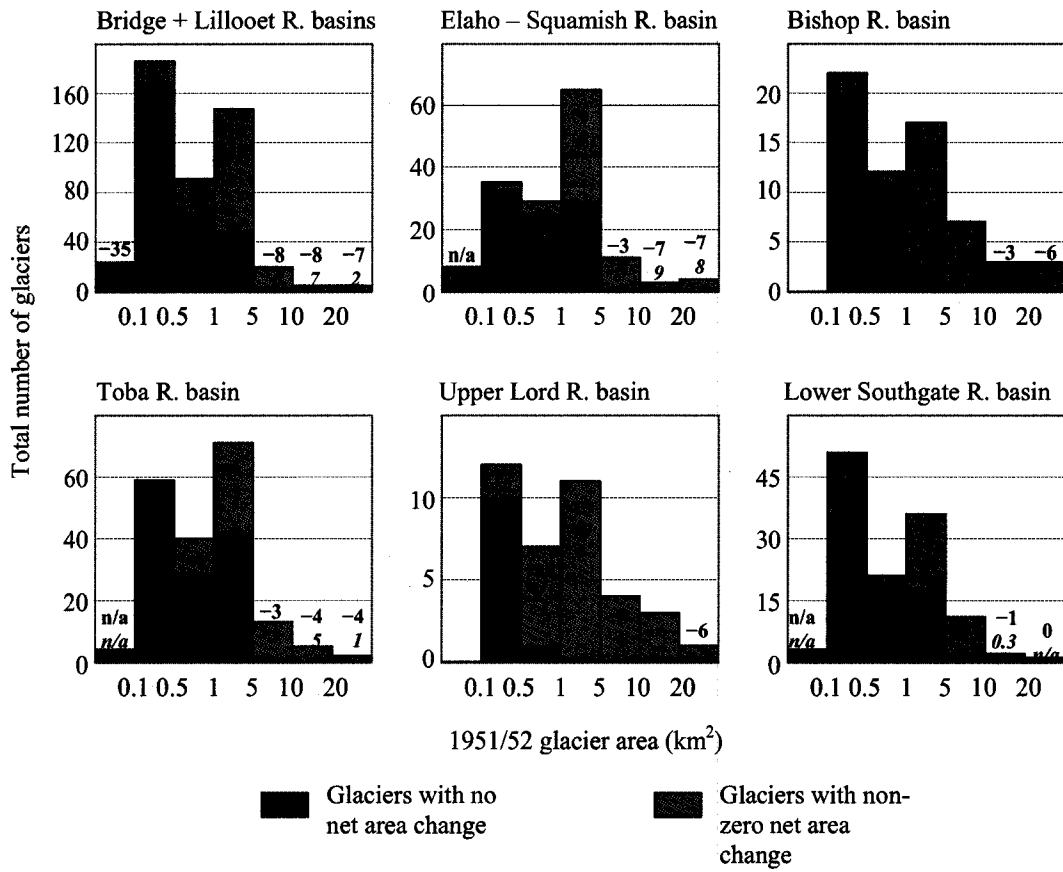


FIGURE 4.10. Histograms showing the size distribution of glaciers in individual drainage basins of the Coast Mountains for 7 distinct size classes (<0.1, 0.1–0.5, 0.5–1.0, 1.0–5, 5–10, 10–20, and >20 km²). The mean percentage area change over the study period (for those glaciers that have undergone a non-zero net change) is given in bold together with the standard deviation (in italics) for each class.

5. ANALYSIS AND DISCUSSION

Variability of changes in glacier area across the study area may be due to regional differences in climatic forcing or differences in the sensitivity of the mass balance and geometry of individual glaciers to climate change. The variability of observed changes between glaciers within specific localities more likely results strictly from differences in their intrinsic sensitivity to climate change, as these glaciers have probably been subject to similar climatic conditions. The sensitivity of these glaciers may vary due to differences in size, surface slope, aspect and shading, elevation, rate of mass turnover, mass balance gradient, and other morphologic and glaciological features unique to individual glaciers. To investigate the effects of such differences on the recent changes in surface area, a number of analyses were performed for glaciers in all parts of the study area. Detailed methodological considerations and results are discussed in the relevant sections.

5.1 REGIONAL CLIMATE TRENDS

5.1.1 Recent Temperature Trends

Mean annual temperatures across the southern Cordillera generally display a gradual increasing trend over the 20th century, rising by 1–2 °C during this time after accounting for the interannual variability (Fig 5.1). The temporal patterns of anomalies observed at stations throughout the region are broadly similar. The first three decades were characterized by relatively cool conditions, followed by a short period of slightly warmer temperatures. During the late-1940s and the 1950s, and again in the late 1960s and the 1970s, temperatures were cooler than usual. Over the final two decades, a gradual warming trend has occurred, and the warm conditions of the 1990s were unprecedented in terms of the climate of the past century at most stations.

More insight into the annual trends is obtained by examining the seasonal temperature trends (Figs. 5.2, 5.3, 5.4). It is clear that much of the interannual variability is due to the winter temperature series. Distinct trends, however, are not readily apparent

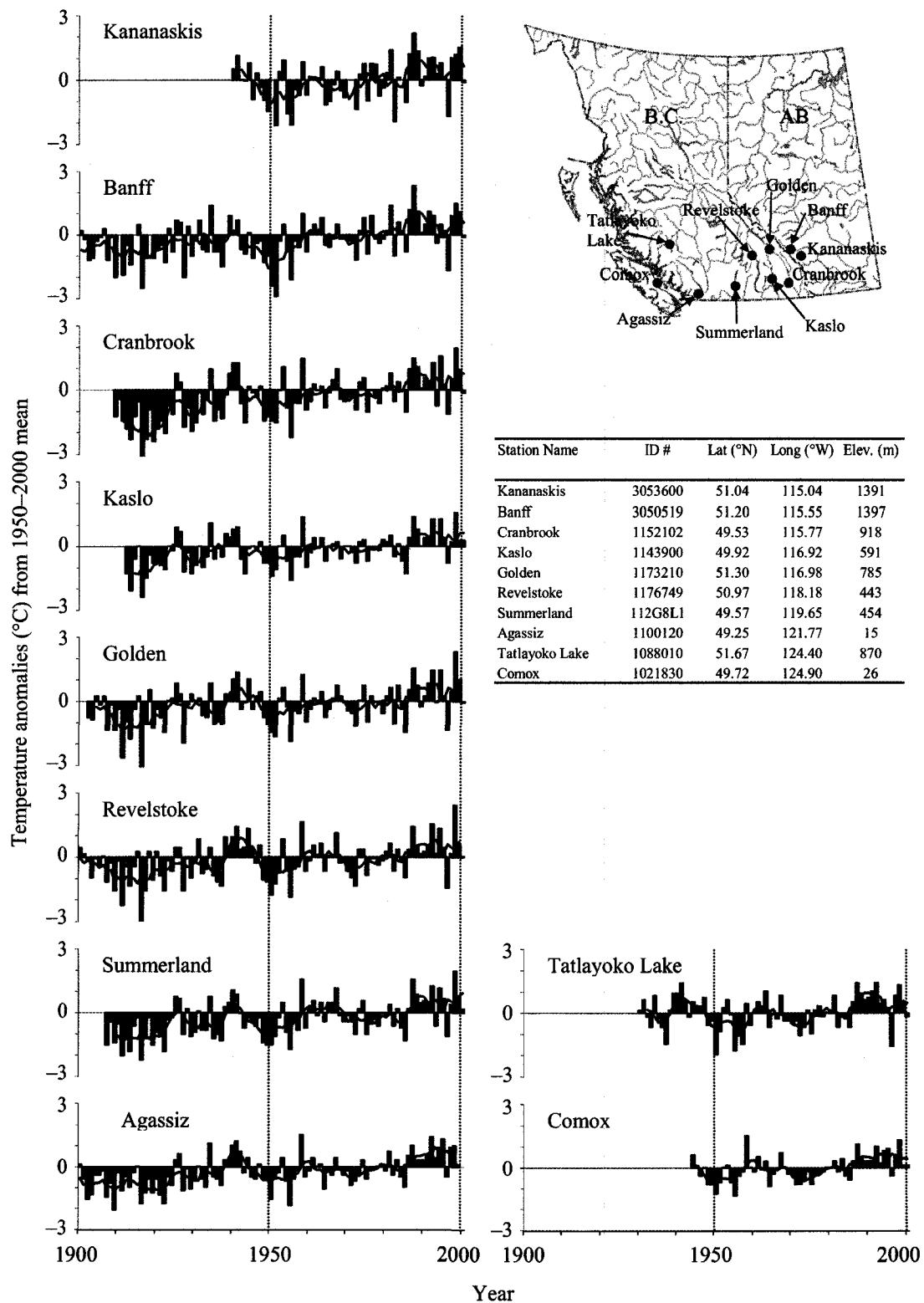


FIGURE 5.1. Local anomalies of mean annual temperature over the period 1900–2000. The anomalies are calculated with reference to the 1950–2000 mean, and are shown together with a 5-year filter. SOURCE: Historical Canadian Climate Dataset (HCCD); (<http://www.cccma.bc.ec.gc.ca/hccd/index.shtml>).

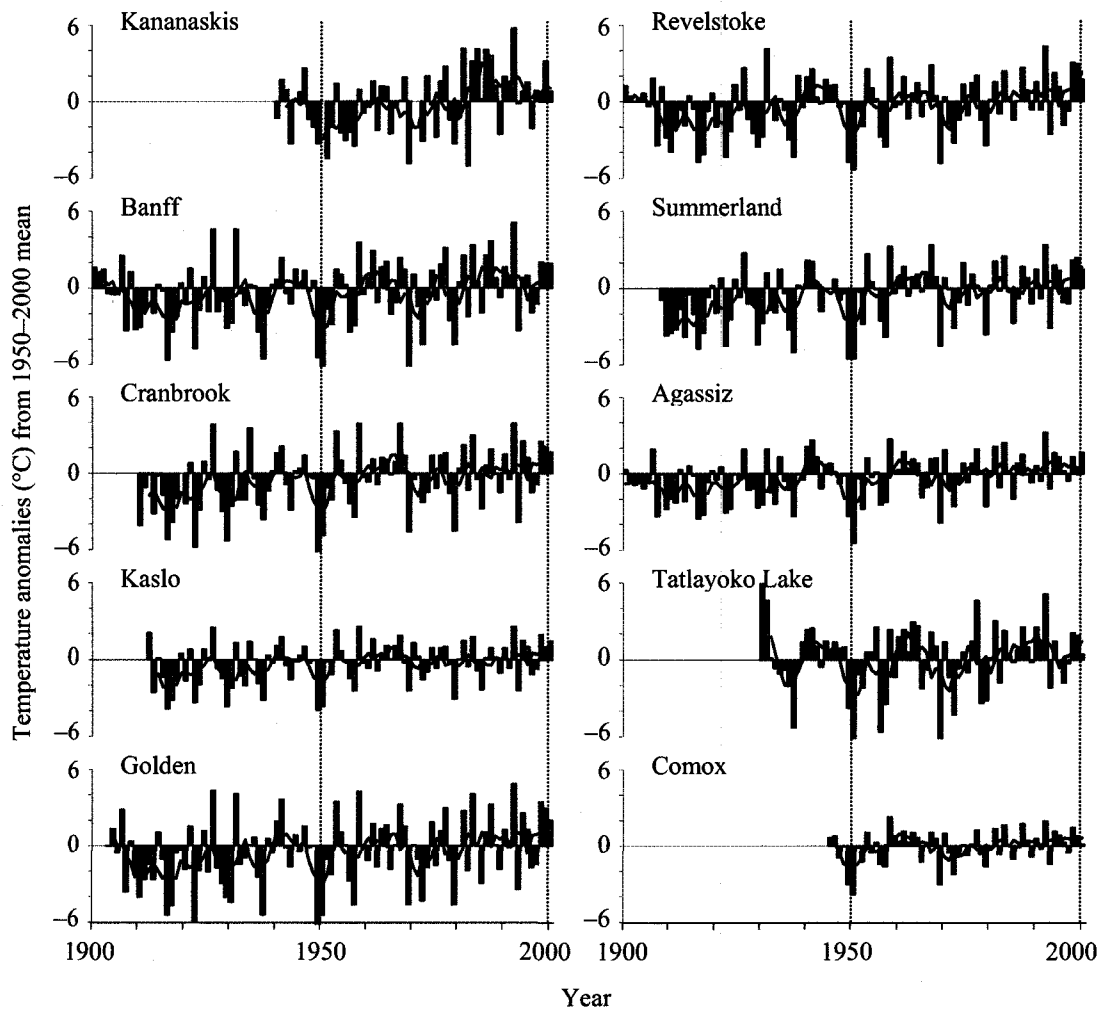


FIGURE 5.2. Local anomalies of mean winter (Dec 21–Mar 21) temperature over the period 1900–2000, shown together with a 5-year filter.

due to the considerable amount of year-to-year variability in the winter anomalies, and even the 5-year filters shown in figure 5.2 are strongly affected by this variability. Despite this, a significant winter warming trend over the period 1950–2000 is present at several stations, including Kananaskis, Golden, Revelstoke, and Agassiz (Table 5.1). The spring and summer series also display interannual variability, but the amplitude of the anomalies is considerably less than that of the winter series. The trends during the spring season closely parallel the annual trends, and an increase in temperature of between 1 and 3 °C is clear for all stations. The spring warming trends between 1950 and 2000 are significant at all stations, and range from 0.028 to 0.056 °C/year (Table

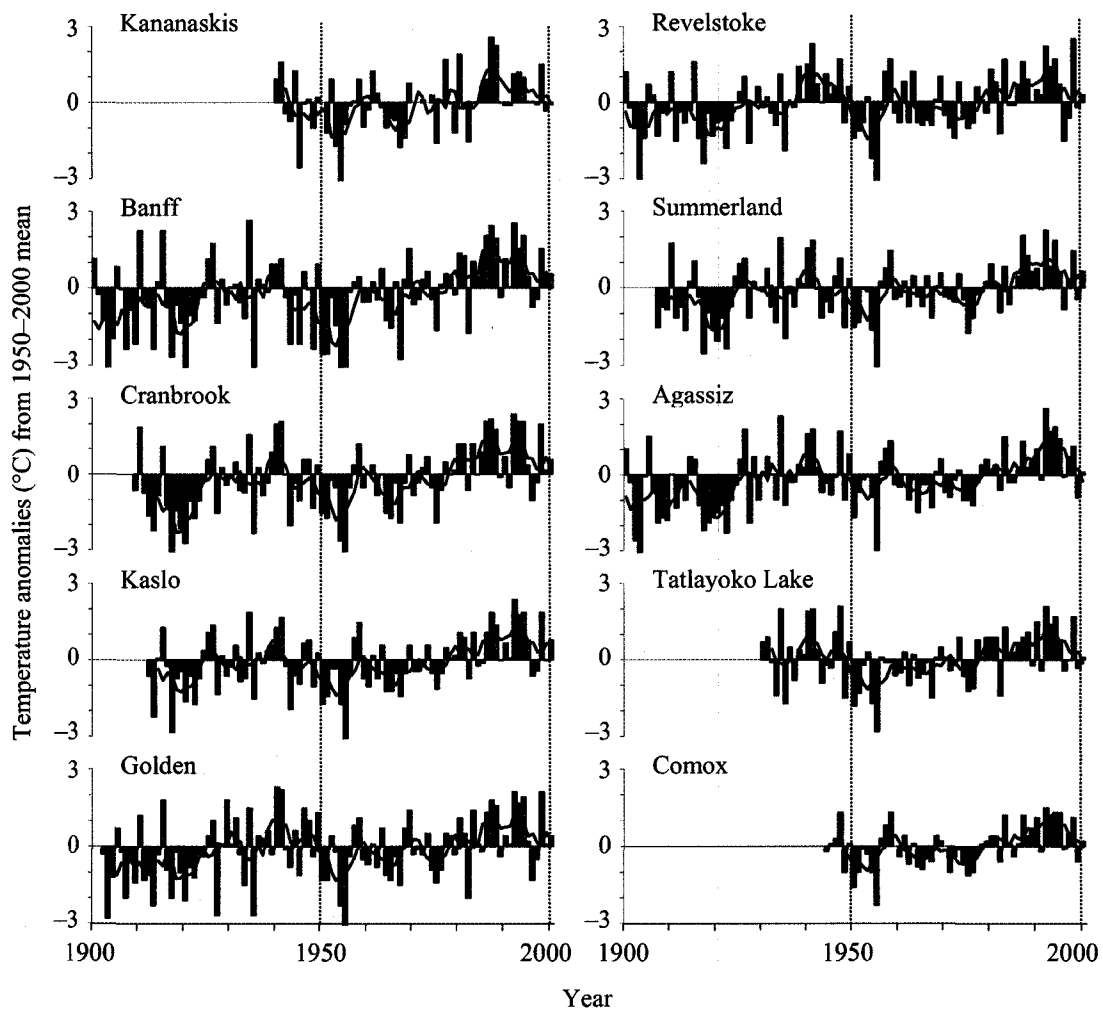


FIGURE 5.3. Local anomalies of mean spring (Mar 21–Jun 21) temperature over the period 1900–2000, shown together with a 5-year filter.

5.1). Strong warming trends during the summer are not apparent in most cases, however, and throughout the second half of the 20th century the temperature anomalies seem to more or less follow the mean of this period. Trends were also absent in the fall temperature series at these stations (not shown). This is consistent with the lack of any trend over the same period reported by Luckman (1998) for the Rocky Mountains as a whole. Together this suggests that the winter and spring seasons have had the most influence on the annual patterns shown in figure 5.1, while the other seasons have been much less influential and have likely only contributed, more or less, to the interannual variability present in the annual temperature series.

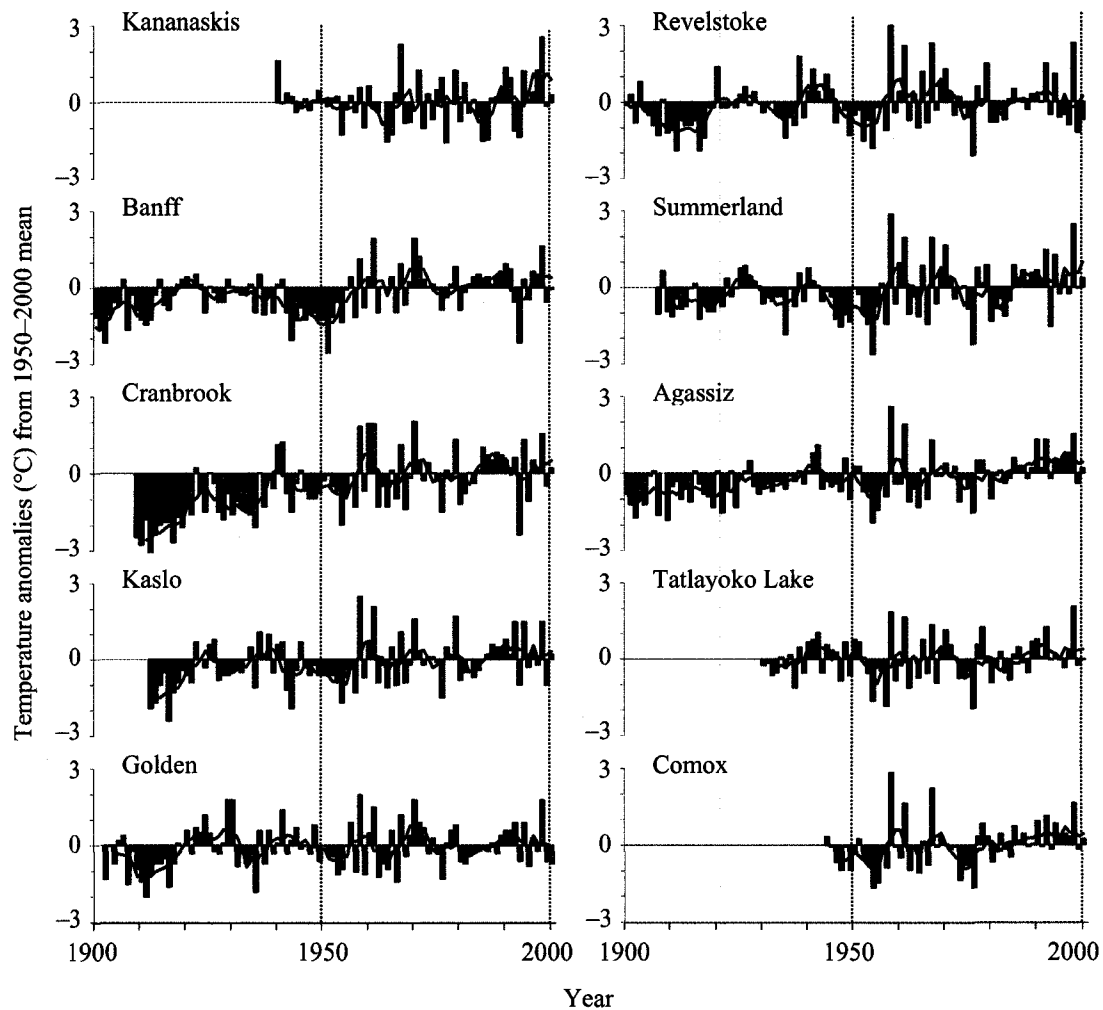


FIGURE 5.4. Local anomalies of mean summer (Jun 21–Sep 21) temperature over the period 1900–2000, shown together with a 5-year filter.

TABLE 5.1. Annual and seasonal temperature warming rates over the period 1950–2000 at individual stations. Significant trends (i.e., those that are significantly different from zero at the 95% confidence level) are shown in bold.

Station name	Annual		Winter		Spring		Summer	
	$^{\circ}\text{C}/\text{year}$	P-value	$^{\circ}\text{C}/\text{year}$	P-value	$^{\circ}\text{C}/\text{year}$	P-value	$^{\circ}\text{C}/\text{year}$	P-value
Kananaskis	0.027	0.009	0.068	0.011	0.032	0.02	0.009	0.155
Banff	0.03	<0.001	0.044	0.07	0.056	<0.001	0.016	0.057
Cranbrook	0.025	0.002	0.028	0.192	0.049	<0.001	0.012	0.2
Kaslo	0.021	0.001	0.014	0.327	0.043	<0.001	0.009	0.101
Golden	0.024	0.003	0.041	0.01	0.035	0.001	0.006	0.485
Revelstoke	0.024	0.003	0.04	0.048	0.033	0.002	0.003	0.746
Summerland	0.021	0.007	0.028	0.158	0.032	<0.001	0.017	0.115
Agassiz	0.025	<0.001	0.035	0.031	0.033	<0.001	0.019	0.021
Tatlayoko L.	0.024	0.001	0.046	0.066	0.037	<0.001	0.008	0.309
Comox	0.019	<0.001	0.019	0.107	0.028	<0.001	0.016	0.053

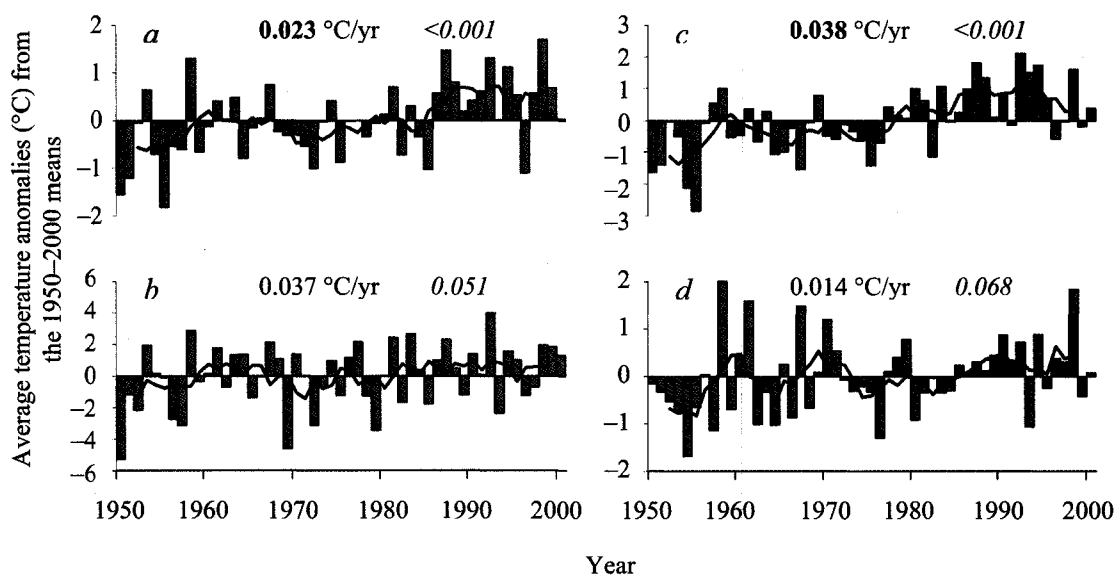


FIGURE 5.5. Regional anomalies of *a*: annual, *b*: winter, *c*: spring, and *d*: summer temperature over the period 1950–2000, shown together with a 5-year filter. The regional series were determined as the average of all the individual stations. Rates of warming are also shown together with their respective *P*-values (italics), and significant trends (at the 95% confidence level) are shown in bold.

Recent changes in temperature have been fairly uniform across the region and it is difficult from visual interpretation of the records to detect significant differences between various parts of the study area. To determine if there are significant regional differences in the trends, the annual and seasonal anomaly series for the period 1950–2000 at all stations were compared using principal component analysis. In each analysis only a single principal component (PC) emerged with an eigenvalue of greater than one, and the loadings of all of the series on this PC were very high (i.e., >0.90). This suggests that there is only one regional signal in the temperature dataset for this period (Fig 5.5).

5.1.2 Recent Precipitation Trends

Moore and McKendry (1996) found that the dominant climatological variable related to glacier mass balance in British Columbia is precipitation, which suggests that greater emphasis should be placed on the interpretation of regional precipitation measurements to explain the heterogeneity of recent glacier changes. The measurements of annual precipitation across the region display notable differences in terms of moisture receipt

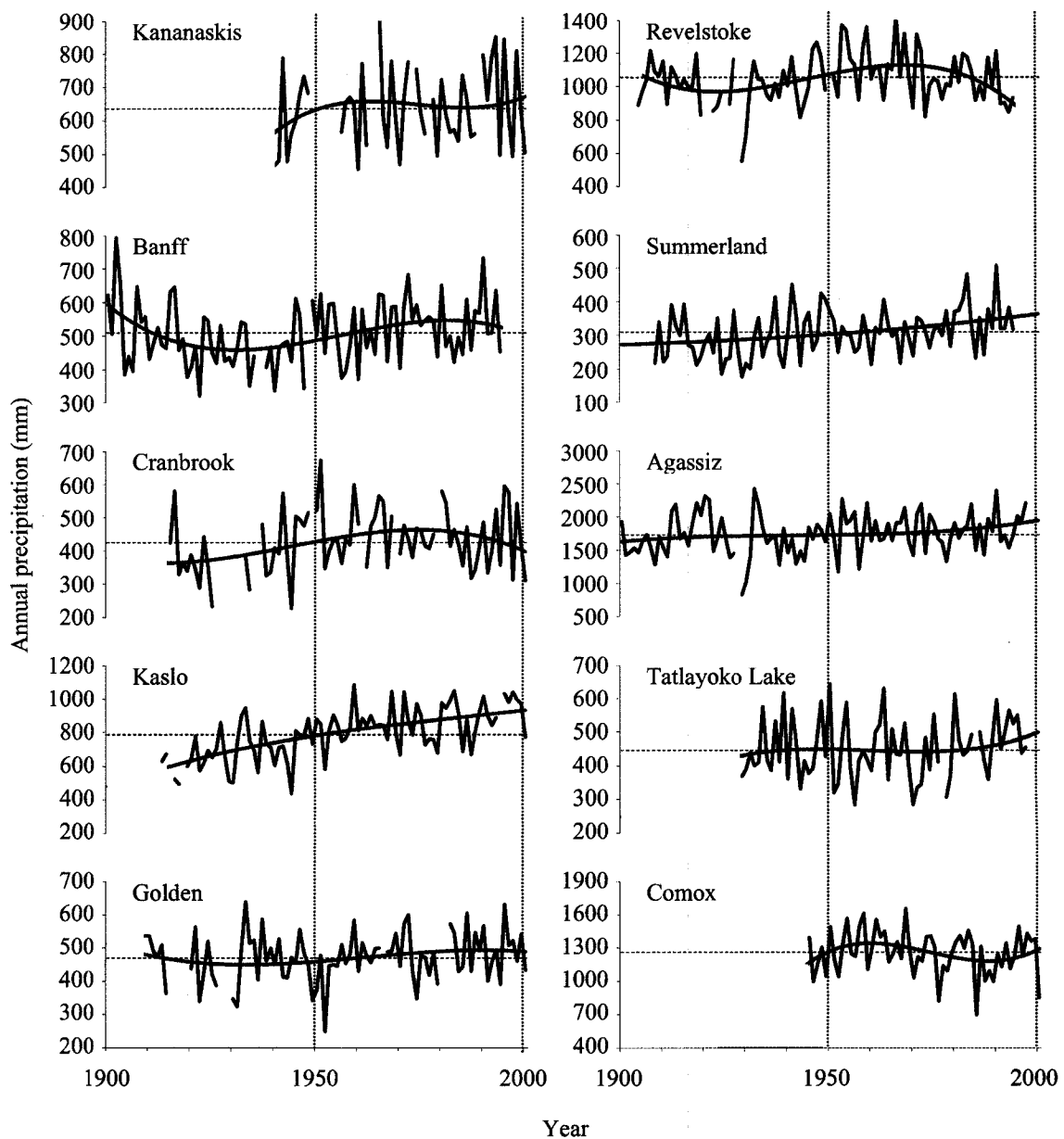


FIGURE 5.6. Annual precipitation records shown together with the mean over the period of record (horizontal dashed line) and a 3rd order polynomial trend line (solid curve). SOURCE: (HCCD).

between different localities (Fig. 5.6). Most obvious is the contrast between the maritime stations and those situated in a more continental setting. Comox and Agassiz have significantly higher mean annual precipitation, receiving more than double that of most other stations considered in this analysis. Tatlayoko Lake is relatively dry because it is located further inland to the east of the highest mountains in the coastal ranges. Average

precipitation increases again from the interior plateau (i.e., Summerland) into the Columbia Mountains, where stations such as Revelstoke and Kaslo have recorded an average of 800–1100 mm of annual precipitation during the study period. Further to the east, precipitation totals decline to between 400–700 mm at stations such as Cranbrook, Banff, and Kananaskis. It is important to note, however, that most of these stations are unlikely to be representative of the precipitation totals over a broader region because of the high degree of local variability and the strong dependence of precipitation on elevation and topography. Still, the changes in the time series of these measurements likely provide a fairly reliable index of the changes that have occurred at more regional scales.

Long term trends in annual precipitation can be seen at some of the stations examined here, but the large range of interannual variability partly masks these. At some stations, including as Golden, Agassiz, and Tatlayoko Lake, such trends are not present, and the polynomial trend lines remain close to the long-term mean or oscillate about it with relatively low amplitude. To determine if there is any regional coherence in the annual precipitation trends, the time series over the period 1950–2000 were standardized and were then compared using principal component analysis. The precipitation values at each station were standardized using the formula:

$$s = \frac{p - \bar{p}}{\sigma} \quad (3)$$

where p is the value for a particular year, and \bar{p} and σ are the 1950–2000 mean and standard deviation. Principal component analysis of the standardized series subsequently revealed three PCs with an eigenvalue of greater than one, with PC1, PC2, and PC3 explaining 42, 17, and 12% of the variance in the 10 series respectively. Figure 5.7 shows the time history of these PCs, and Table 5.2 gives the correlations between the component scores and the original standardized series at each station. From this analysis it appears that there is some degree of regional coherence, as many of the series are most highly correlated with PC1. Trends at stations in the Rockies and parts of the Columbia Mountains (i.e., Kananaskis, Banff, Cranbrook, and Kaslo) have a strong positive correlation with this component and a negative or very low correlation with the other two components. This is also true for Summerland, Agassiz, and Tatlayoko Lake in the

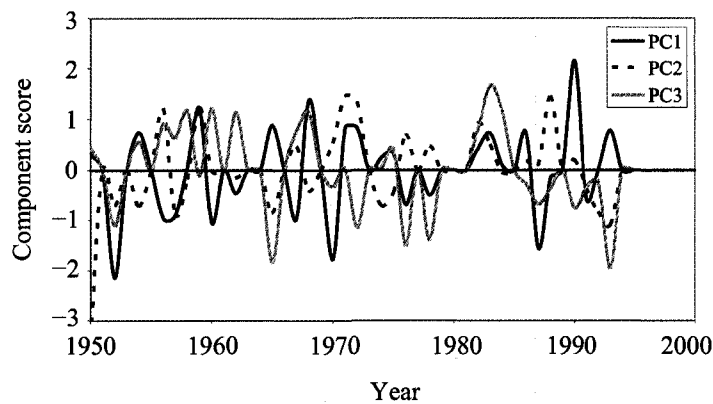


FIGURE 5.7. Time series of the component scores derived from the principal component analysis of the standardized annual precipitation series.

TABLE 5.2. Matrix of loadings for the three extracted components of the standardized annual precipitation series.

Station name	Component		
	1	2	3
Kananskis	0.654	-0.327	-0.463
Banff	0.772	0.042	-0.539
Cranbrook	0.694	-0.225	-0.128
Kaslo	0.868	0.083	0.304
Golden	0.600	0.615	0.011
Revelstoke	0.318	0.728	0.144
Summerland	0.693	0.057	-0.048
Agassiz	0.713	0.222	0.276
Tatlayoko L.	0.550	-0.660	0.095
Comox	0.401	-0.423	0.687

interior and coastal regions. Many stations show a period of drier than usual conditions during the 1930s and 1940s, followed by increasingly wet conditions through the late-1940s and the 1950s, as well as during parts of the 1960s and the early 1970s in a number of instances, and this is likely the regional signal represented by PC1. It is noted that most of the wetter periods coincide with periods of cooler than average annual and seasonal temperatures (see Fig 5.5), indicating that climatic conditions during these times were more favorable for the preservation and growth of glaciers. The remaining stations show trends that have a slight positive correlation with PC1, but that have greater loadings on the other components. Aside from a regional pattern, the correlations with the other components and the differing sign of the coefficients at many individual stations indicate a high degree of local variation in the annual precipitation series. Thus, although

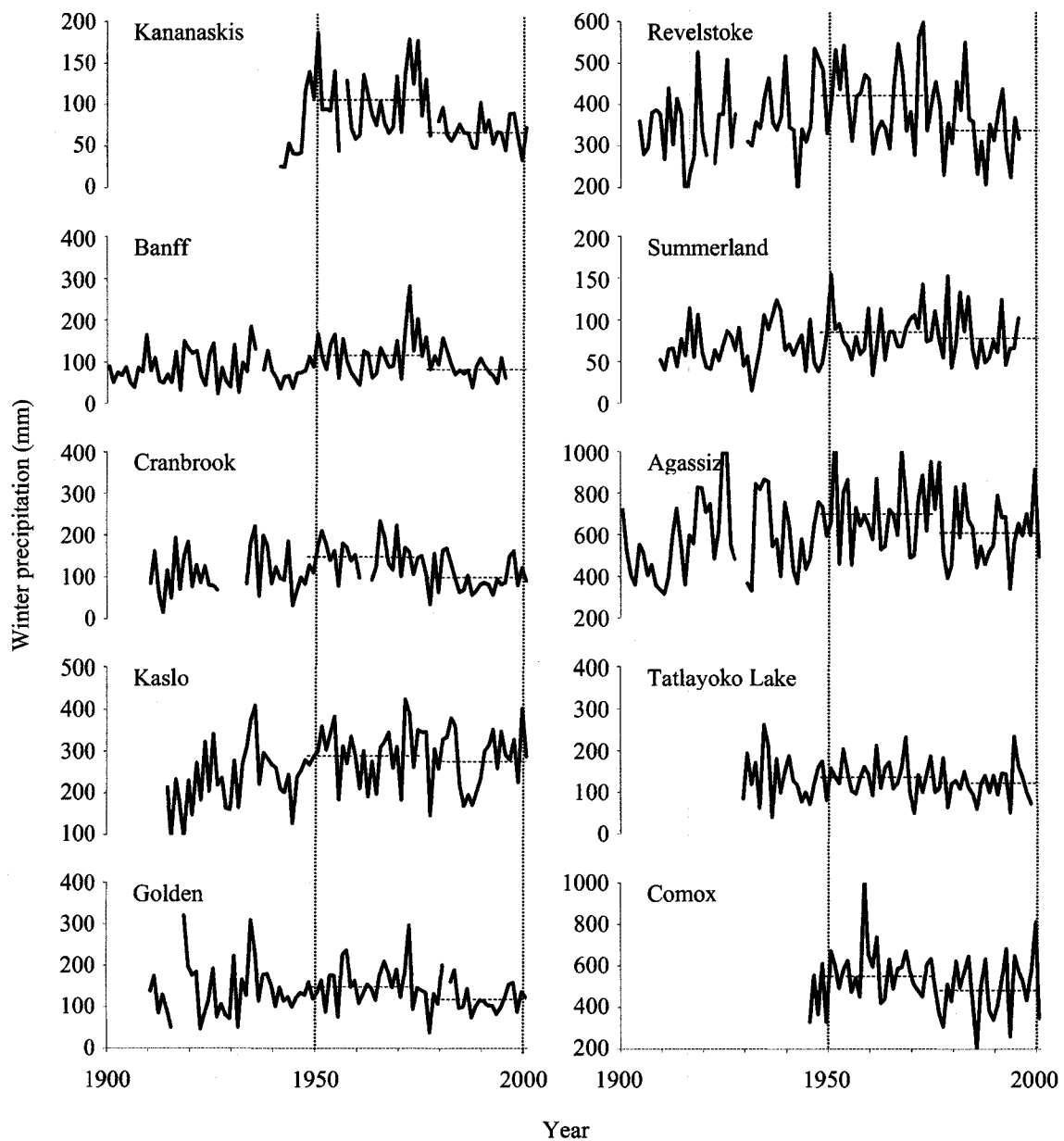


FIGURE 5.8. Winter (Dec 21–Mar 21) precipitation records shown together with the means over each of the periods 1947–1976 and 1977–2001 (horizontal dashed lines).

the trends are broadly similar in many respects, annual precipitation variations across the study area are influenced significantly by site-specific factors.

Regional differences in the local patterns of winter precipitation are likely more important than temperature or annual precipitation in terms of the disparate regional behavior of glaciers here, as changes during this time of year translate more or less into

changes in accumulation. The winter series are shown in figure 5.8, and the 1950–2000 series at each station were compared in the same manner as the annual series to determine if there is a single regional signal. The principal component analysis yielded two PCs with eigenvalues of greater than one, with PC1 and PC2 explaining 50 and 16% of the variance of the 10 series respectively. There is indeed a strong regional coherence as most of the series have a high positive correlation with PC1, and only two of the series (i.e., Tatlayoko Lake and Comox) show a stronger positive correlation with PC2 (Table 5.3). The most distinct feature that is apparent in the time series of the component scores of PC1 is the shift to primarily negative values beginning in 1976. This reflects the PDO regime shift, and the strong positive correlation of most of the series with PC1 indicates that the PDO signal has been manifested in the winter precipitation across the entire study area.

Seasonal mass balance data for Place and Peyto Glaciers confirm that the ‘step-change’ in winter accumulation that took place between 1976–77 as a result of the PDO regime shift has had a much more significant influence on the annual mass balance than variations in summer temperature (Demuth and Keller, 2000; Moore and Demuth, 2001). It may be that local differences in the magnitude of this change have contributed to the observed differences in glacier response in various parts of the study area. To gain more insight into this possibility, the pre- and post-1976 mean winter precipitation totals at each of the climate stations were compared (Fig 5.8, Table 5.4). These means were taken over the period of 1947–1976, which corresponds to the negative PDO regime identified

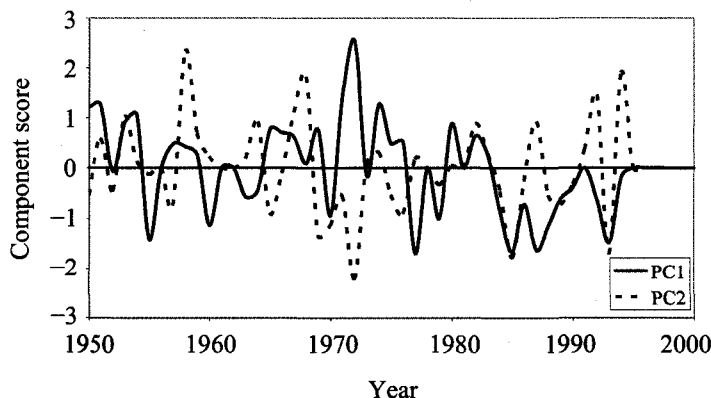


FIGURE 5.9. Time series of the component scores derived from the principal component analysis of the standardized winter precipitation series.

TABLE 5.3. Matrix of loadings for the two extracted components of the standardized winter precipitation series.

Station name	Component	
	1	2
Kananskis	0.712	-0.379
Banff	0.802	-0.318
Cranbrook	0.781	-0.143
Kaslo	0.841	0.156
Golden	0.817	-0.162
Revelstoke	0.869	0.066
Summerland	0.596	-0.190
Agassiz	0.737	0.274
Tatlayoko L.	0.264	0.762
Comox	0.394	0.735

TABLE 5.4. Changes in winter precipitation associated with the 1976–77 PDO regime shift. All the changes, with the exception of that at Summerland, are significant at the 95% confidence level.

Station name	1947–	1977–	Change (mm)	Change (%)
	1976 mean (mm)	2001 mean (mm)		
Kananaskis	107	67	-40	-38
Banff	117	87	-30	-26
Cranbrook	145	96	-49	-34
Kaslo	298	271	-26	-9
Golden	156	118	-37	-24
Revelstoke	419	339	-80	-19
Summerland	82	79	-3	-4
Agassiz	712	603	-109	-15
Tatlayoko Lake	138	115	-22	-16
Comox	557	487	-70	-13

TABLE 5.5. Changes in spring snowpack depth measured at snow survey locations across the region associated with the 1976–77 PDO regime shift. All changes are significant at the 95% confidence level. SOURCE: Alberta Environment Water Supply Outlook: <http://www3.gov.ab.ca/env/water/WS/WaterSupply/Index.html>; and B.C. Ministry of Environment River Forecast Center: http://www.env.gov.bc.ca/rfc/river_forecast/data.htm.

Mountain range	Snow survey location (lat/long)	Elev. (m)	1967-76	1977-2001	Absolute change (mm)	Mean St. Dev.	Relative change (%)	Mean St. Dev.
			mean s.w.e.	mean s.w.e.				
Coast	50° 41'; 122° 36'	1800	737	563	-174		-23	
	50° 32'; 122° 56'	1680	1435	1143	-292		-20	
	49° 23'; 123° 05'	1100	1815	1039	-776	-335	-43	-30
	51° 36'; 124° 20'	1700	314	215	-99	304	-32	10
Monashee	51° 02'; 118° 09'	1830	1495	1231	-264		-18	
	50° 04'; 118° 21'	1620	584	469	-115	-189	-20	-21
	50° 12'; 118° 02'	1480	731	542	-189	74	-26	4
Selkirk	51° 15'; 117° 30'	1250	850	655	-195		-23	
	51° 14'; 117° 42'	1870	1485	1280	-205		-14	
	50° 26'; 117° 42'	1800	1464	1270	-194	-206	-13	-17
	50° 43'; 117° 12'	1860	1303	1071	-232	18	-18	5
Purcell	50° 38'; 116° 56'	2030	1068	905	-163		-15	
	50° 58'; 116° 56'	1520	624	334	-290	-234	-46	-29
	49° 37'; 116° 39'	1910	1003	753	-250	65	-25	16
Rocky	50° 23'; 114° 38'	1493	529	430	-99		-19	
	50° 54'; 115° 37'	2230	695	469	-226	-143	-32	-25
	50° 32'; 115° 07'	1750	457	352	-105	72	-23	7

by Mantua et al. (1997), and the period of 1977–2001, corresponding to the recent shift to warm phase PDO conditions. In addition, the average depths (measured as mm of snow

water equivalent [s.w.e.]) of the spring snowpack over the 10-year period prior to 1976 were compared with those for the period of 1977–2001 at 17 manual snow survey and automatic snow pillow sites across the region (Table 5.5). The 10-year period prior to 1976 was the longest possible period that could be considered due to the short duration of records at most of the survey locations.

In general, from Table 5.4 it appears that the greatest relative reductions in winter precipitation occurred in the Rocky and eastern Columbia Mountains, while relative reductions in the Coast Mountains were more limited. This is not supported by the data in Table 5.5, however, which show a large amount of variability in relative reductions in spring snowpack depth within individual mountain ranges. What is clear from each of these datasets is that most of the greatest absolute reductions in winter precipitation and spring snowpack depths occurred in localities with a wetter climate. This suggests that the glaciers within the highest precipitation regimes have undergone the largest reductions in winter accumulation. This pattern is most notable in the western ranges of the Coast Mountains, where snowpack reductions of 300–800 mm in mean s.w.e. have been observed. A more detailed assessment of the regional variability of winter precipitation is not possible due to the low density of stations with long term records throughout the study area.

5.1.3 Glacier – Climate Interactions

A recent warming trend has been observed in all parts of the study area, with the greatest increases in temperature occurring during the spring, and to a lesser extent, the winter seasons. Warmer conditions during the spring may imply that in recent decades, there has been an earlier onset of melt on most glaciers. This would likely result in an earlier disappearance of the snowpack over the ablation zone, exposing ice with a lower albedo, and would thereby increase melt rates throughout the summer season. The reductions in winter snowfall observed across the study area would tend to reinforce this effect. Warmer temperatures during the winter season may also have affected the mass balance of some glaciers, particularly the larger glaciers in the coastal region that extend to very low elevations. This is because warming at this time could lead to a significant change in

the fraction of precipitation falling as snow, and because melting may occur throughout much of the year on the tongues of such glaciers.

More widespread retreat of glaciers would be expected in the Coast Mountains given a uniform change in climate across the study area, as glaciers with a large mass turnover are inherently more sensitive, and the sensitivity of mass balance to changes in temperature and precipitation increases dramatically with the amount of annual precipitation (Meier, 1984; Oerlemans, 1992; Oerlemans and Fortuin, 1992; Oerlemans and Reichert, 2000). This is primarily because albedo feedbacks are more significant when the snowpack is thicker and lasts longer, and because, as mentioned above, the change in the fraction of precipitation falling as snow with a change in temperature is large. Climatic changes have not been uniform across the region, however, as greater reductions in winter precipitation have occurred in the wetter localities. Together this helps to partly explain the substantial retreat of many of these glaciers and the large ice loss that has been observed in the coastal region.

Glaciers in the Columbia Mountains are also situated within a rather wet climatic setting that is somewhat maritime in nature. Some of the glaciers here, especially those within the Monashee Mountains, descend to elevations similar to the large glaciers in the coastal region (i.e., <2000 m), and may therefore be sensitive to winter warming. Large reductions in winter precipitation and spring snowpack depth associated with the recent PDO shift have been observed at some localities here, and thus many of these glaciers may have undergone a similar response to those in the Coast Mountains.

The glaciers of the Rocky Mountains are situated within a much more continental climate regime. Changes in winter temperature have likely had less of an effect on the mass balance and terminal response of glaciers in the Rocky Mountains, since these glaciers are at higher elevations in a cooler climatic setting. Bitz and Battisti (1999) and Hodge et al. (1998) noted that glaciers in an interior, continental regime have a net balance that is driven more by the summer ablation than the winter accumulation. Ablation rates in this region during the summer have likely been affected significantly by the rise in spring temperatures and the post-1976 decline in winter precipitation as a result of albedo feedbacks. The lack of any clear recent trends in summer temperatures here suggests that this decline has been the primary mechanism affecting the summer

balance of these glaciers. Finally, because many of the glaciers here have a very high mean elevation (i.e., 2600–2800 m), changes in precipitation that have occurred outside the winter months have likely affected the annual balance to some degree, as precipitation at these times may still fall as snow over much of the glacier. Drier annual conditions were observed during the late-1950s – early-1960s, and again in the 1980s at Kananaskis and Banff. These periods coincided with periods of warmer temperatures in all seasons, as well as relatively lower winter precipitation, and therefore during these times the mass balance of most glaciers was probably characterized as strongly negative.

These generalizations concerning the linkage between regional climate trends and the behavior of glaciers are not useful for explaining the heterogeneity of changes in glacier extent at local scales. Aside from the maritime to continental gradient in climatic conditions across the study area, it is even difficult to interpret regional variations in glacier changes in terms of differences in local climate. Much of the variation is likely explained by complex local climatic conditions that cannot be resolved with the existing network of observation stations. Furthermore, differences in the morphologic and glaciological characteristics of individual glaciers make it difficult to generalize how glaciers in a region have responded to climatic changes. Such differences between individual glaciers at local scales are therefore considered in the following sections in an attempt to explain some of the observed variability.

5.2 RESPONSE TIME

The response time of a glacier is a measure of the time it takes to complete its adjustment to a climatic change, and is of fundamental importance when interpreting the relationship between past glacier variations and climatic history. Glacier response time is best represented by the volume time scale, which is the length of time over which ice is added to or removed from a glacier until it reaches a new state of equilibrium following a sudden and permanent change in its mass balance. Johannesson et al. (1989) showed that this time scale can be expressed under fairly general conditions by:

$$t_v = \frac{H}{-b_t}, \quad (4)$$

where H is a thickness scale of the glacier and b_t is the mass balance rate at the glacier terminus. The time scale of (4) provides an estimate of the duration of the glacier's response to a change in climate, but it does not incorporate all of the dynamics of a glacier, and is therefore only useful as an order of magnitude estimate. For example, (4) does not take into account the positive mass balance feedback that occurs as a result of the fact that the mass balance of glaciers increases/decreases with increasing/decreasing elevation. A negative mass balance perturbation will lead to a decrease in the surface elevation of the glacier, which will in turn result in a further decrease in mass balance. The final mass balance perturbation may be much larger than the initial one, and the change in volume of the glacier will therefore be greater, leading to an increase in the volume time scale relative to the value determined using (4). Nevertheless, this estimate of the time scale can be used to provide simple physical insight into the complicated response of a glacier, and may serve as a useful order of magnitude index of the relative sensitivity of individual glaciers to climate change.

Response times were estimated for individual glaciers in all regions of the study using (4) with H taken as the mean ice thickness. Paterson (1994) suggested that is possible to estimate mean glacier thickness by using glacier slope and an assumed constant shear stress for an infinitely-wide glacier with laminar flow. This follows from the relation:

$$\tau = \rho g H \sin \alpha \quad (5)$$

where τ is the basal shear stress, ρ is the density of ice, g is the acceleration of gravity, and α is the surface slope. H was estimated from this relation assuming a constant shear stress of 1 bar (1 bar = 10^5 Pascals) for each glacier, and using the mean slope measured over the entire length of the individual glaciers. The melt rate at the terminus in (4) was estimated with a positive degree-day model (Hock, 2003);

$$\sum_{i=1}^n M = \text{DDF} \cdot \sum_{i=1}^n T^+ \Delta t \quad (6)$$

where the amount of melt M (mm) during a period of n time intervals, Δt (d), is related to the sum of positive daily air temperatures in each time interval, T^+ ($^{\circ}\text{C}$), multiplied by a degree-day factor (DDF). DDF's of 8.0 and 4.5 $\text{mm d}^{-1} \text{ } ^{\circ}\text{C}^{-1}$ were used for snow and ice respectively (Braithwaite and Zhang, 1999), with the model first used to simulate

snowmelt until depletion of the spring snowpack had occurred, and then to simulate the ablation of ice through the remainder of the summer. Average monthly temperature series from Environment Canada stations (HCCD: <http://www.cccma.bc.ec.gc.ca/hccd/index.shtml>) were extrapolated to the elevation of each individual glacier terminus using a lapse rate of $6.5 \times 10^{-3} \text{ }^\circ\text{C m}^{-1}$. These series were used together with spring snowpack data from Alberta Environment (<http://www3.gov.ab.ca/env/water/WS/WaterSupply/Index.html>) and the B.C. Ministry of Environment (<http://www.env.gov.bc.ca/rfc/river/forecast/data.htm>) as inputs to the model.

Since (4) may potentially underestimate the actual time for the glacier to adjust to a change in climate, another formulation of glacier response time (Harrison et al., 2001) was used for comparison:

$$\tau_v = \frac{1}{\frac{-b_t}{H} - G_e} \quad (7)$$

H and b_t have the same meaning as in (4), and G_e is the gradient of the specific balance rate with elevation. τ_v accounts for the effect of the changing surface elevation of the glacier on the balance rate via the G_e term in the denominator of (7). This formulation was applied to 6 glaciers with mass balance – elevation records (i.e., Bridge, Place, and Sentinel Glaciers in the Coast Mountains, and Peyto, Ram, and Haig Glaciers in the Rockies).

Theoretical response times on the order of 10–40 years are predicted by (4) for the glaciers in all regions of the study. Including mass balance gradients in the formulation of τ_v does not result in significantly longer response times. These glaciers have a typical ablation rate of 2–4 m a^{-1} near the terminus, mean thickness of 30–150 m, and specific balance gradient of $4\text{--}10 \times 10^{-3} \text{ m W.E. m}^{-1}$. Therefore, the G_e term in (7) is roughly an order of magnitude smaller than $-b_t/H$, and τ_v is only several years longer than t_v so that the estimates of response time are not significantly affected.

The estimates of glacier response time do not show a strong relationship with the observed differences in relative area change between individual glaciers in any part of the study area (not shown). Response times were also estimated using a value of H that was based on the slope measured in the lower ablation zone over a distance of 1 km up from the terminus of the individual glaciers. This value of the slope was not influenced by the

presence of steep upper slopes or plateaus that occur on many glaciers, and therefore seemed to be more representative of the region on the glaciers where changes were observed to take place. Based on these estimates of slope and mean thickness, measurements of the percentage area change of individual glaciers show a negative relationship with the calculated response times in all regions (Fig 5.10). All of the glaciers that have undergone a net advance over the study period have a typical response time of less than 15 years. Glaciers that have undergone larger relative reductions in area (i.e., >10%) have response times of 20–50 years or more, but the variability in relative area changes becomes much greater for glaciers with a longer response time. This is presumably due to the influence of other site-specific factors that affect the sensitivity of the glacier to climatic change.

Major glaciers that have undergone only minor area reductions or that have advanced over the study period have very steep fronts with extensive crevassing. This is an indication that longitudinal strain rates and glacier velocity are relatively high, and therefore such glaciers can react faster to changing climatic conditions (Bahr et al., 1998; Paterson, 1994). The observed behavior of these glaciers seems counter-intuitive, as one would expect that these glaciers would have undergone the most marked terminal retreat in response to the observed recent changes in climate. However, the findings of Pelto

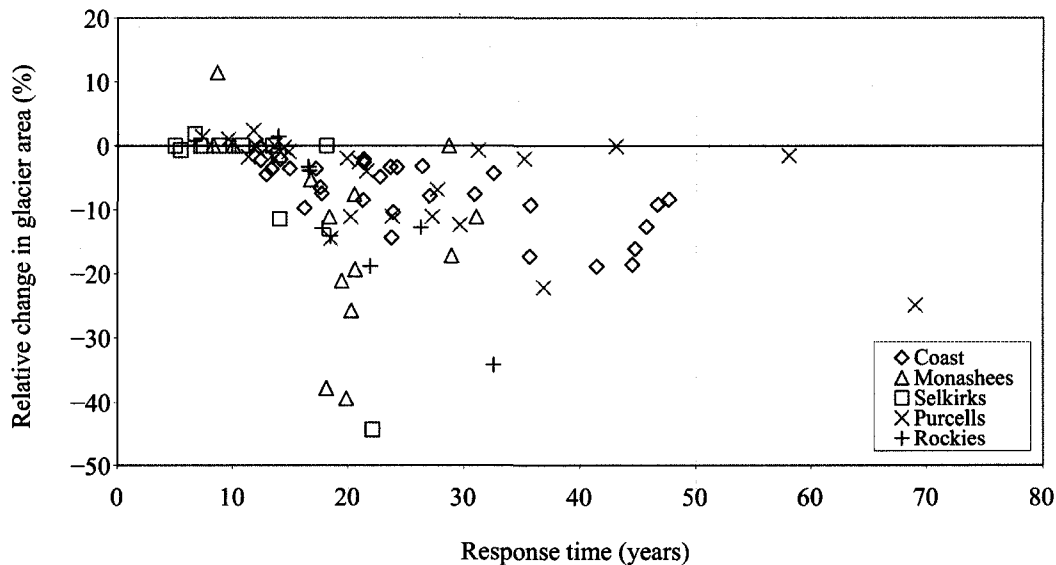


FIGURE 5.10. Relative changes in glacier area plotted against the calculated response times. Values of response time are derived using an estimate of H that is based on the lower slope of the individual glaciers.

and Hedlund (2001) in their study of the terminus variations of 38 glaciers in the North Cascade Mountains, Washington, provide some insight on the possible behavior of the glaciers in this study. The authors found that the glaciers with the most rapid response to climatic change (Type 1 glaciers; 20–30 year response time) are those with steep slopes, heavily crevassed surfaces, and high terminus-region velocities. These glaciers had come close enough to equilibrium conditions that the climate shifts beginning in 1947 and 1976 initiated rapid changes from retreating to advancing, and subsequently back to retreating conditions. For the glaciers with a very low slope, limited crevassing, and generally low velocities for their size, response times of at least 60–100 years were estimated based on terminus observations (Type 3 glaciers). Such glaciers are known to have a longer period of adjustment to climatic change as a consequence of the surface height – mass balance feedback (Oerlemans, 1989; Harrison et al., 2001). The behavior of these glaciers has been characterized by continuous retreat from 1890 to the present. None have approached a steady state since the end of the LIA; rather, they are all still adjusting in part to the post-LIA climate change, which has been reinforced by recent warming (Pelto and Hedlund, 2001; 502). Type 2 glaciers have an intermediate slope and terminus-region velocity with response times of 40–60 years, and underwent rapid retreat from 1890 until ~1950, followed by slow retreat or equilibrium to 1976, and moderate to rapid retreat since 1976.

It is possible that the glaciers of this study have responded to climatic changes in a similar manner. All of the glaciers that have undergone minor advance have the same characteristics as the Type 1 glaciers of Pelto and Hedlund (2001) (Fig 5.11). Therefore, although their termini are presently at an advanced position relative to 1951/52, they are likely in a retreating mode at present, following a period of advance sometime between 1947 and 1976 when climatic conditions were more favorable for glacier growth. Figure 5.11 shows the terminus position at 3 different times for two contrasting glaciers in the central Purcell Mountains. The terminus of the Covenant Glacier, which had a frontal slope of 0.54 or 28°, and a response time of 11.7 years, was at its most advanced observed position between 1984 and 1987. This confirms that during the final 2 decades of the study period this glacier was indeed in a state of retreat, and that it has likely responded rapidly to recent climate shifts. All the other glaciers that have undergone a

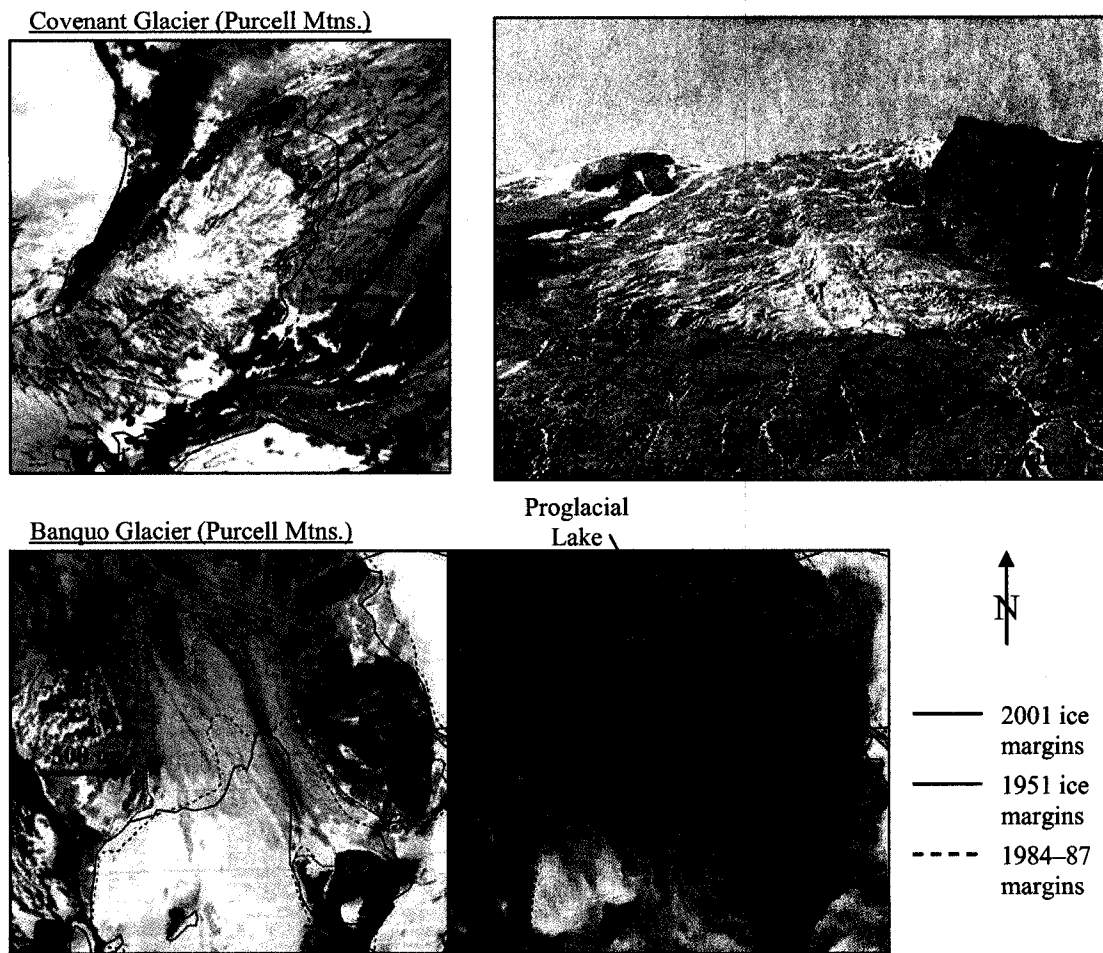


FIGURE 5.11. Terminus positions at different times for the Covenant and Banquo Glaciers (unofficial names) in the central Purcell Mountains. The surface of the Covenant Glacier is very steep and heavily crevassed (top right), while the recent formation of a large proglacial lake below the terminus of the Banquo Glacier (bottom right) attests to the very low initial bed slope in this region. The 1984-87 glacier margins are represented by the Terrain Resource Information Mapping (TRIM) digital maps of the Ministry of Sustainable Resource Management, Government of British Columbia.

net advance exhibit the same pattern. In contrast, the 1984-87 terminus position of the Banquo Glacier, which had a frontal slope of 0.08 or 5°, and a response time of 69 years, was transitional between the 1951 and the 2001 positions. This pattern was also observed for most other glaciers with a moderate or low slope, and less extensive crevassing. These glaciers are similar in nature to the type 2 and 3 glaciers of Pelto and Hedlund (2001), and have likely been retreating continuously over the study period. No formal measurements of the rate of retreat or advance over the study period are made because

the error associated with the TRIM glacier margins is unknown. Rather, these data provide a qualitative assessment of the state of these glaciers at that time.

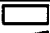




5.3 GLACIER GEOMETRY AND RESPONSE

The geometric characteristics of a glacier (i.e., shape, size, elevation, surface slope, and aspect) are of fundamental importance in terms of its sensitivity to climatic change and the response it will undergo. Further analyses were conducted to investigate the effects of specific geometric characteristics of individual glaciers, as well as various geographic and topographic characteristics of these glaciers, on their observed response to recent climate changes. The roles of these characteristics are discussed below.

5.3.1 *Glacier Shape*

Furbish and Andrews (1984) examined the response of the terminus to changes in the equilibrium line altitude (ELA) of glaciers situated within five idealized valley-basin shapes (Table 5.6). They showed that for a rectangular glacier, a unit change of the ELA is exactly compensated for by a similar unit change of the terminus altitude (though not necessarily equal to Δ ELA). The response of glaciers with other shapes is non-linear (Fig 5.12). For example, due to its shape, the initial response of the terminus to a rise in the ELA of a type-B glacier is very large, but becomes smaller with successive unit rises in the ELA. Because the rate at which surface area becomes available for ablation decreases progressively in the downslope direction, these glaciers generally extend to lower elevations where the specific melt rates are higher. For a given change in mass balance, the response at the terminus of these glaciers is greater than that of glaciers with other shapes because the terminus must retreat farther up-valley to locations where specific melt rates are reduced in order to achieve a new balance between mass input and output. In addition, the sensitivity of mass balance to climate change for glaciers with a long and narrow tongue is relatively higher due to potential feedbacks between ablation and the advective heat flux from the surrounding ice-free ground (Oerlemans, 1989). As the glacier retreats, more rock is exposed and the increased flux of sensible heat from

TABLE 5.6. Summary of the five basic (idealized) glacier shapes considered by Furbish and Andrews (1984). Ice flow direction is to the left in the diagrams.

Shape	Glacier type	Description
	A	Rectangular shaped glaciers
	B	Glaciers that taper in width downslope
	C	Glaciers that increase in width downslope
	D	Glaciers similar in form to shape B in the lower region, and shape C in the upper region
	E	Glaciers similar in form to shape C in the lower region, and shape B in the upper region

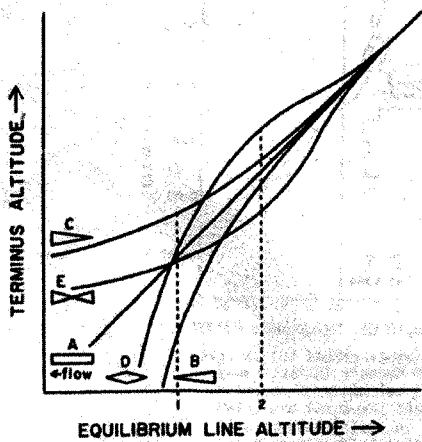


FIGURE 5.12. General relation between terminus altitude (TA) and ELA for the five idealized glaciers in Table 5.3. FROM: Furbish and Andrews (1984).

peripheral regions leads to increasing air temperature over the glacier (apart from regional climate perturbations). Glaciers that are characterized as type C, in contrast, generally have relatively high terminus positions and reduced sensitivity of their termini to changes in mass balance. This is due to the fact that the rate at which surface area becomes available for ablation increases progressively at lower elevations. The response of the terminus to changes in the ELA is small, but becomes greater with successive unit rises in the ELA. The remaining shapes are essentially end-to-end combinations of shapes B and C. Thus the response of D to a unit lowering of the ELA is similar to that of C over high ELA values, and similar to the response of B over lower ELA values. This is the opposite for shape E. (Furbish and Andrews, 1984; 202–203). Together this implies that if several glaciers occupying distinct valley shapes are subjected to a similar change in climate, they should exhibit essentially unique responses at their termini.

The planimetric shape of individual glaciers was classified according to the types listed in table 5.6. Within most regions of the study area, glacier shape appears to have had a significant effect on the response of the glaciers to recent changes in climate.

Many of the glaciers that have undergone significant reductions in area are characterized as type B in shape, while those that have undergone only minor changes are of type A or C. Specific glaciers within individual regions are discussed below.

5.3.1.1 Rocky Mountains

In the Rocky Mountains most of the glaciers are either type A or B in shape (see Fig 4.1 and Appendix B), and the linkage between glacier shape and response to climate change is evident. For example, the Robertson, Northover, and Mangin – Marlborough Glaciers, which are all type B in shape with long and narrow snouts, have undergone substantial terminal retreat and lost a significant portion of their initial area. The Haig and Tipperary Glaciers are also type B shaped glaciers that underwent a large change in area. Glaciers that underwent very limited or no change in area, including the King, Smith-Dorrien, Castelnau, French, and Beatty Glaciers, are generally type A in shape. The Queen Glacier, which changed in area by only -1% from an initial area of 0.63 km^2 , is best represented by shape D. This glacier has a high ELA and thus its response would be expected to be similar to that of shape C. In contrast, an unnamed glacier to the northwest of the Abruzzi Glacier (GLIMS ID: G295238E50461[N]) that is also type D in shape has a relatively low steady-state ELA, and thus its response should theoretically be similar to that of shape B. This glacier underwent a change in area of -33% from an initial size of 1.03 km^2 . These two glaciers differ in other respects (most notably surface slope and elevational range), but nonetheless, this example is consistent with the findings of Furbish and Andrews (1984).

5.3.1.2 Columbia Mountains

The shape of most individual glaciers in the Purcell Mountains appears to have influenced their response to recent climate changes, but there are a number of cases where shape has clearly not been a major factor in the response of the glacier. All but one of the major glaciers in the Purcell Mountains that have undergone $>10\%$ reductions in area are type B in shape. An excellent example of this is the Starbird Glacier (Fig.

5.13), which is confined by a narrow valley in the lower ablation zone and had an initial terminus elevation (1940 m) over 200 m below the regional average. This glacier lost over 1.7 km² (~15%) of its surface area and retreated nearly 2 kilometers over the period 1951–2001. There are, however, several glaciers that are characterized by shape B that have either undergone only minimal retreat or have advanced slightly. The Bugaboo and Commander Glaciers are prime examples of this, and for these glaciers their rapid response time has been the primary influence on their recent behavior. Major glaciers in the Purcells that are characterized as type C in shape have a higher than average terminus elevation and typically underwent extremely limited (i.e., >–1%) changes in area. For example, the MacCarthy Glacier (Fig 5.13) has a very broad terminus that is approximately 150 m higher than the regional average over most of its length, and it showed no measurable change in area over the period. Glaciers that are type A in shape have generally undergone changes in area that are intermediate between those of glaciers with other shapes. Glaciers in this class include the Conrad, Horseshoe, Catamount (see Fig. 4.3 and Appendix B), and several other glaciers, which have changed anywhere from 0 to –3% in area.

In the Selkirk Mountains, glacier shape appears for the most part to be unrelated to the recent behavior of the glaciers. Only in one locality is the effect of glacier shape

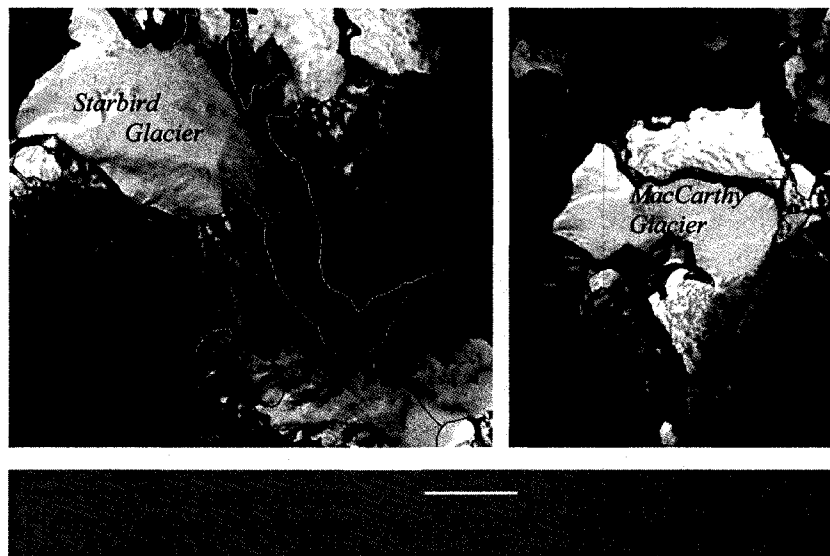


FIGURE 5.13. Changes in surface extent of 2 glaciers in the Purcell Mountains with differing planimetric shapes.

evident. The group of glaciers surrounding the Tenderfoot and Spyglass Mountains in the central Selkirks (Fig 5.14) displays a highly variable pattern of area change between individual glaciers. The Tenderfoot Glacier had an initial shape that was characteristic of type B. This glacier is one of only a few in the Selkirks to have undergone a significant reduction in area, and its retreat accounts for most of the ice loss in these mountains. The other major glaciers in this locality, which are type C in shape, have retreated to a far less extent or have advanced slightly.

Glacier shape has clearly had a significant influence on the response of glaciers in the Monashee Mountains (see Fig. 4.5 and Appendix B). The initial terminus elevation (1760 m) of the Cranberry Glacier, which is type B in shape, was over 300 m below the regional average, and this glacier underwent a substantial amount of terminal retreat and ice loss. The glacier immediately southwest of the Cranberry Glacier, which is type C in shape, has a terminus elevation (2410 m) nearly 400 m higher than the regional average, and underwent no measurable change in area. Other type C glaciers that underwent only minor retreat or slight frontal advance include the western portion of the Blanket Icefield and the glacier in the southern central part of this region just north of the Frigg Glacier. The Frigg Glacier and the glacier in the far northwestern part of this region have a shape that is characteristic of type D, and have ELAs that are situated near the widest part of the glacier. Their response should therefore theoretically be somewhere between that of the

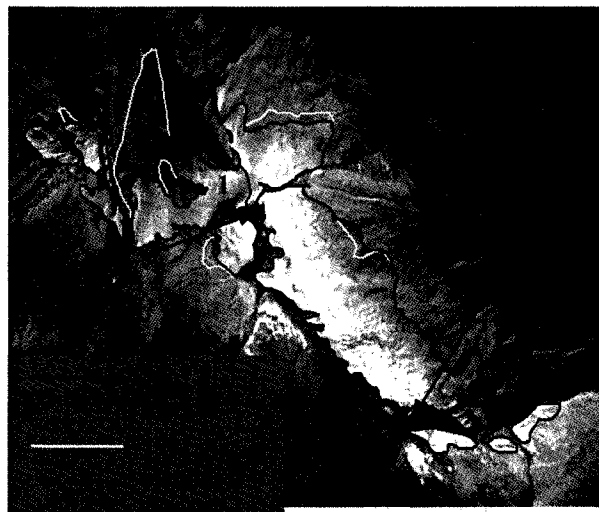


FIGURE 5.14. Retreat of the Tenderfoot Glacier (1) and neighboring glaciers in the Slocan Ranges of the central Selkirk Mountains.

glaciers characterized as type B and type C. They changed in area by -11 and -8% respectively, which is intermediate between the extremes of other glaciers in the region. The Gates Glacier had an initial shape that is best characterized as type E, with an ELA that is situated high on the glacier. This partly explains the significant reduction in area, as the response to a change in climate should theoretically be similar to that of shape B.

5.3.1.3 Coast Mountains

In the Coast Mountains, most of the larger glaciers and the outlet glaciers of ice fields are type B in shape. These glaciers are confined by the valley walls in their ablation zones and they must extend large distances downvalley in order to allow ablation of the large amounts of accumulated ice. At such low elevations the air temperature is high and melt may occur throughout much of the year. Together with the elongated shapes of their tongues, this makes them inherently more sensitive to climate change and helps to explain the large overall loss of ice in the region. Many of the smaller glaciers that have undergone little or no change in area are type A or C in shape and have a relatively high terminus elevation. This is due to the fact that these glaciers have smaller accumulation areas, and thus, a smaller total mass input than the much larger glaciers. Therefore, the rate of mass turnover of these glaciers is lower and they do not need to push as far into the ablation zone (where valley topography is more restrictive) to maintain equilibrium conditions.

Across the coastal region, glacier shape has not been a major control on the response of glaciers to recent climatic changes. There are numerous type B glaciers that have undergone little or no net change in area. Rather, it appears that the pattern of changes across this region is controlled primarily by the distance of glaciers from the regional moisture source, their response time, and other intrinsic characteristics including their slope (section 5.3.3) and hypsometry (section 5.4).

5.3.2 Area and Elevation

The discussion in the previous section has already highlighted the relationship between glacier area and terminus elevation, where, other factors held constant, larger glaciers descend to lower elevations to balance mass input and output. For glaciers confined in a narrow valley this effect is amplified, while the opposite is true for glaciers in less confined topographic settings. This interrelation between glacier size and elevation range controls the amount of surface melt and accumulation, and is therefore useful for explaining some of the differences in the observed responses of glaciers in this study.

Figure 5.15 shows how strongly the initial area of individual outlet glaciers of the Bridge Icefield in the Coast Mountains (see Fig. 4.8 for reference) has influenced their relative and absolute change in area. With the exception of the smallest glaciers, both the average relative area loss and the variability of this loss between individual glaciers become smaller with increasing glacier size. The greater variability amongst the smaller glaciers likely reflects the variability in climatic or environmental conditions (such as snow drifting or avalanching) at highly local scales, which may or may not have a significant impact on a glacier, depending on its location. These smaller glaciers may be highly sensitive to changes and would respond more quickly than the larger glaciers (Bahr et al., 1998). The larger glaciers would integrate such variation over a wider region and take longer to fully adjust, and would therefore exhibit a more uniform response. The greater relative changes of many glaciers are due to the fact that even a small absolute change can represent a large fraction of a small glaciers' surface.

Absolute changes become greater with increasing glacier size (Fig 5.15b). This is because a given reduction in specific accumulation rates occurs over a larger region, representing a greater total reduction in mass input. This is balanced by a greater loss of mass and surface area at lower elevations. In addition, because the large glaciers have a significant amount of surface area situated at very low elevations where melt rates are high, ice wastage and absolute changes in area are more substantial.

In other regions of this study the relationship between changes in area and glacier size is much weaker. In some cases a similar pattern was observed for the relative changes in surface area, where the average change and the variability of changes of

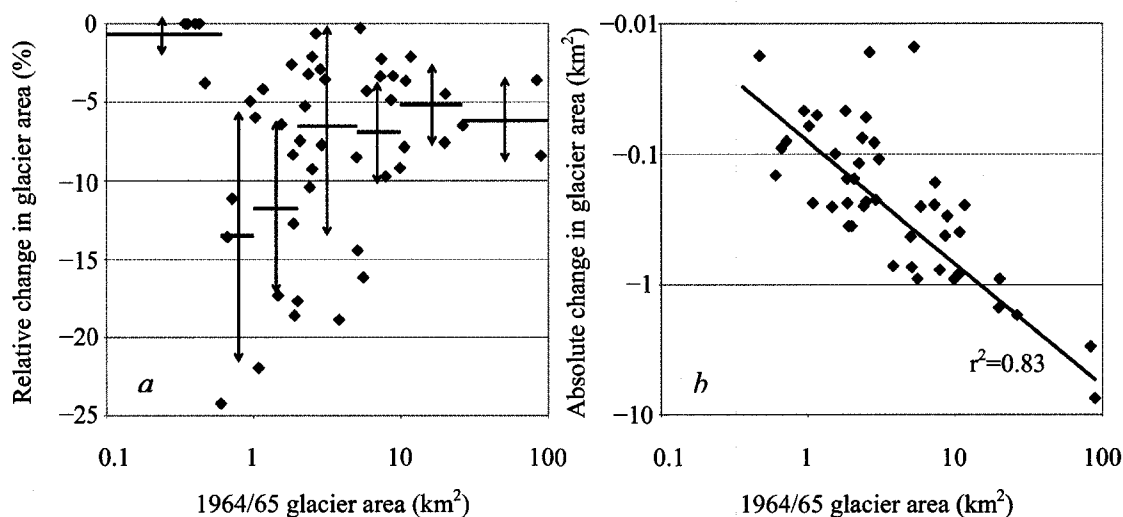


FIGURE 5.15. Relative (a) and absolute (b) changes in area of individual glaciers of the Bridge Icefield plotted against their initial area. Mean values of relative glacier area change (horizontal bars) are given together with \pm one standard deviation for seven distinct area classes (<0.5, 0.5–1.0, 1.0–2.0, 2.0–5.0, 5.0–10, 10–25, and >25 km²).

individual glaciers decreases with increasing glacier size, but this trend was not found in all regions. Larger glaciers have generally undergone greater absolute reductions in area, but the trends are not as significant as that shown in Figure 5.15b. This may be partly due to the more limited range in size (and thus area changes) of individual glaciers outside the Coast Mountains. Plots of absolute area change vs. glacier size for the Columbia Mountains contain many outliers from the general trend, which are probably due to the fact that glacier hypsometry (section 5.4) and other geometric characteristics such as shape and slope have had a greater effect on the response of glaciers here. The variability in shape and slope between individual glaciers of the Bridge Icefield is much more limited, so differences in glacier response across the icefield are more likely to have resulted from differences in area and elevation range.

Figure 5.16 shows the relative change in area plotted against the area-weighted mean elevation of individual glaciers in all parts of the study area. The relative change in glacier area shows a very slight positive trend with the area-weighted mean elevation of glaciers in the Columbia Mountains. This reflects the fact that, other factors held constant, glaciers with a large portion of area situated at lower elevations are relatively more sensitive to climatic change than neighboring glaciers with a smaller fraction of their surface area at such elevations. Large ice masses situated at low elevations are

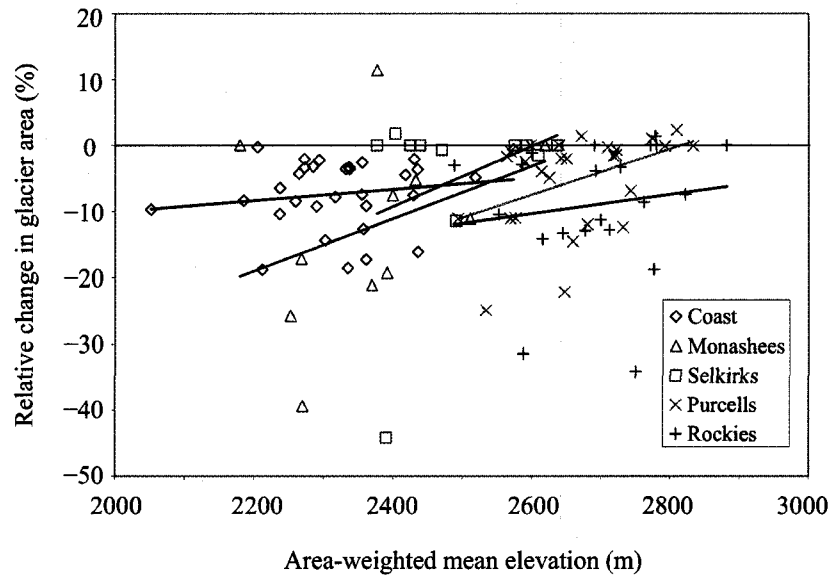


FIGURE 5.16. Plot of relative change in area against mean elevation of glaciers situated within different parts of the study area. The area-weighted mean elevation was determined as: $\bar{z} = \sum z_i (S_i / S_{tot})$, where z_i and S_i are the median elevation and surface area respectively of individual hypsometric bins, and S_{tot} is the total glacier area.

vulnerable to climatic warming and reduced snowfall since melt rates are higher here. This also implies that as the terminus of a glacier retreats to higher elevations, its overall sensitivity to further climatic change is reduced (discussed further in section 5.3.4).

In the Rocky Mountains, the trend is less distinct, and it seems to be almost non-existent in the Coast Mountains where the changes that have been observed are unrelated to the mean elevation of individual glaciers. Across the region, mean glacier elevations decrease toward the west, reflecting the increasingly moist conditions in this direction. The overall pattern in figure 5.16 may partly reflect the transition to an increasingly maritime regime. For glaciers in the Coast Mountains, represented here by those of the Bridge Icefield, those that descend to lower elevations have typically undergone smaller relative changes. At the same time, however, these glaciers tend to have very wide and extensive accumulation areas that act to compensate for the effect of the low elevation of their termini on their mean elevation. These conflicting factors result in a lack of any coherent pattern in the plot of relative area change vs. mean elevation.

5.3.3 Glacier Slope

It is well known that the position of the glacier terminus will be more sensitive to changes in the ELA when the longitudinal slope of the bed is small. The importance of slope can be seen in a simple formula derived by Oerlemans (1989), which gives the equilibrium length L for a glacier of constant width resting on a bed of constant slope γ :

$$L = \frac{2\left(\frac{\Lambda}{\gamma} + b_0 - E\right)}{\gamma} \quad (8)$$

where Λ , assumed to be constant, is the product of the thickness and the surface slope, $H(dh/dx)$, b_0 is a reference elevation for the bed, and E is the equilibrium line altitude. (8) shows that the feedback between glacier surface height and mass balance, reflected in the term Λ/γ , becomes more important when the bed slope is small. It can also be seen that by taking the derivative of L with respect to E , ($\partial L/\partial E = -2/\gamma$) the sensitivity of glacier length to changes in the ELA is inversely proportional to the bed slope. Similar behavior is expected of glaciers with more complicated geometry (Oerlemans, 1989). Glacier slope is therefore an important geometric characteristic to consider in terms of variability of glacier response at local scales.

The mean surface slope ($\bar{\alpha}$) of individual glaciers was measured by differencing the maximum and minimum elevation and dividing this by the length of the glacier. For glaciers with complicated geometry or multiple tributaries, the average elevational range and average length were used to derive a value of $\bar{\alpha}$. The mean surface slope in the vicinity of the terminus ($\bar{\alpha}_t$) was also measured. This was typically determined over a length of 1 km up from the terminus along an ice-flow line, but for exceptionally short (i.e., <2 km) and long (i.e., >10 km) glaciers, slope was measured over a distance of 500 m and 3 km up from the terminus respectively.

Measurements of slope were compared with the percentage area change of individual glaciers. The relative change in area is unrelated to $\bar{\alpha}$ for individual glaciers in all regions of the study area with the exception of the Monashee Mountains. Even here, however, the relationship between these two variables is rather weak (i.e., $r^2=0.42$). In contrast, $\bar{\alpha}_t$ has had a significant effect on the relative area change of glaciers in most

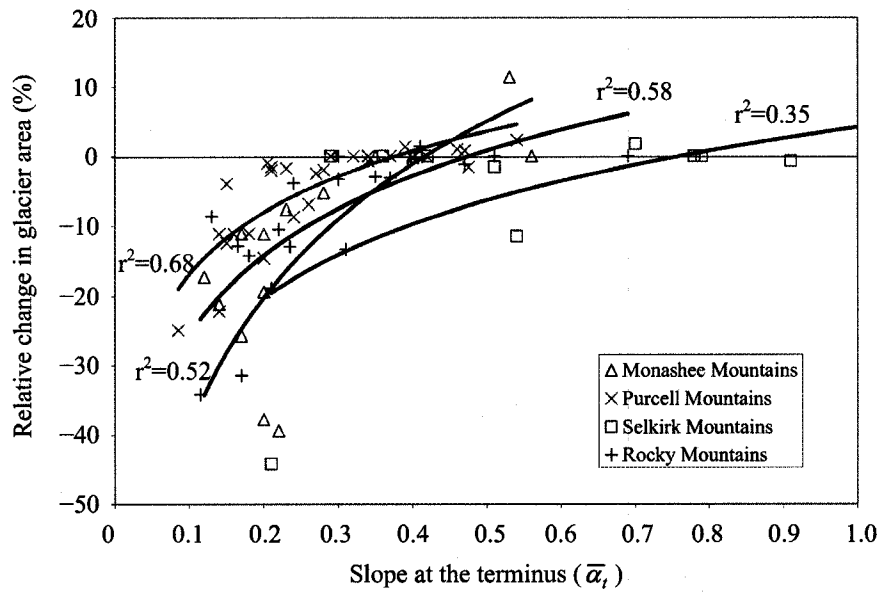


FIGURE 5.17. Plot of the relative change in area against the slope at the terminus for major glaciers of the Rocky, Purcell, Selkirk, and Monashee Mountains.

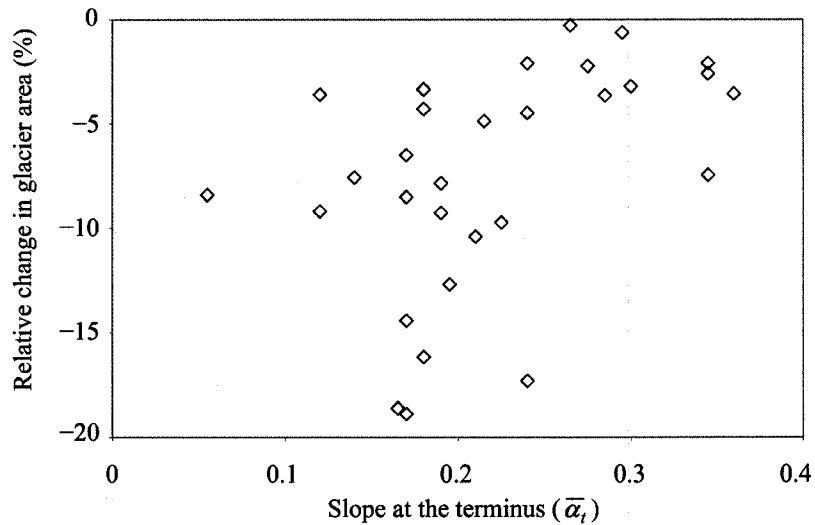


FIGURE 5.18. Plot of the relative change in area against the slope at the terminus for outlet glaciers of the Bridge Icefield.

regions, and in certain cases appears to be the dominant control on the response of individual glaciers to recent climate changes. The percentage area change of individual glaciers displays a logarithmic relationship with $\bar{\alpha}_t$ (Fig 5.17), and the coefficient of determination, r^2 , is equal to 0.58, 0.68, 0.35, and 0.52 in the Rocky, Purcell, Selkirk, and

Monashee Mountains respectively. For the glaciers of the Bridge Icefield, the relative change in area of individual glaciers appears to be only marginally related to $\bar{\alpha}_t$ (Fig 5.18). This may, however, be due to the fact that these glaciers have only a limited range in the values of their slope. For example, the pattern is still consistent with that of the glaciers in other regions, such that glaciers with a value of $\bar{\alpha}_t$ greater than 0.25 have typically lost less than 5% of their initial area, and glaciers that have undergone the largest relative reductions in area have a $\bar{\alpha}_t$ value of 0.1–0.25. Therefore, the response of these glaciers is likely still linked to a large extent with the slope at the terminus.

Greater relative loss of ice from glaciers with a gently sloping terminus has likely occurred because the overall mass balance of such glaciers has been more strongly affected by recent climatic change. For a glacier with a gentle slope over its lower ablation zone, the positive feedback effect of surface lowering on specific melt rates has a greater impact on the overall balance because this occurs over a relatively large region where melt rates are initially the highest. The effects of this feedback on the overall balance are less significant for surface changes over relatively flat sections higher up on the glacier. At locations far above the ELA, the specific balance is positive and is likely to remain so even with a rise in the ELA and an increase in specific melt rates through positive feedback. Over flat sections near the ELA, changes in specific balance are only minor and should not significantly affect the adjustment of the glacier. This may explain why $\bar{\alpha}$ is less important than $\bar{\alpha}_t$ in terms of the observed glacier response, as is clearly illustrated by the behavior of some of the glaciers within the Purcell Mountains. There are several glaciers here that have gently sloping plateaus above their ELA with $\bar{\alpha} < \bar{\alpha}_t$, and which have undergone only minimal area reductions or even minor advance. The MacCarthy Glacier, for example, has a $\bar{\alpha}$ value of only 0.23 as a result of 2 extensive upper plateaus, but steepens to a slope of 0.37 near its front (Fig. 5.19). This glacier underwent no observable change in area over the study period, which may partly be explained by the fact that the surface elevation – mass balance feedback is insignificant over both of the upper plateaus (situated between 2400–2500, and 2600–2700 m), and over the steep lower section of the glacier. There are some glaciers in the Purcell Mountains that have very steep upper slopes, with the result that $\bar{\alpha} > \bar{\alpha}_t$, and which have

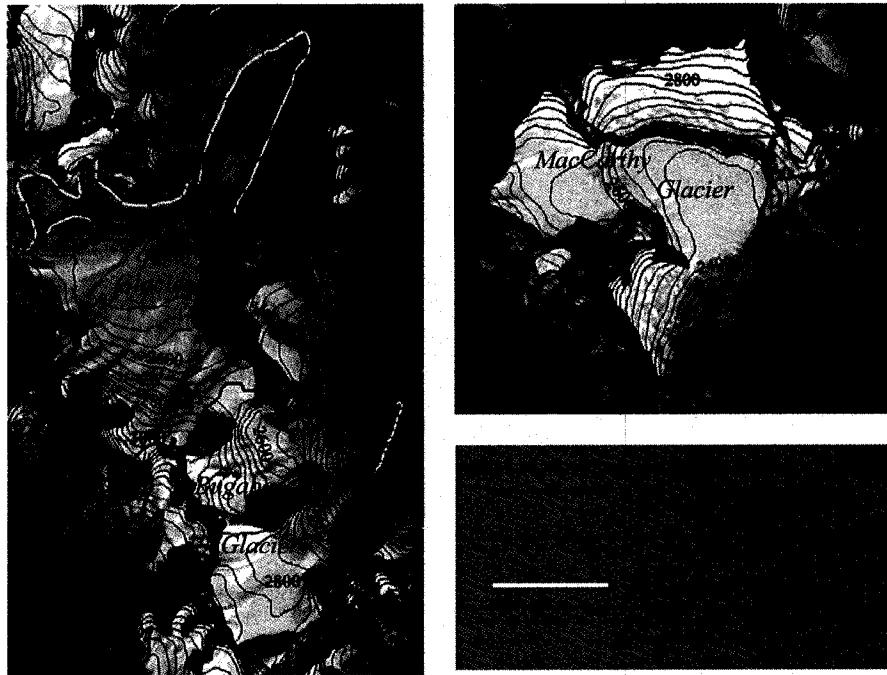


FIGURE 5.19. Surface topography and glacier margins of glaciers with unique surface slope characteristics in the Purcell Mountains (contour interval is 40 m).

undergone relatively large changes in area. For example, the Jumbo Glacier has $\bar{\alpha}$ and $\bar{\alpha}_t$ values of 0.39 and 0.14 respectively, and underwent a large amount of terminal retreat that reduced its area by ~22%. This glacier calves into a large lake, however, which was likely also a contributing factor in the extensive retreat of its terminus. The contrasting response of the Vowell and Bugaboo Glaciers (Fig. 5.19), which are similar in almost all respects, is likely primarily a result of the difference in slope at their termini. The Vowell Glacier (~11% area loss) has a low slope over its entire ablation zone, and appears to have thinned and retreated not only at its front, but also higher up along the northwest margin of the glacier where it has disintegrated into several separate ice masses. The Bugaboo Glacier, which is very steep over its entire length except for a small plateau above ~2700 m, has advanced by ~150 m and increased in area by ~1.5% over the same period.

The slope of the individual glaciers has a large effect on their calculated response time though its effect on the estimate of H . The strong relationship observed between relative changes in glacier area and slope near the terminus is a reflection to some degree

of the differences in response time of the individual glaciers. Essentially, the glaciers with a moderate or low slope not only undergo a greater overall response to climatic change as a result of the surface height – mass balance feedback, but they also have a longer period of adjustment to this change (Oerlemans, 1989; Harrison et al., 2001).

5.3.4 Dynamic Sensitivity

In addition to the positive feedback between mass balance perturbations and changes in glacier surface elevation, negative feedbacks involving mass balance and glacier geometry also act to reduce the sensitivity and the overall response to a change in climate. For example, a perturbation in mass balance that results in a retreat of the terminus will be partly offset by the fact that as the glacier front retreats to higher elevations and the ablation zone assumes a smaller area, overall melt rates decrease and the final response is less than would occur if the melt continued at a constant rate (Oerlemans et al., 1998). This must be taken into consideration in an interpretation of the observed changes in glacier area, as the dynamic sensitivity due to changes in glacier geometry may provide a partial explanation for the differential responses of individual glaciers.

In all regions of this study, most of the very small (i.e., $<0.2 \text{ km}^2$) glaciers underwent no change in area. These glaciers are generally isolated ice aprons and small cirque and hanging glaciers that are situated in shaded depressions or at very high elevations where melt rates are low, or below steep slopes that contribute snow to the ice surface by avalanching. Such sites are favorable locations for ice preservation, and glaciers situated within these marginal locations may be less sensitive to climatic change as reduced snowfall and/or warmer temperatures would have less impact on their overall mass balance than that of larger glaciers in more exposed sites. To provide insight into the location of these glaciers an analysis was conducted for a sample of 103 small (i.e., generally $<1 \text{ km}^2$) glaciers in the central Purcell Mountains (NTS sheets 82K07 and 82K08) that underwent no net change in area. These seem to have similar characteristics to very small glaciers in other regions of this study, and are therefore considered to be representative of all of such glaciers. For each glacier the minimum and maximum

elevation, aspect, and fraction of its surface shaded by the surrounding slopes at a typical sun angle during times of peak ablation were determined. A sun altitude of 45° above the horizon at an azimuth of 245° clockwise from north was initially chosen to represent the mid-afternoon position of the sun in mid-July for this region. This position, however, gives rise to shadows falling on <20% of the glaciers analyzed, so to increase the number of glaciers with some percentage of shaded area the sun elevation was reduced by 10° .

Figure 5.20 shows the relationship between the fraction of shaded surface area of each glacier and its median elevation. A slightly negative trend is apparent, with lower glaciers having a greater portion of their surface shaded by the surrounding topography. 74% of the glaciers analyzed have a median elevation that is higher than the regional average ELA, and glaciers situated below this elevation generally have some portion of their surface that is shaded. Only 18% of the glaciers with a median elevation below the regional ELA have a shaded fraction of 0, while this is observed for 51% of the glaciers with a median elevation above the regional ELA. All glaciers that are situated far below the regional ELA have a relatively high shaded fraction (i.e., >0.25).

The relationship between fractional shaded area and median elevation is not very strong and there exists a considerable amount of scatter. This is partly due to the effects

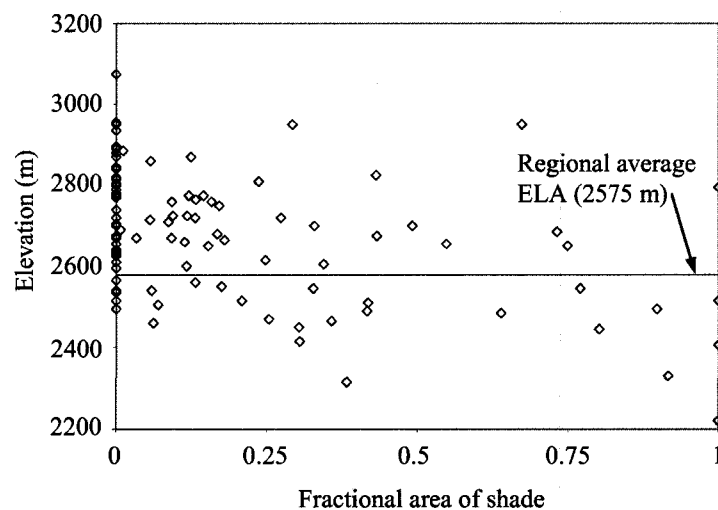


FIGURE 5.20. Plot of the median elevation of individual small glaciers (in the central Purcells) that underwent no net change in area against the fraction of their surface area shaded by the surrounding topography during times of peak ablation. The regional ELA is based on the surrounding larger glaciers, none of which were included in this analysis.

of glacier aspect, and also because a lower fraction of shaded surface area does not necessarily imply a greater rate or total amount of ablation. Even a very small fraction of shade is significant because this implies that the glacier is situated within a somewhat sheltered site. Additionally, these small glaciers are generally very steep so that for sections of ice facing away from the sun, the angle between incoming radiation and the ice surface is quite low.

Figures 5.21 and 5.22 show how glacier location depends on aspect. Glaciers situated on southern and western slopes have a median elevation that is well above average. Some of these are also situated within deep cirque basins that may provide shelter and enhanced inputs of snow; the glaciers to the southwest of the Commander Glacier and that to south of the Horseshoe Glacier provide clear examples. The glaciers facing north and east are much more common and have a greater range of median elevation, with all the lowest glaciers found to be facing these directions. In cases where they are extremely low, such as the glaciers to the north and southeast of the Delphine Glacier and those near the Macbeth Icefield, they are situated within deep cirques and are highly shaded.

Many of these glaciers have well-defined LIA moraines and trimlines (i.e., erosional ‘tidemarks’ on valley sides) that are clearly identifiable in the aerial photography. They extend from several hundred meters up to a kilometer or more downvalley

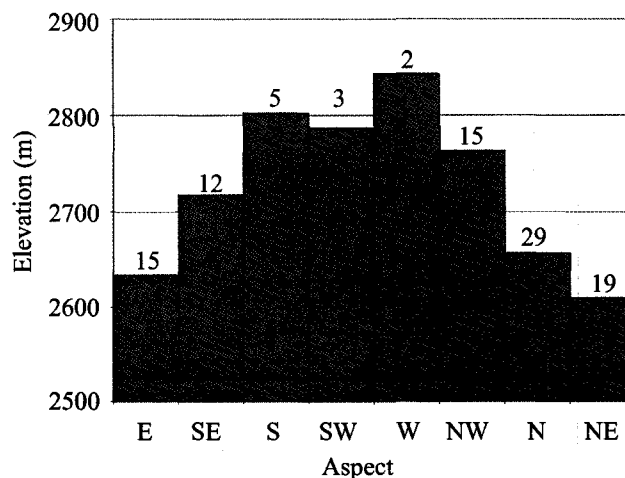


FIGURE 5.21. Average median elevation of glaciers with differing aspect shown together with the percentage of the sample these glaciers represent.

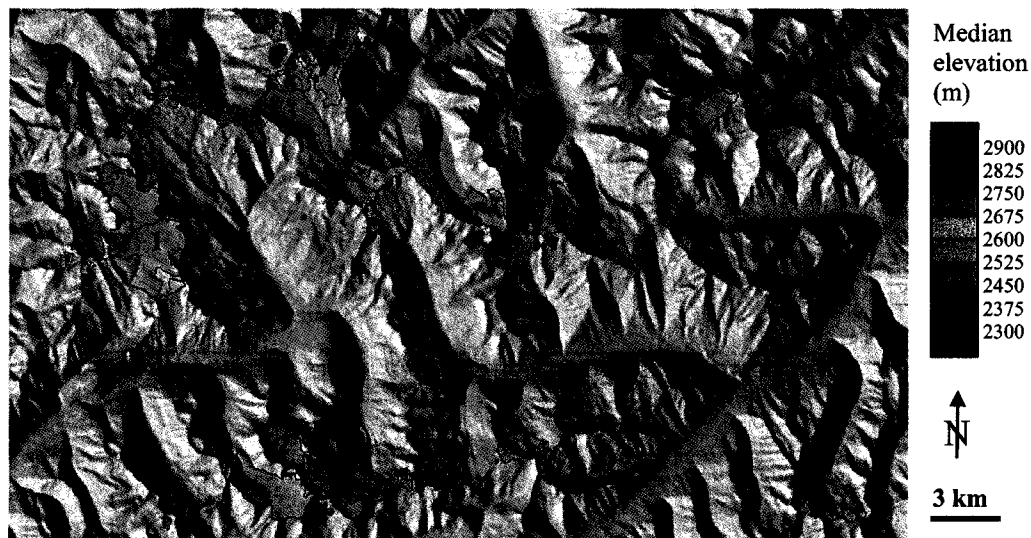


FIGURE 5.22. Distribution and elevational characteristics of small glaciers in the central Purcell Mountains that underwent no net change in area, shown over shaded relief map. 1: Macbeth Icefield; 2: Horseshoe Glacier; 3: Starbird Glacier; 4: Commander Glacier; 5: Delphine Glacier.

from the present terminus position, indicating that these glaciers have undergone considerable retreat since their LIA maximum extent. Given that no measurable changes in area were observed over the study period and that all of these glaciers are situated within favorable sites for preservation, it is likely that they had undergone full adjustment to the post-LIA warming before the start of the study period, and in doing so, substantially reduced their sensitivity to climatic change that occurred during the study period.

5.4 GLACIER HYPSONOMETRY

Glacier hypsometry, or the distribution of surface area with respect to elevation, plays an important role in determining the adjustment of a glacier to climate change as valley topography restricts where the ablation zone can or cannot expand or contract in response to a change in mass balance. The influence of valley topography on observed glacier response was investigated through analysis of the hypsometry of individual glaciers and icefield drainage catchments. Glacier hypsometry was characterized by two parameters: a geometric balance ratio, which is used to compare the distribution of area in the accumulation zone to that in the ablation zone (Furbish and Andrews, 1984), and a basin

sensitivity index that is used to quantify the relative change in glacier accumulation area ratio (AAR; i.e., the ratio of the area of the accumulation zone to the entire glacier surface area) that results from a prescribed change in the ELA (Burgess and Sharp, 2004).

5.4.1 Geometric Balance Ratios

Furbish and Andrews (1984) explored the way in which valley topography is linked to long-term glacier response through glacier hypsometry and the distribution of mass balance with elevation. Their discussion relies on three assumptions:

- i. The net mass balance curve of a glacier (water equivalent depth in relation to elevation) can be approximated as two linear functions of elevation above (accumulation zone) and below (ablation zone) the ELA.
- ii. The net mass balance curve reflects a steady-state condition.
- iii. Valley topography sufficiently confines a glacier such that a change in mass balance results only in a change in the elevation of the terminus.

Rather than a rectilinear coordinate system, which is not well-suited for treatment of mass transfers over a glacier because of the complexity of spatial variations in width and slope, Furbish and Andrew's approach is based on the hypsometric curve of a glacier's planimetric area in relation to elevation (Fig. 5.23). They showed that under steady-state conditions, the ratio of the gradient of mass balance with elevation in the ablation zone to that in the accumulation zone (balance ratio; BR) can be approximated from the glacier's geometry as:

$$BR = \frac{m_c}{m_b} \quad (9)$$

where,

$$m_c \approx \sum_{i=1}^n S_{c_i} z_{c_i}, \quad (10a)$$

$$m_b \approx \sum_{i=1}^n S_{b_i} z_{b_i}. \quad (10b)$$

S_c and S_b are the areas of individual hypsometric bins in the accumulation and ablation zones respectively, and z_c and z_b are the altitudinal distances of the bins from the steady-

state ELA, measured as positive. m_c and m_b are geometric moments of area in the accumulation and ablation zones with respect to the ELA.

(9) describes the relationship between the steady-state mass balance of a glacier and the distribution of its surface area with respect to elevation. By setting the values of BR and m_c (which is equivalent to setting the ELA for a particular area of accumulation), the importance of valley topography becomes clear. The value of m_b , and hence the terminus altitude, becomes essentially set by the physical limits of the valley floor and walls to the extent that ice must fill the valley until an equality between mass input and output is achieved (Furbish and Andrews, 1984; 202). Assuming the value of BR remains fixed following a change in climate that leads to a vertical translation of the net-balance curves and an increase in the ELA, the value of m_b must change together with that of m_c as a new steady-state condition is established. For a glacier with an initially low BR value (i.e., <1.0) the change in the value of m_b is necessarily greater than that of m_c in order to maintain a constant BR . This change is achieved either by the removal of ice situated at a large distance below the ELA (which contributes relatively more to the geometric moment, m_b) or by significant area reduction of the ablation zone. A glacier with a higher initial BR value (i.e., >1.0) would undergo more limited ice loss in the ablation zone following a change in climate, as the change in value of m_b is necessarily less than that of the moment, m_c , in order to maintain a constant BR . Therefore, if several

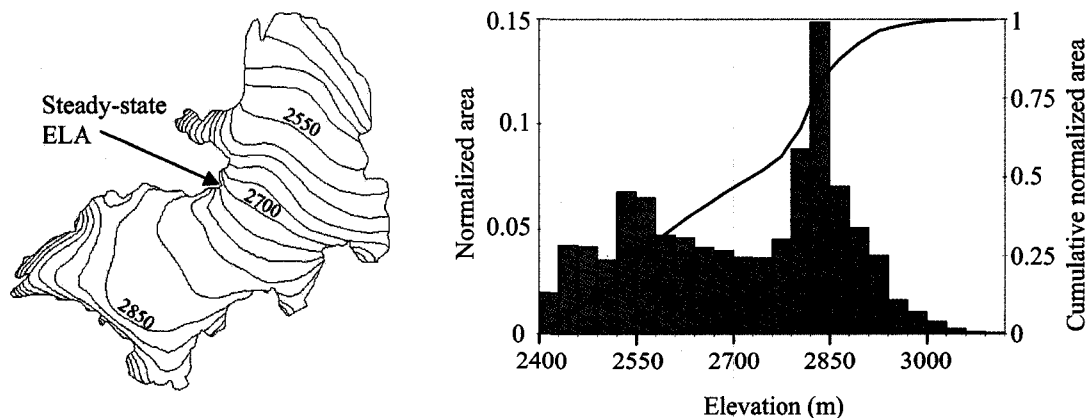


FIGURE 5.23. Hypsometric distribution of planimetric area in relation to elevation, and hypsometric curve relating the cumulative area to elevation for the Pétain Glacier in the southern Rocky Mountains. The steady-state ELA is selected based on the change in contour curvature, which occurs at an elevation of 2700 m on this glacier (contour interval is 30 m).

glaciers with distinct BR values are subjected to a similar change in climate, they should exhibit essentially unique responses at their termini.

Values of BR were calculated for the initial surface topography of individual glaciers using (9). The glaciers chosen for this analysis include the major glaciers of the Rocky and Columbia Mountains, and outlet and surrounding glaciers of the Bridge Icefield in the Coast Mountains. Steady-state ELAs of individual glaciers were estimated from the ice topography by choosing the elevation where contour curvature changes from concave to convex down-valley (Leonard and Fountain, 2003; Fig. 5.23). Glaciers were typically divided into 20–30 hypsometric bins, and a minimum of 15 bins was chosen to allow for a reasonable approximation of BR . Balance ratios were also determined by comparing the gradients of the estimated steady-state ablation zone (b_{nb}) and accumulation zone (b_{nc}) mass balance curves for Bridge, Place, and Haig Glaciers.

5.4.1.1 Comparison of BR calculations

The calculated geometric BR values may not realistically reflect the ratio b_{nb}/b_{nc} as the assumptions relied on in this analysis may not hold. Table 5.7 compares the results of the two approaches used to calculate BR for glaciers with mass balance records in the study area. There is reasonable agreement between the results of the two approaches for Bridge and Haig Glaciers, and similarity between those for Place Glacier. Some of these calculations are based on a limited series of mass balance data (i.e., 5 and 2 years for Bridge and Haig Glaciers respectively), which may result in considerable uncertainty in the estimated steady-state mass balance curves and thus explain some of the difference between the results. It is clear from all of the observational mass balance series (not shown), however, that assumption (i) of Furbish and Andrews (1984) is satisfied to a reasonable degree. Rather than error in the mass balance curves, the primary cause of the discrepancies between calculated BR s for each glacier is uncertainty in the estimation of the steady-state ELA. This is because even minor variations in the estimates of the ELA significantly affect the terms m_b and m_c , while possible variations of b_{nb} and b_{nc} lead to only subtle changes in their ratio. Nonetheless, the similarity between all of the results suggests that (9) provides a reasonable approach for determining the BR of glaciers here.

TABLE 5.7. Comparison of the balance ratio calculated from both mass balance data and ice surface topography.

	b_{nb} (10^{-3} m W.E. m^{-1})	b_{nc} (10^{-3} m W.E. m^{-1})	b_{nb}/b_{nc}	m_c/m_b
Bridge Glacier	6.77	4.57	1.48	1.17
Place Glacier	10.9	4.24	2.58	3.33
Haig Glacier	7.98	6.95	1.15	1.23

5.4.1.2 BR values and glacier area changes

The calculated BRs display a logarithmic relationship with the percentage area change of the outlet glaciers of the Bridge Icefield ($r^2=0.63$; Fig 5.25) and the larger glaciers in the Monashee Mountains ($r^2=0.79$; Fig 5.28). This pattern is characteristic of glaciers in other regions as well, but the relationship is not as strong and the shape is controlled to a large extent by a very limited number of observations. Discussion of these results is presented first for the glaciers of the Bridge Icefield, and then for those of the Monashee Mountains.

a) Bridge Icefield

Glaciers that have undergone losses of more than 10% of their initial surface area have a BR of less than 1.0 and typically have a large fraction of their area situated below the ELA. Conversely, those glaciers that have experienced only limited retreat generally have a higher BR, resulting from an extensive accumulation area, or equivalently, a large portion of the accumulation zone situated far above the ELA. For example, glacier # 34 (Fig. 5.24) has an AAR of 0.76 and elevational range above the ELA of almost twice that below the ELA. Several other glaciers that have similar characteristics include # 23, 37, and 39 (Fig 5.26). In contrast, glaciers such as # 24 and # 43 have AARs of ~ 0.3 and a much smaller elevation range above their ELA. Glacier # 24, however, does have a greater elevation range above the ELA than below the ELA, but the calculated BR is still very small because of the relatively limited surface area at higher elevations.

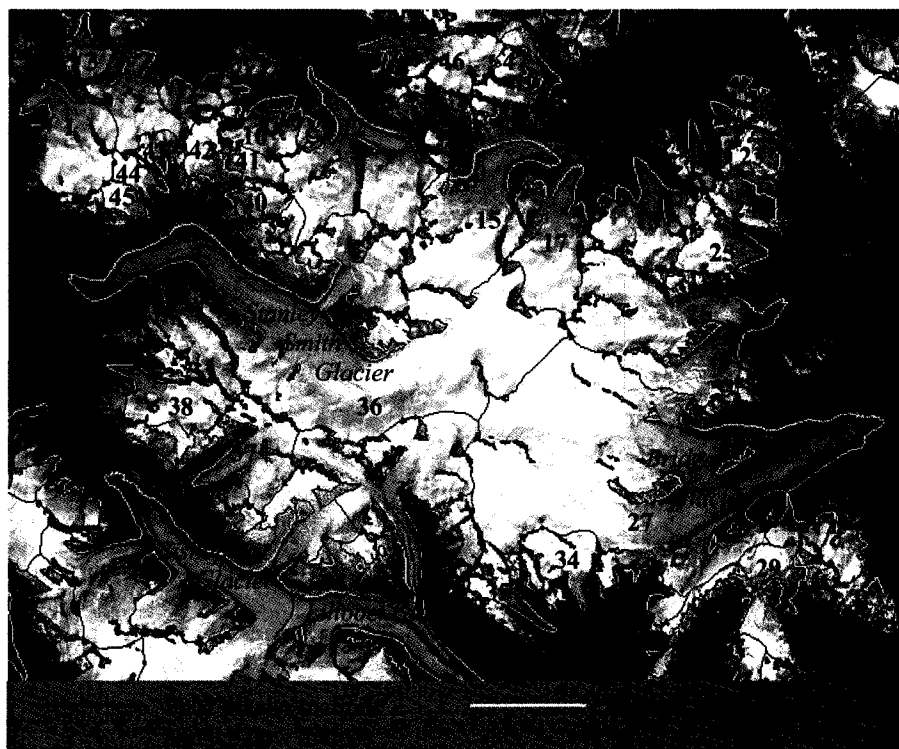


FIGURE 5.24. Net changes in surface extent of outlet glaciers of the Bridge Icefield over the period 1964/65–2002.

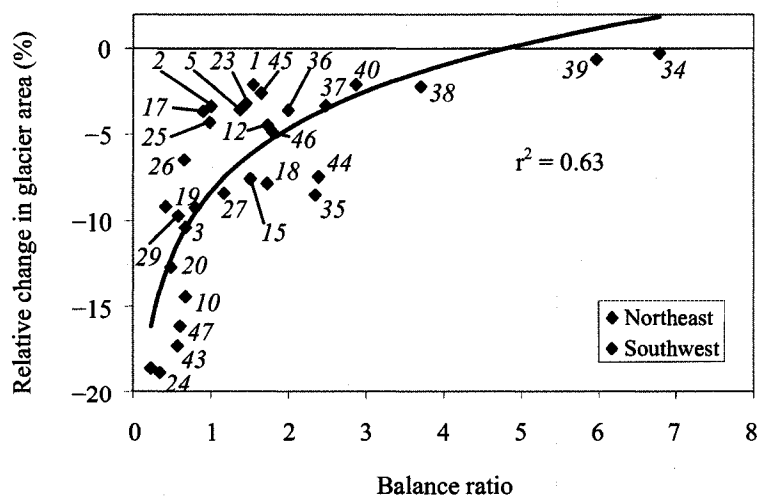


FIGURE 5.25. Plot of the relationship between calculated balance ratios and relative area change for outlet glaciers of the Bridge Icefield. The glaciers are separated based on the side of the icefield on which they are situated.

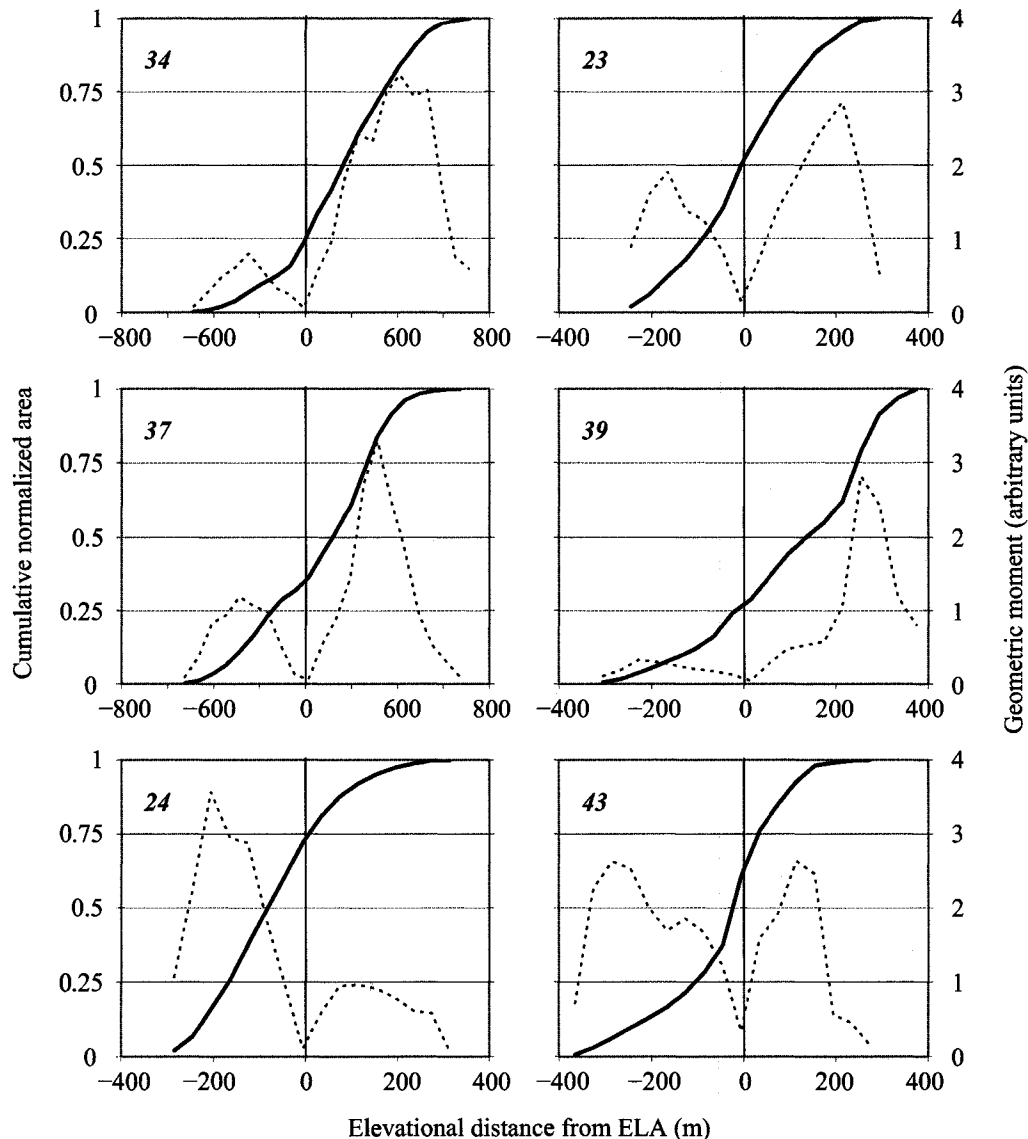


FIGURE 5.26. Sample hypsometric curves for selected outlet glaciers of the Bridge Icefield in relation to elevational distance from the estimated ELA. The distribution of geometric moments calculated from (8) is also shown (dashed lines).

There appears to be a spatial pattern of variation in BR values across the Bridge Icefield. Glaciers situated along the southwestern side of the icefield tend to have larger BR values and have typically undergone less dramatic changes than those along the northeastern side of the icefield. Many of the glaciers along the southwest margin have ELAs and terminus elevations that are 100–150 m or more below the regional average (~ 2300 m), indicating that average winter snowfall is greater on this side of the icefield. Evans (1990) identified a strong gradient in the glaciation level (altitudinal threshold for

glacier generation) across this locality, and related this to the presence of high mountain ranges that obstruct and likely divert air flow from the southwest. This suggests that the assumption that these glaciers are affected by similar climatic conditions (and climatic changes) may be false, which could account for some of the scatter about the trendline in Figure 5.25. Considering the distinction in the *BR* values on opposite sides of the icefield, and the fact that there is a considerable range of *BR* values with only minor differences in the relative area change of most glaciers along the wetter southwest margin of the icefield, it is possible that these glaciers are less sensitive to climatic change than those of the drier northeastern portion of the icefield. However, this seems to contradict the established notion that the sensitivity of mass balance to changes in temperature and precipitation increases with increasing annual precipitation (Meier, 1984; Oerlemans, 1992; Oerlemans and Fortuin, 1992; Oerlemans and Reichert, 2000). Alternatively, it may be that the changes in mass balance and ELA over the southwestern glaciers have been less significant than those over the glaciers to the northeast. A similar spatial pattern in relative area loss of individual glaciers is apparent across the entire central Coast Mountains. Typical relative losses become increasingly large over short (i.e., <50 km) distances toward the northeast, which suggests either that the glaciers further removed from the regional moisture source have undergone a greater response to recent climate forcing as a result of their more continental nature, or that they have been subjected to greater changes in mass balance.

b) Monashee Mountains

As with the glaciers of the Bridge Icefield, the larger glaciers of the Monashee Mountains that have undergone a significant loss of area (i.e., >20%) have a *BR* value that is generally less than 1.0. These glaciers have small AAR values (i.e., 0.26, 0.5, and 0.44 for glaciers # 2, 5, and 8 respectively), and with the exception of glacier # 5, have a greater elevational range above their ELA than below it. If the *BR* values of these glaciers were to have remained more-or-less the same over the period, given a rise in their ELA, this would have been achieved by significant area reduction of their ablation zones. An example of why this is the case is provided in figure 5.29, which shows

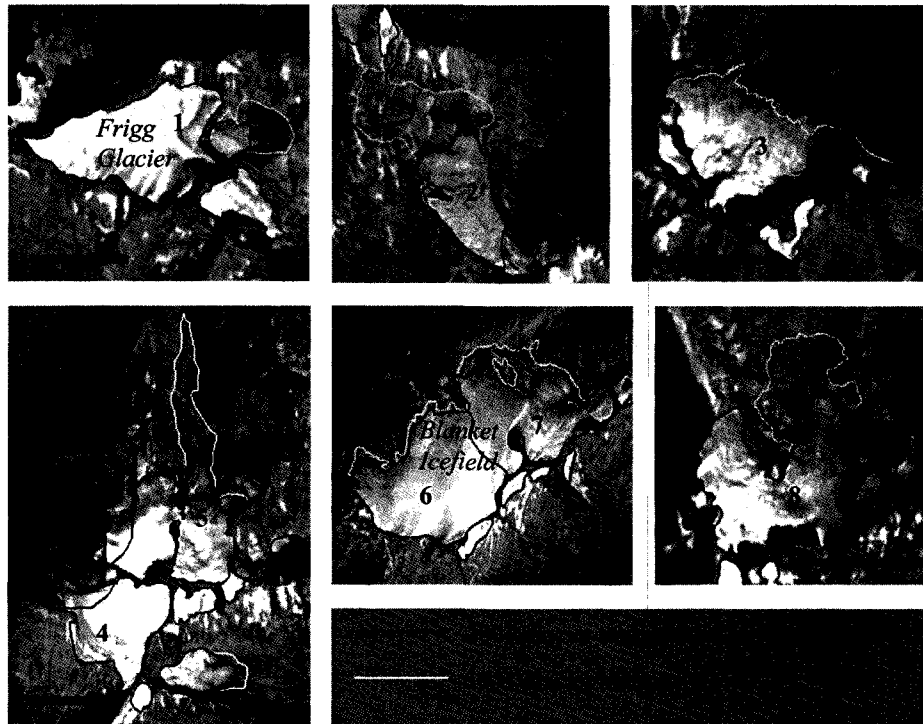


FIGURE 5.27. Net changes in surface extent of major glaciers of the southern Monashee Mountains over the period 1951–2001. The solid bars indicate a distance of 1 km.

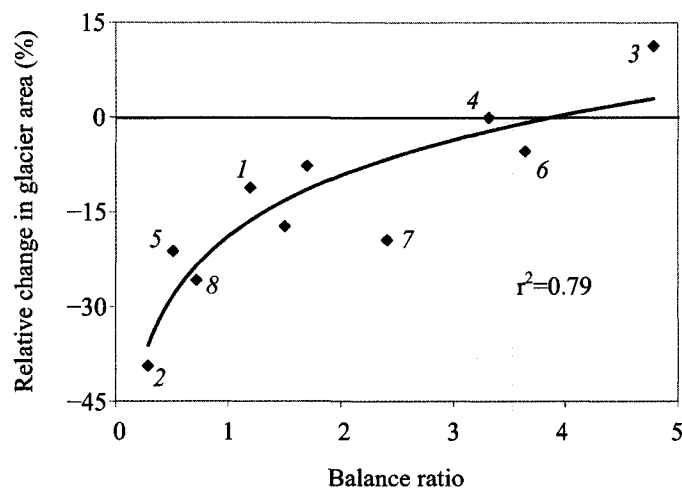


FIGURE 5.28. Plot of the relationship between calculated balance ratios and relative area change for major glaciers of the Monashee Mountains.

graphically how the values of m_c and m_b for glacier # 2 change given a 50 m rise in the ELA. The initial values of m_c and m_b are 2.05 and 7.08 (arbitrary units) respectively, giving a BR value of 0.29. A 50 m rise of the ELA from its initial state leads to a decrease in the value of m_c to 0.95. However, the value of m_b increases to nearly 11.0 because the large portion of area initially situated only a short distance below the ELA contributes substantially more to the moment m_b as it becomes further removed from the ELA. To maintain a constant BR value this term must decrease to ~ 3.3 , and this can only be achieved by the wastage of a significant amount of the ice within the range of 2100–2260 m. Comparison of figures 5.27 and 5.29 confirms that this has indeed begun to occur over the study period, and even without further changes in climate, frontal recession is likely to continue. A similar argument can be given for glaciers # 1 and 8. The situation is somewhat different for glacier # 5, where the ablation zone is confined to a narrow and gently sloping valley basin. As a result, the terminus of this glacier extends a long distance downvalley and is situated far below the ELA. A significant portion of the moment, m_b , is contributed by relatively small amounts of area that are situated at a large elevational distance below the ELA, leading to a situation in which a substantial amount of terminal retreat would be necessary to attain a new steady-state value of m_b following even a modest rise in the ELA. This is due in part to the low slope of the ice front (so that a large retreat corresponds to a relatively modest change in terminus

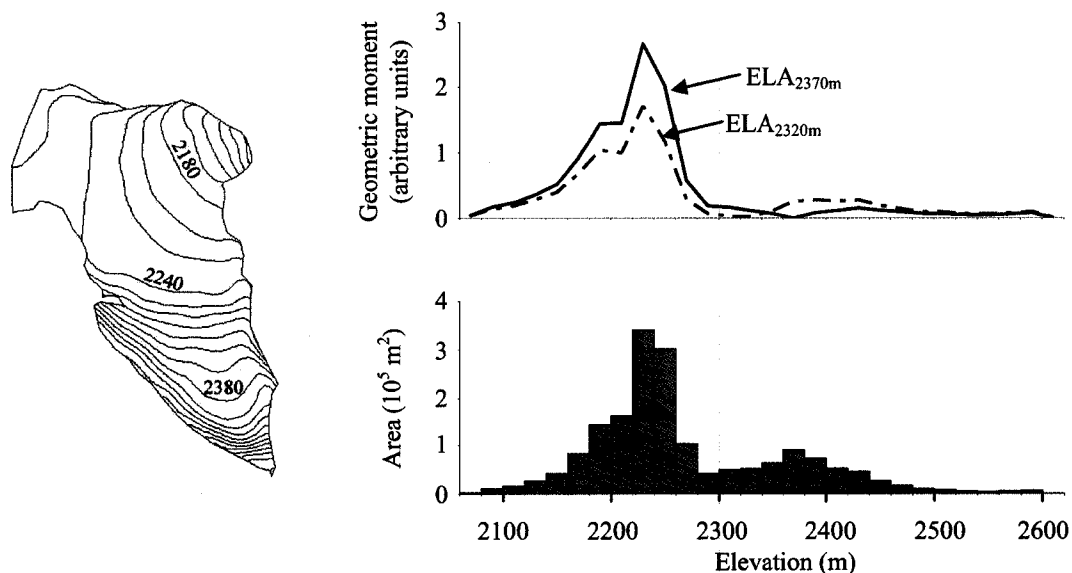


FIGURE 5.29. Hypsometric distribution of area and distribution of geometric moments calculated from (10) for glacier # 2 in the Monashee Mountains (contour interval is 20 m).

elevation), and to the shape of the upper glacier, where the value of m_c decreases rapidly as the ELA rises.

Glaciers that have undergone only limited retreat or advance have a BR value that is generally over 2.0, and have extensive accumulation zones with a greater elevation range above than below their ELA. Glaciers # 3, 4, and 6 each have a relatively wide and steep ablation zone, and taper in width in the upslope direction. To maintain a constant BR value following a change in the ELA, the moment m_c of these glaciers must necessarily change more than m_b . The retreat of their termini must therefore be limited as their planimetric area increases in the downslope direction and even minor frontal retreat could result in large changes of m_b .

No obvious spatial patterns of BR values or relative area change were observed in the Monashee Mountains. This implies that changes in climate have occurred uniformly across this region and that disparate responses of individual glaciers here are primarily a result of differences in valley basin topography, and hence, intrinsic sensitivity to climate change.

5.4.1.3 Uncertainty in ELA estimates

The calculated geometric BR values may be subject to error as a result of the subjective method used to determine steady-state ELAs. Estimates of BR values may vary by as much as $\pm 50\%$ or more as a result of only minor variations in the estimate of the ELA (Table 5.8). Although this uncertainty is large, it does not significantly alter the observed relationship between BR and relative area change. For example, glaciers of the Bridge Icefield that have experienced only very minor changes in area still have a BR value considerably greater than 1, even if the true ELA is 50–100 m higher than estimated. Similarly, those glaciers which have experienced the most significant relative loss of area typically have a BR of ~ 1 or less, even if the ELA is up to 50 m lower than estimated. Multiple years of mass balance – elevation data for Bridge and Place Glaciers confirm that the ELA is within this range of estimates. Furthermore, because the ice topography represented in the DEM reflects the mass balance conditions of the previous decades, it is more likely that ELAs during the study period are underestimated as a result of

TABLE 5.8. Variability of the balance ratio with different choices of ELA for several different glaciers of the Bridge Icefield.

Glacier ID	Area Change (%)	Calculated Balance Ratio			
		ELA-100m	ELA-50m	ELA+50m	ELA+100m
34	-0.3	17.6	10.9	4.1	2.4
38	-2.2	10.0	6.1	2.2	1.2
27	-8.4	2.2	1.6	0.8	0.6
20	-12.7	2.5	1.1	0.2	0.1
24	-18.9	2.6	0.9	0.1	0.05

systematic error. Therefore, the values of *BR* calculated with a higher ELA shown on the right side of table 5.8 provide a better indication of the direction of potential error associated with calculated *BR* values.

5.4.2 Basin Sensitivity

To further examine the influence of the hypsometry of individual glaciers on their observed area changes, a basin sensitivity index (*BS*) was used (Burgess and Sharp, 2004);

$$BS = \frac{\Delta AAR_{+120m}}{AAR}$$

(11)

where *AAR* is the accumulation area ratio of each individual glacier, and ΔAAR_{+120m} is the change in the *AAR* resulting from a 120 m rise in the ELA. (11) represents the fractional change in the accumulation area ratio resulting from a prescribed change in the ELA. For glaciers with a high *BS* value, a given rise in the ELA would result in a relatively large reduction in the glacier's accumulation area, and concomitantly, a large increase in the glacier's ablation area. Therefore, the mass balance of a glacier with a high *BS* value would be affected to a greater extent than that of a glacier with a lower *BS* value. This index was derived for the same glaciers as those in the previous analyses.

The relative changes in glacier area are only marginally related or unrelated to the *BS* index in all regions of this study with the exception of the Bridge Icefield. Here the

relative change in area of individual outlet glaciers displays a negative linear trend with the *BS* index ($r^2=0.44$), where glaciers with a relatively high *BS* value have lost a greater

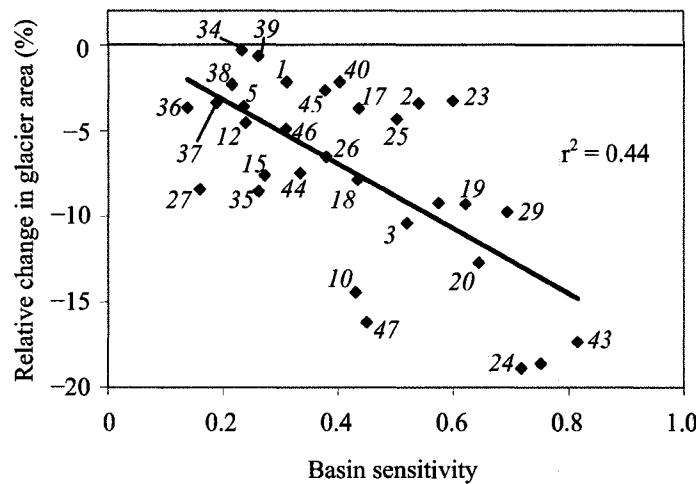


FIGURE 5.30. Plot of the relationship between calculated basin sensitivity index values and relative area change for outlet glaciers of the Bridge Icefield.

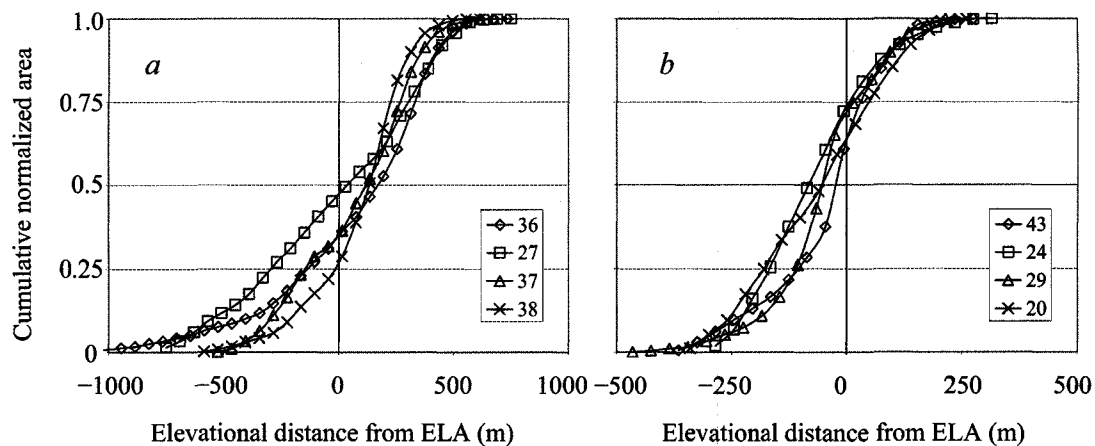


FIGURE 5.31. Hypsometric curves of selected outlet glaciers of the Bridge Icefield with a: low basin sensitivity values, and b: high basin sensitivity values.

fraction of their area than those with a relatively low *BS* value (Fig. 5.30). The glaciers with relatively low *BS* values (i.e., <0.3) have an initially low ELA and a high value of the AAR, which make them less susceptible to climatic changes. These glaciers typically have less than $\sim 40\%$ of their cumulative area situated below the ELA (Fig. 5.31a). Also,

the ELAs of these glaciers generally intersect relatively gently sloping sections of their hypsometric curve so that moving the ELA from its current location results in changes in accumulation area that are small relative to the total drainage basin area. Glaciers with a high *BS* value (i.e., >0.5), in contrast, have higher ELAs that intersect near the steepest section of their hypsometric curves, and low AARs with over 60% of their area situated below the ELA (Fig 5.31b). It is the elevation range of individual glaciers, however, that is the primary difference between glaciers with high and low basin sensitivity values, as the AAR of larger glaciers with a greater range of elevation is much less sensitive to changes in the ELA. This is essentially because a given change in the ELA covers a smaller fraction of the total elevation range, and thus the total area of these glaciers (e.g., the normalized hypsometric curve of these glaciers has a much lower overall slope than glaciers with a high *BS* value). Therefore, a significant amount of the variation in the calculated values of basin sensitivity is due to differences in the area of individual outlet glaciers, and part of the relationship in figure 5.31 is simply a reflection of this dependency (Fig 5.32; see also Fig 5.15).

Many of the glaciers of the southwest margin of the Bridge Icefield have characteristically low *BS* values, while others along the northeast margin have a higher *BS* value (Fig 5.30). This suggests that for a uniform increase in the ELA over all parts of the icefield, many of the glaciers along the northeastern side would experience the greatest relative change in mass balance, and depending on their shape and size, undergo more extensive terminal retreat. This partly explains the observed spatial pattern of glacier area changes across the icefield and the relationship shown in figure 5.30. The remaining variance is likely accounted for by differences in the slope and response time,

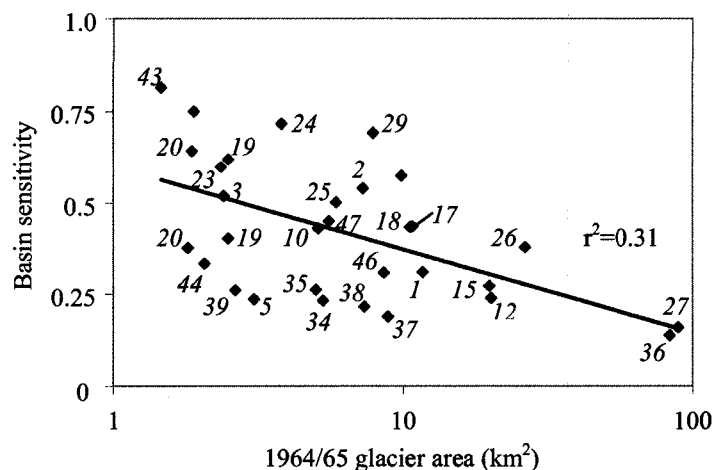


FIGURE 5.32. Dependence of basin sensitivity index on area of individual outlet glaciers of the Bridge Icefield.

balance ratio, and the climate regime (increasingly drier over short distances to the northeast) of individual glaciers.

The dependence of *BS* values on glacier area (and thus elevational range) provides simple insight into the greater relative change in area observed for many of the smaller glaciers. A given rise in the average ELA across a region due to a spatially uniform change in climate results in a large relative change in the AAR and the overall mass balance of small glaciers. The overall mass balance of larger glaciers is not affected as significantly by a given rise in the ELA, and therefore the magnitude of the relative change in area is not as large. However, because the decrease in specific balance rates occurs over a more extensive area on larger glaciers, the total change in mass is greater, and absolute changes in surface area and volume are therefore larger (Fig 5.15b).

The dependence of *BS* values on glacier area also helps to explain the lack of any significant correlation between *BS* values and relative changes in area in the Columbia and Rocky Mountains (not shown). Because size has not been as significant a factor in the response of these glaciers compared with those of the Bridge Icefield, it follows that changes in area should show less dependence on *BS* values.

5.5 SENSITIVITY TO FURTHER CLIMATIC CHANGE

In addition to identifying regional variability in the recent changes of glaciers that have taken place in the southern Cordillera, part of the objective of this work is to highlight regions where the present ice cover may be sensitive to further climatic change. This task is facilitated by the identification and more thorough understanding of the principal factors affecting the sensitivity and response of these glaciers. In general, the most sensitive glaciers are those which have some combination of:

- i. a large amount of surface area situated at large distances below the ELA,
- ii. a very gentle slope over the lower ablation zone, and

- iii. a shape that decreases in width in the downslope direction, with a narrow valley confining the lower ablation zone.

Glaciers that possess these general characteristics and are relatively large in size are likely to undergo continued retreat and lose a significant amount of ice, even if further climatic change is minimal. This is because such glaciers generally respond more slowly than smaller glaciers due to their size and slope (Bahr et al., 1998; Paterson, 1994; Pelto and Hedlund, 2001), and will probably continue to adjust to the recent reduction in mass balance for some time. The longer response time implies that not only will the period of adjustment be longer, but that the overall magnitude of the final response will be greater (Harrison et al., 2001). Therefore, it is these glaciers that must be identified in order to better understand the changes in ice cover and regional water resources that may take place over the next several decades.

5.5.1 Coast Mountains

The Pacific Ranges of the Coast Mountains contain numerous large valley and outlet glaciers that have the general characteristics listed above. These glaciers are situated within a very high precipitation climate regime and have a high melt rate over their lower ablation zone, which implies a high rate of mass turnover and thus high sensitivity to climatic change (Meier, 1984; Oerlemans and Fortuin, 1992). As previously mentioned, melting may occur throughout much of the year on the lower reaches of the larger glaciers, and so even an increase in winter temperature can lead to significant reductions in mass balance. In addition, the change in the fraction of precipitation falling as snow with a change in temperature is large. Within the region analyzed in this study, the largest glaciers are found along the central ranges where a strong gradient in climate exists. The transition from maritime to more continental-like conditions occurs over a very short distance here (Evans, 1990), so it is likely that under any climate change scenario the glaciers in this region will be affected differentially. Based on their observed recent behavior, glaciers further removed from the coast will likely undergo relatively greater reductions in area and volume because of their more continental nature. The greatest loss of ice, however, will occur on the larger glaciers along the central

ranges, as they have likely not yet adjusted to the recent climatic changes, and because they remain highly sensitive to further changes in temperature and precipitation.

A simple analysis was conducted to estimate the possible extent of further retreat of the Bridge Glacier. Figure 5.33 shows the distribution of the geometric moments of

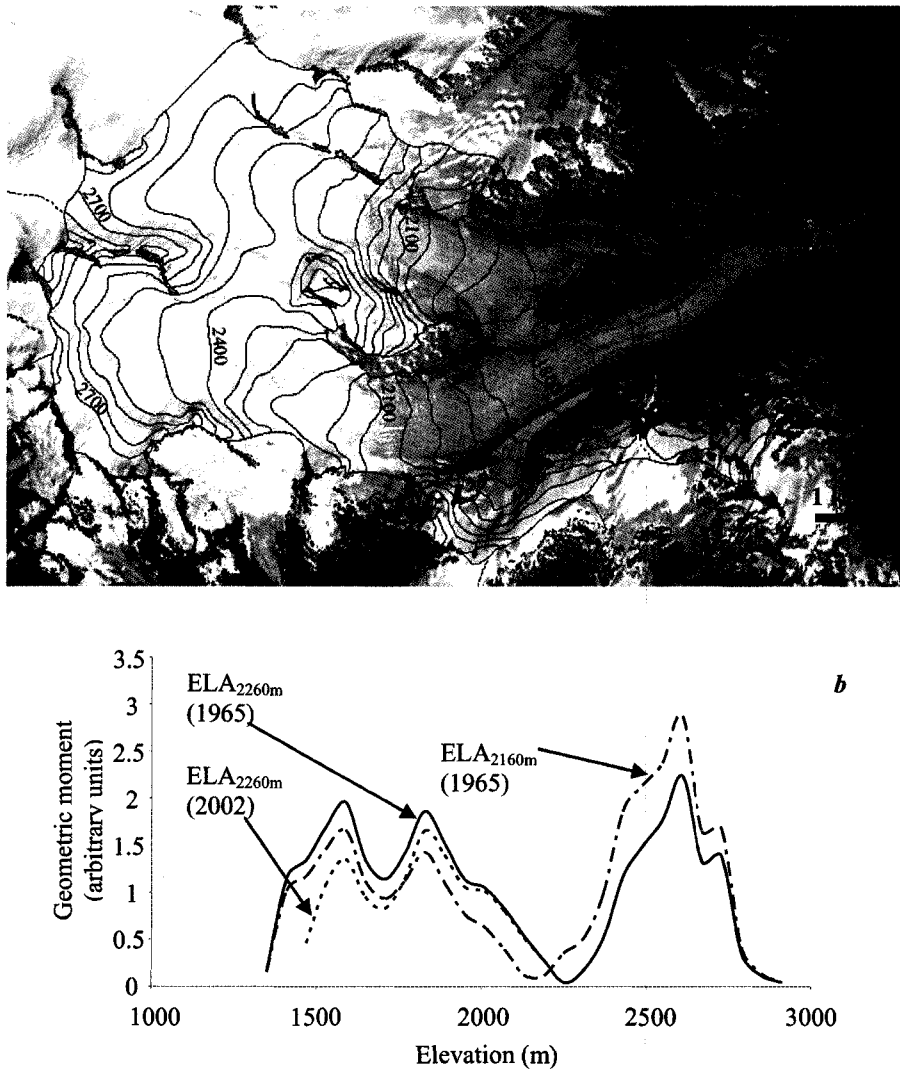


FIGURE 5.33. Hypsometry of the Bridge Glacier; (a) ice margin and surface topography of the Bridge Glacier in 1965 shown over the 2002 ETM+ image; (b) distribution of geometric moments calculated from (10) for different ELAs and surface extents. The distribution for the 2002 surface does not take into account changes in ice surface elevation that have occurred over the ablation zone.

area with respect to the ELA. The calculated BR for the 1965 ice surface is 1.17, with a steady-state ELA of 2160 m and values of 15.1 and 12.9 (arbitrary units) for m_c and m_b

respectively. A 100 m rise in the ELA results in a decrease of the value of m_c to 10.6, and an increase of m_b to 17.5, and so to maintain a constant value of BR , a significant amount of ice wastage must occur in the lower ablation zone. Over the period 1965–2002 the glacier did indeed undergo a frontal retreat of nearly 2 km in addition to decreasing in width over a large portion of the ablation zone. This resulted in the value of m_b decreasing to 12.5. In order for the glacier to reach a new equilibrium condition this value must continue to decrease to ~ 9.1 , and this would be achieved by a further terminal retreat of ~ 1 km and reduction in width of 100–200 m over the lower ablation zone. This assumes, however, that the surface elevation of the glacier at any given location remains fixed, which is an invalid assumption. In fact, the ice surface elevation over the lowermost portion of the ablation zone has decreased by an average of 4–5 m W.E. each year over the 1970s and 80s (personal communication B. Menounos, May 2005). By taking the effect of this surface lowering into consideration, the current value of m_b is estimated to be 14.6, despite the fact that a large portion of the lower ablation zone has disintegrated. The glacier surface situated below ~ 1700 m (with reference to the 1965 hypsometry) contributes significantly to the geometric moment, as does the wide section between ~ 1750 and 1900 m. Frontal retreat of as much as 3 km or more, along with a significant reduction in width from the present margins will be necessary to bring the moment, m_b , to its new equilibrium value.

This retreat is based on a 100 m rise of the ELA from its steady-state position, which has likely occurred during the study period. This is therefore the adjustment the glacier will undergo in the absence of any further forcing. Assuming the ELA rises by another 50 m, the reduction of the value of m_c and increase of the value of m_b would require the terminus to retreat by as much as 7–8 km from its present position in order to re-establish an equilibrium state. The retreat and loss of ice could be even greater considering that lowering of the surface would also occur.

This simple analysis shows that this glacier and many others in the region with similar characteristics are still adjusting to recent changes in climate, and are highly sensitive to any further reduction in snowfall or increase in temperature. The results are only useful as a general estimate of the magnitude of the final response, however, as uncertainty in the calculation of BR and the influence of other factors may result in

considerable variation in the estimates. For example, the lack of topographic control for the glacier surface in 2002 is problematic for an accurate calculation of BR , and it may be that the changes in surface topography are not realistically reflected by the simple change in elevation assigned to the individual hypsometric bins in this analysis. Rotation of either or both of the curves b_{nb} and b_{nc} in addition to vertical translation could result in a change in the value of BR , thereby changing the magnitude of the final adjustment necessary to restore equilibrium. Also, surface lowering over the ablation zone increases the slope of the glacier, which increases the strain rate and ice velocity, shortens the response time, and reduces the magnitude of the final response. Nonetheless, it is clear that this glacier, and likely many others here, will continue to shrink in the coming decades, and remain sensitive to further climatic change.

5.5.2 Other Regions

A similar analysis was not performed for glaciers of the Columbia or Rocky Mountains, but the relative sensitivity of the larger glaciers in this region was estimated based on their present geometric characteristics. In the Purcell Mountains, the influence of slope near the terminus was observed to be the most important factor controlling the response of the larger glaciers. Based on this, the sensitivity of glaciers to further climatic change was assessed by estimating how the slope over the present ablation zone may have changed over the study period. For example, the absence of changes along the lateral margins just up from the terminus on the Conrad Glacier suggests that surface lowering has been minimal over the period 1951–2001 (Fig 5.34). Since the surface slope over this region has remained low over a distance of many kilometers, the glacier is highly sensitive to a further increase in its ELA. Should the terminus retreat beyond the short, steeper section where the tributaries converge, rapid rates of retreat over the eastern arm of the glacier may follow. In contrast, the lateral margins of the Starbird Glacier have changed substantially over the same period, indicating that surface lowering has occurred here and that the present front is now considerably steeper. Its sensitivity has therefore been reduced as a result of the wastage of ice in its ablation zone. The difference in sensitivity between these two glaciers is also highlighted by the fact that their present

termini have an elevation difference of nearly 500 m. The terminus elevation of the Starbird Glacier is now ~2300 m, having retreated ~2 km upvalley from an elevation of ~1950 m, while that of the Conrad Glacier is now ~1840 m, having retreated ~700 m from an elevation of ~1720 m. This may also be due in part to differences in the response time of these glaciers, where the larger Conrad Glacier has been slower to adjust

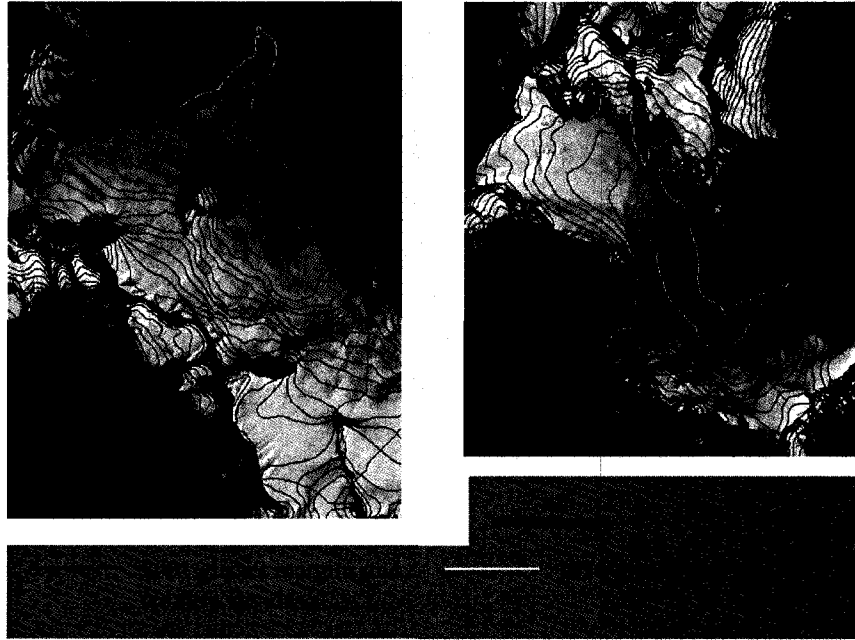


FIGURE 5.34. Surface topography (ca. 1950) and margins of the Conrad (left) and Starbird (right) Glaciers in the Purcell Mountains (contour interval is 40 m).

to recent changes in climate.

Other than the Conrad, Vowell and Jumbo Glaciers, most of the large glaciers in the Purcell Mountains appear to be less sensitive than they were at the start of the study period. Glaciers that have retreated substantially have lost large portions of their ablation area that were gently sloping, and have either become steeper at their terminus or have retreated to steeper sections along their longitudinal profile. Because of the low slope over a large portion of the ablation zone of the Vowell Glacier, and the fact that most of the ablation zone of the Jumbo Glacier appears to calve into a lake, which may facilitate its disintegration, these glaciers remain highly sensitive. Glaciers with an initially steep terminus have maintained this profile and are therefore no more sensitive than at the start of the study period. A further change in the ELA of all glaciers here would still result in

their retreat, but other variables constant, the declining sensitivity indicates that it would not have as great an effect as the recent change in climate.

The same pattern was observed in other parts of the Columbia Mountains and the Rocky Mountains. Most of the highly sensitive glaciers have adjusted in a manner that has reduced their sensitivity to further change. This is clear for the glaciers of the Monashee Mountains, where those with a large amount of area situated below their ELA

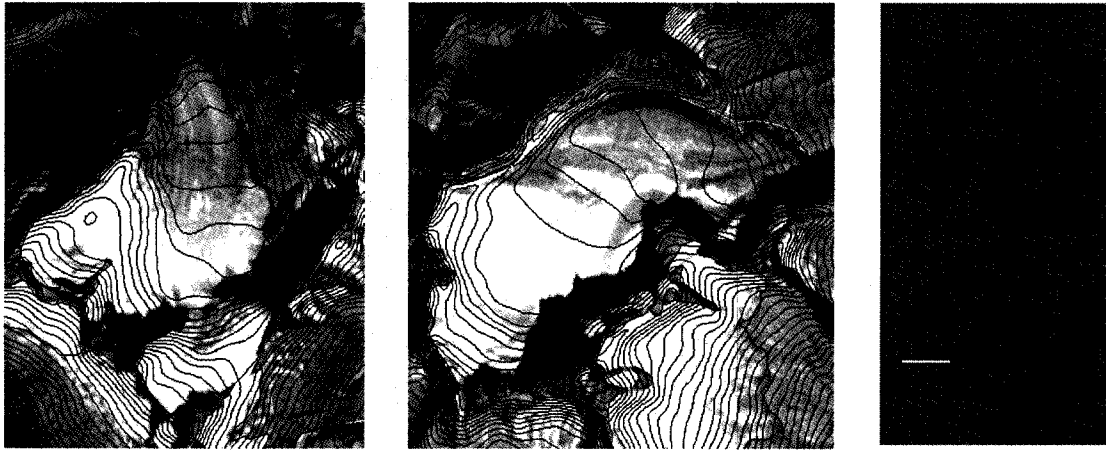


FIGURE 5.35. Surface topography (ca. 1950) and margins of the Wrong (left) and Nemo (right) Glaciers in the Selkirk Mountains (contour interval is 30 m).

have lost a substantial portion of their ablation zone. Long and narrow valley glaciers such as # 5 in the Monashee Mountains, and the Mangin – Marlborough Glaciers in the Rocky Mountains have retreated far upvalley to locations where specific melt rates are greatly reduced. The Tenderfoot Glacier in the Selkirk Mountains, which has significantly altered its planimetric shape in the previous decades, has responded in a similar manner by retreating far upvalley.

Several glaciers in the Selkirk Mountains, including the Wrong and Nemo Glaciers, have large sections with a relatively low slope situated not far upglacier from their present terminus (Fig 5.35). If future changes in their ELAs are sufficient to cause retreat of their termini beyond the short, steep sections near their fronts, these glaciers could potentially become very sensitive. Although these glaciers underwent little or no change in area over the study period, it appears that if a low climatic threshold is surpassed, these glaciers may once again resume a state of rapid retreat. With greater climatic change and rising regional ELAs, the large distribution of upland ice in the

Purcell Mountains (e.g., the Conrad, Four Squatters, and Macbeth Icefields) could become highly sensitive and undergo a substantial response. Much of this ice is situated on broad plateaus, which may be subjected to persistent melting conditions as the ELA migrates large distances across them. Therefore, although the sensitivity of glaciers to a minor rise in the ELA has likely been reduced, more significant changes in climate may yet cause extensive wastage of ice in this region.

6. SUMMARY AND CONCLUSIONS

This study has compared the extent of glaciers at two different time periods using remotely sensed imagery acquired in 1951/52 over the southern Columbia and Rocky Mountains, 1964/65 over the southern Coast Mountains, and 2001/02 over all regions. Across the study region, glacier surface area has decreased by $146 \pm 10 \text{ km}^2$, which corresponds to a loss of $\sim 5\%$ of the initial ice covered area. The use of an empirical volume – area scaling relationship indicates that this retreat has resulted in a loss of $13 \pm 3 \text{ km}^3$ of ice, which corresponds to a 0.03 mm rise in sea level. Most of this wastage is due to the retreat of large glaciers in the Coast Mountains, many of which retreated by up to several kilometers over the study period. The retreat of glaciers in the Purcell Mountains has also contributed significantly to the overall wastage. Some of the larger glaciers here have retreated by 1–2 km and undergone significant reductions in area and volume. Many of the largest glaciers in the Rocky and Monashee Mountains have undergone a substantial relative reduction in size over this period, losing over 20% of their area in many cases. Their comparatively small size, however, has limited the overall loss of ice volume from these regions. Few glaciers in the Selkirk Mountains have undergone any noticeable change in area, and ice volume loss here was the lowest from any mountain range in this study.

Changes in climate have occurred in a consistent manner across the region during the study period. A recent increasing trend in average winter, spring, and annual temperature has been observed at stations in all parts of the study area. Apart from changes in temperature, the 1976–77 PDO regime shift has disparately affected winter snowfall amounts in different parts of the study area. The greatest reductions have occurred in the Coast Mountains, where winter snowpack depths have declined by some

300–800 mm s.w.e, or an average of 30%. In other parts of the study area the reduction in winter snowfall has been between 100 and 300 mm s.w.e. At a regional scale, differences in the response of glaciers to recent climatic changes have likely resulted from differences in the climate regime (maritime or continental) of specific parts of the study area. The greater sensitivity of maritime glaciers, together with the fact that reductions in winter accumulation have been greatest near the coast, may partly explain the more extensive amount of frontal retreat and ice wastage that has been observed in the Coast Mountains.

In all parts of the study area, the response of glaciers to recent climate trends was observed to be highly variable at the local scale. This is thought to be a result of both strong local gradients in climatic regime, and differences in the intrinsic sensitivity of individual glaciers to climate change. For the glaciers of the Bridge Icefield along the central ranges of the Coast Mountains, there appears to be a spatial pattern in the area changes of the individual outlet glaciers, where glaciers to the northeast have undergone relatively greater reductions in size. This may be due to the fact that they are further removed from the regional moisture source. Further variation in the response of the individual glaciers here is explained by differences in their slope, response time, and hypsometry. Glacier slope and response time have had a significant influence on the behavior of glaciers throughout the study area. All of the glaciers that have undergone only very minor changes or a slight net advance are among the steepest in their respective regions, while those with a very low slope (near the terminus) have generally undergone considerable retreat. This is likely due to the fact that steep glaciers with rapid response times have advanced at one or more times during the study period, while more gently sloping glaciers with longer response times have been in a continuous mode of retreat. In addition, as a result of the increasing importance of the surface height – mass balance feedback for glaciers with a low slope, these glaciers typically undergo a greater overall adjustment. Glacier hypsometry has been important in controlling the response of individual glaciers in some localities, most notably the Bridge Icefield area and the Monashee Mountains. Glaciers with a significant area of ice situated at large distances below the ELA are more sensitive and must undergo a greater geometric adjustment to reach a new equilibrium state following a rise of the ELA. Several other geometric

variables, including glacier size, shape, and elevation, have also been found to be of importance in terms of the sensitivity of the glaciers here. Glaciers that descend to low elevations or taper in width in the downslope direction underwent the greatest changes in many instances. Many of the smaller glaciers have lost a greater fraction of their surface area and volume, but most of the observed loss of ice in this study is due to the retreat of a few of the largest glaciers in individual mountain ranges. Finally, in all regions of this study, the smallest glaciers have remained essentially unchanged as a result of their sheltered location and reduced sensitivity to climatic change.

Many of the glaciers in the coastal region, as well as some larger glaciers in the Columbia and Rocky Mountains remain very sensitive to further climatic change. In the following decades the retreat of many of these glaciers should continue, even in the absence of additional climate forcing. Continued warming or reduction of snowfall will result in even greater losses of ice, which could further impact the volume of meltwater contributed to rivers during the late summer and the regulatory capability of these glaciers on regional streamflow. As glacier cover becomes increasingly reduced in these watersheds, runoff patterns will tend to become more characteristic of those from unglaciated basins. This would imply further reductions in mean flow during the late summer and an increase in year-to-year flow variability.

The results of this study will contribute to ongoing glacier inventory work in the Canadian Cordillera, and will facilitate efforts to assess the impact of changes in regional glacier cover on streamflow. Further research should compare the changes in glacier extent to streamflow variations at individual stations throughout the region. An improved understanding of the connection between runoff from glacierized catchments and the loss of glacier surface area and volume after accounting for variations in regional precipitation and temperature will assist glacio-hydro-meteorological modeling studies. Such modeling studies are necessary to predict runoff under future climate scenarios, which is essential for future water resource management planning, and the models that are developed will be able to more accurately simulate and predict runoff given an improved parameterization of regional glacier coverage.

Glacier inventory work remains to be completed for a large portion of the Canadian Cordillera, including more northerly regions in British Columbia and much of

the Yukon Territory. This work will benefit from the use of automated procedures of image analysis together with digital terrain data and GIS technology, as manual delineation of ice boundaries is time-consuming, labor intensive, and impractical over very extensive regions. Semi-automatic methods that combine multispectral classification with digital terrain analysis and GIS-based neighborhood relation and change detection (e.g., Paul et al., 2004b) may reduce errors that result from the misclassification of late-lying snow and debris-covered ice. Manual correction of the results will likely be necessary, however, since these procedures cannot fully resolve all the error inherent in the classification of the imagery. Finally, the data produced from such an approach will be in a suitable format for submission into the GLIMS digital database to inventory the world's glaciers. Therefore, the data may be distributed to other GLIMS collaborators and used for an improved understanding of global-scale glacier – climate interactions and sea-level change, in addition to impacts on regional water resources.

REFERENCES

- Bahr D., M. Meier and S. Peckham, 1997. The physical basis of glacier volume-area scaling. *Journal of Geophysical Research*, **102** (B9), pp. 20,355-20,362.
- Bahr D., T. Pfeffer, C. Sassolas, and M. Meier, 1998. Response time of glaciers as a function of size and mass balance. *Journal of Geophysical Research*, **103** (B5), pp. 9777-9782.
- Bishop M., J. Olsenholler, J. Shroder, R. Barry, B. Raup, A. Bush, L. Copland, J. Dwyer, A. Fountain, W. Haerberli, A. Käab, F. Paul, D. Hall, J. Kargel, B. Molnia, D. Trabant, and R. Wessels, 2004. Global Land Ice Measurements from Space (GLIMS): remote sensing and GIS investigations of the Earth's cryosphere. *Geocarto International*, **19** (2), pp. 57-84.
- Bitz C. and D. Battisti, 1999. Interannual to decadal variability in climate and the glacier mass balance in Washington, Western Canada, and Alaska. *Journal of Climate*, **12**, pp. 3181-3196.
- Braithwaite R., and Y. Zhang, 1999. Modelling changes in glacier mass balance that may occur as a result of climate changes. *Geografiska Annaler*, **81** A, pp. 489-496.
- Burgess D. and M.J. Sharp, 2004. Recent changes in areal extent of the Devon Ice Cap, Nunavut, Canada. *Arctic, Antarctic, and Alpine Research*, **36** (2), pp. 261-271.
- Chen J. and A. Ohmura, 1990. Estimation of glacier water resources and their change since the 1870s. In: *Proceedings of the two Lausanne Symposia, August 1990*. IAHS Publication no. 193, pp. 127-135.
- Cogley J. and P. Adams, 1998. Mass balance of glaciers other than the ice sheets. *Journal of Glaciology*, **44** (147), pp. 315-325.
- Demuth M. and R. Keller, 2005. An assessment of the mass balance of Peyto Glacier (1966–1995) and its relation to recent and past-century climatic variability. In: *Peyto Glacier: One Century of Science*. Demuth, M.N., Munro, D.S., Young, G.J. (eds). National Hydrological Research Institute Scientific Report 8, pp. 83-132.
- Demuth M. and A. Pietroniro, 2002. The impact of climate change on the glaciers of the Canadian Rocky Mountain eastern slopes and implications for water resource-related adaptation in the Canadian Prairies: phase I—headwaters of the North Saskatchewan River basin. *Climate Change Action Fund—Prairie Adaptation Research Collaborative Project P55*, 162 pp. and technical appendices.
- Dyurgerov M., 2001. Mountain glaciers at the end of the twentieth century: global analysis in relation to climate and water cycle. *Polar Geography*, **25** (4), pp. 241-336.
- Dyurgerov M. and M. Meier, 1997. Mass balance of mountain and subpolar glaciers: a new global assessment for 1961-1990. *Arctic, Antarctic and Alpine Research*, **29** (4), pp. 379-391.
- Dyurgerov M. and M. Meier, 2000. Twentieth century climate change: evidence from small glaciers. *Proceedings of the National Academy of Sciences of the USA*, **97** (4), 1406-1411.
- Dyurgerov M. and M. Meier, 2005. Glaciers and the changing Earth system: a 2004 snapshot. *Occasional paper No. 58, Institute of Arctic and Alpine Research*, University of Colorado, Boulder, 117 pp.
- Evans I., 1990. Climatic Effects on glacier distribution across the Southern Coast Mountains, B.C., Canada. *Annals of Glaciology*, **14**, pp. 58-64.
- Evans I., 2004. Twentieth-century change in glaciers of the Bendor and Shulaps Ranges, British Columbia Coast Mountains, *Quaternary Newsletter*, ISSN 0 143-2826 (104), pp. 70-72.
- Fountain A., and W. Tangborn, 1985. The effect of glaciers on streamflow variations, *Water Resources Research*, **21**, pp. 579–586.

- Furbish D., and J. Andrews, 1984. The use of hypsometry to indicate long-term stability and response of valley glaciers to changes in mass transfer. *Journal of Glaciology*, **30** (105), pp. 199-211.
- Haerberli W., 1990. Glacier and permafrost signals of 20th-century warming. *Annals of Glaciology* **14**, pp. 99-101.
- Haerberli W., R. Frauenfelder, M. Hoelzle and M. Maisch, 1999. On rates and acceleration trends of global glacier mass changes. *Geografiska. Annaler.*, **81 A** (4), pp. 585-591.
- Harrison W., D. Elsberg, K. Echelmeyer, and R. Krimmel, 2001. On the characterization of glacier response by a single time-scale. *Journal of Glaciology*, **47** (159), pp. 659-664.
- Hock R., 2003. Temperature index melt modeling in mountain areas. *Journal of Hydrology*, **282** (1-4), pp. 104-115.
- Hodge S., C. Trabant, R. Krimmel, T. Heinrichs, R. March and E. Josberger, 1998. Climate variations and changes in mass of three glaciers in Western North America. *Journal of Climate*, **11** (9), pp. 2161-2179.
- Holland S., 1976. *Landforms of British Columbia: A Physiographic Outline*. Bulletin 48, British Columbia Department of Mines and Petroleum Resources, Victoria, B.C., 138 pp.
- Hopkinson C. and G. Young, 1998. The effect of glacier wastage on the flow of the Bow River at Banff, Alberta, 1951-1993. *Hydrological Processes*, **12** (10-11), pp. 1745-1762.
- IPCC (Intergovernmental Panel on Climate Change), 2001. *Climate Change 2001: Impacts, Adaptation and Vulnerability. Contribution of Working Group II to the Third Assessment Report of the Intergovernmental Panel on Climate Change*, edited by J.J. Mc Carthy, O.F. Canziani, N.A. Leary, D.J. Dokken, and K.S. White, Cambridge University Press, Cambridge.
- Jansson P., R. Hock and T. Schneider, 2003. The concept of glacier storage: a review. *Journal of Hydrology*, **282** (1-4), pp. 116-129.
- Johannesson T., C. Raymond, and E. Waddington, 1989. A simple method for determining the response time of glaciers. In: *Glacier fluctuations and climate change* J. Oerlemans (ed.), Kluwer Academic Publishers, pp. 343-352.
- Leonard K. and A. Fountain, 2003. Map-based methods for estimating glacier equilibrium-line altitudes. *Journal of Glaciology*, **49** (166), pp. 329-336.
- Luckman B., 1998. Landscape and climate change in the central Canadian Rockies during the 20th century. *Canadian Geographer*, **24** (4), pp. 319-336.
- Luckman B., 2000. The Little Ice Age in the Canadian Rockies. *Geomorphology*, **32**, (3-4), pp. 357-384.
- Luckman B., 2005. The Neoglacial history of Peyto Glacier. In *Peyto Glacier – one century of science*. Edited by M.N. Demuth, D.S. Munro, and G.J. Young. National Hydrology Research Institute (NHRI), Saskatoon, Sask., Science Report 8, pp. 25-57.
- Luckman B., K. Harding, and J. Hamilton, 1987. Recent glacier advances in the Premier Range, British Columbia. *Canadian Journal of Earth Sciences*, **24** (6), pp. 1149-1161.
- Mantua N., S. Hare, Y. Zhang, J. Wallace and R. Francis, 1997. A Pacific interdecadal climate oscillation with impacts on salmon production. *Bulletin of the American Meteorological Society*, **78** (6), pp. 1069-1079.
- McCabe G., A. Fountain and M. Dyurgerov, 2000. Variability in winter mass balance of northern hemisphere glaciers and relation with atmospheric circulation. *Arctic, Antarctic, and Alpine Research*, **32** (1), pp. 64-72.
- McCarthy D. and Smith D, 1994. Historical glacier activity in the vicinity of Peter Lougheed Provincial Park, Canadian Rocky Mountains, *Western Geography*, **4**, pp. 94-109.
- Meier M., 1984. Contribution of small glaciers to global sea level. *Science*, **266** (4681), pp. 1418-1421.
- Meier M., M. Dyurgerov and G. McCabe, 2003. The health of glaciers: Recent changes in glacier regime. *Climatic Change*, **59** (1-2), pp. 123-135.
- Moore R., 1996. Snowpack and runoff responses to climatic variability, southern Coast Mountains, British Columbia. *Northwest Science*, **70** (4), pp. 321-333.
- Moore R. and I. McKendry, 1996. Spring snowpack anomaly patterns and winter climatic variability, British Columbia, Canada, *Water Resources Research*, **32** (3), pp. 623-632.
- Moore R. and M. Demuth, 2001. Mass balance and streamflow variability at Place Glacier, Canada, in relation to recent climatic fluctuations. *Hydrological Processes*, **15** (18), pp. 3473-3486.
- Natural Resources Canada (NRCan), 2006. Landsat 7 orthorectified imagery over Canada, *GeoGratis*, <http://geogratias.cgdi.gc.ca/clf/en>, Accessed January 2005.

- Oerlemans J., 1989. On the response of valley glaciers to climatic change. In: *Glacier Fluctuations and Climatic Change*, J. Oerlemans (ed.), Kluwer Academic Publishers, pp. 353-371.
- Oerlemans J., 1992. Climate sensitivity of glaciers in southern Norway: application of an energy-balance model to Nigardsbreen, Hellstrugubreen and Alfotbreen. *Journal of Glaciology*, **38** (129), pp. 223-232.
- Oerlemans J., 2000. Holocene glacier fluctuations: is the current rate of retreat exceptional? *Annals of Glaciology*, **31**, pp. 39-44.
- Oerlemans J., and J. Fortuin, 1992. Sensitivity of glaciers and small ice caps to greenhouse warming. *Science*, **258** (5079), pp. 115-117.
- Oerlemans J., B. Anderson, A. Hubbard, P. Huybrechts, T. Johannesson, W. Knap, M. Schmeits, A. Stroeven, R. van de Wal, J. Wallinga, and Z. Zuo, 1998. Modeling the response of glaciers to climate warming. *Climate Dynamics*, **14** (4), pp. 267-274.
- Paterson W.S.B., 1994. *The physics of glaciers*, 3rd ed. Pergamon Press, Oxford, England, 481 pp.
- Paul F., A. Kääb, M. Maisch, T. Kellenberger and W. Haeberli, 2004a. Rapid disintegration of Alpine glaciers observed with satellite data. *Geophysical Research Letters*, **31** (21), L21402, doi:10.1029/2004GL020816.
- Paul F., C. Huggel, and A. Kääb, 2004b. Combining satellite multispectral image data and a digital elevation model for mapping debris-covered glaciers. *Remote Sensing of Environment*, **89** (4), pp. 510-518.
- Pelto M., and C. Hedlund, 2001. Terminus behavior and response time of North Cascade glaciers, Washington, U.S.A. *Journal of Glaciology*, **47** (158), pp. 497-506.
- Sidjak R., and R. Wheate, 1999. Glacier mapping of the Illecillewaet icefield, British Columbia, Canada, using Landsat TM and digital elevation data. *International Journal of Remote Sensing*, **20** (2), pp. 273-284.
- Stahl K. and D. Moore, 2006. Influence of watershed glacier coverage on summer streamflow in British Columbia, Canada. *Water Resources Research*, **42** (6), W06201, doi:10.1029/2006WR005022.
- Young G., 1981. The mass balance of Peyto Glacier, Alberta, Canada 1967-1978. *Arctic and Alpine Research*, **13** (3), pp. 307-318.
- Young G., 1991. Hydrological interactions in the Mistaya Basin, Alberta, Canada. In: *Snow, Hydrology and Forests in High Alpine Area: Proceedings of the Vienna Symposium*, August 1991. International Association of Hydrological Sciences, Wallingford, UK, Publication 205, pp. 237-244.
- Zhang Y., J. Wallace and D. Battisti, 1997. ENSO-like interdecadal variability: 1900-93. *Journal of Climate*, **10** (5), pp. 1004-1020.

APPENDIX A

FIELD MEASUREMENT OF GLACIER VOLUME CHANGES

Field investigations were carried out in August, 2005 to evaluate the validity of the volume – area scaling relationship for glaciers within this region. The sites chosen for this work included the Rae (50.62° N, 114.99° W) and Robertson (50.73° N, 115.33° W) Glaciers in Kananaskis Country, Alberta, as well as the Cauldron (50.31° N, 116.66° W) and Covenant (50.32° N, 116.67° W) Glaciers in the Lardeau Provincial Forest (Purcell Mountains), British Columbia. At each of these sites, measurements of the horizontal and vertical position of the present glacier margin as well as clearly defined LIA moraine systems were obtained using a Garmin Ltd. 12XL hand-held Global Positioning System (GPS) and a Suunto Ltd. Escape203 hand-held electronic altimeter. X, Y, and Z readings were taken every ~50 meters or wherever a significant change in direction or slope occurred while traversing the moraine ridges and the glacier boundary.

The horizontal and vertical accuracy of these measurements is estimated to be ± 5 m and ± 3 m respectively based on repeated measurements of the same location at several different times. Accuracy is reduced in situations where readings were taken in close proximity to steep valley walls, as fewer satellites were in view due to the high relief of the mountains. During these times positions could only be given by the GPS in 2 dimensions. Before surveying each glacier and moraine system, the altimeter was calibrated at a spot of known elevation. Such spots were derived from the NTS maps or from the vertical coordinate given by the GPS after leaving it stationary for an extended period of time.

Following the field data collection, three-dimensional surfaces were constructed from the point measurements using ArcMap™ GIS. These virtual surfaces represent the

present glacier surface, as well as the glacier surface and bed corresponding to the LIA maximum extent. Some additional points were added at this time, based on features visible in the imagery. These were necessary because some parts of individual moraine systems, trimlines, and ice boundaries were inaccessible due to the hazards involved.

TABLE A.1. Summary and comparison of volume loss measured from glacier surface reconstructions and estimated with different variations of the scaling parameters of Equation (1). The various coefficients are taken from Chen and Ohmura (1990).

Measured Vol. Loss (10^{-3} km ³)	Rae Glacier		Robertson Glacier		Cauldron Glacier		Covenant Glacier		
	13.8		49.2		76.7		28.7		
	Est. Vol		Est. Vol		Est. Vol		Est. Vol		
$V = c_0 S^{c_1}$	Loss	%	Loss	%	Loss	%	Loss	%	
c_0	c_1	10^{-3} km ³	Diff.	10^{-3} km ³	Diff.	10^{-3} km ³	Diff.	10^{-3} km ³	Diff.
28.5	1.36	6.7	51.5	44.7	9.2	100	30.2	29.9	4.3
24.6	1.39	5.7	58.8	40.1	18.4	92.9	21.0	27.0	5.9
16.1	1.52	3.5	74.8	30.7	37.6	81.8	6.6	21.1	26.6
27.6	1.36	6.5	53.1	43.1	12.4	96.2	25.4	28.8	0.6
30.8	1.41	7.1	48.7	51.1	3.9	120	56.5	34.5	20.1
48.0	1.19	12.2	11.9	60.0	22.0	111	44.8	39.1	36.5
21.3	1.15	5.5	60.2	25.2	48.7	44.7	41.8	16.4	43.0
36.1	1.41	8.3	40.1	59.8	21.6	141	83.5	40.3	40.1

Extrapolation of elevation values for individual points along the moraines and glacier margins to points within these boundaries was done manually using the contour lines produced from the DEM. In a similar fashion, points were added along contour lines that represent the former surface topography of the glacier. The curvature of these contours was based on surface contours of similar glaciers nearby or on linear morphological features on the former bed that are visible in the imagery. These features provide an indication of the direction of former ice flow, and thus contours were drawn perpendicular to them, as the ice flows in the direction parallel to the surface slope. Surfaces were then constructed from both sets of points as Triangulated Irregular Networks (TINs) using the Spatial Analyst extension of ArcMapTM. Both surfaces were tied along the boundaries so that the volume between the upper and lower surfaces represents the loss of ice associated with the retreat of the glacier margin. Subtraction of the lower surface from the upper surface yields this volume loss, which was subsequently compared with the loss predicted by different variants of the volume – area scaling relationship (Table A.1).

Variations of the parameters used in the volume – area scaling relationship lead to significant differences in the estimated volume loss from the individual glaciers, and in many cases the relative difference between measured and estimated volume loss is high. This is because some glaciers have specific geometric characteristics (e.g., multiple tributaries) that result in systematic error in the estimates of their volume, and because some values of c_0 and c_1 are not appropriate for glaciers in this region. It is apparent that for the very small Rae Glacier (initially $<0.5 \text{ km}^2$), which lost a large percentage of its volume since the LIA, most variations of the volume – area scaling relationship underestimate the actual volume loss. The values of c_0 and c_1 in Table A.1 are not ideal for such glaciers as few of the observations from which these values are derived were made on very small glaciers. In the case of the Cauldron Glacier, the actual volume loss is overestimated by most variations of this relationship. This may be due to the more complicated geometry of this glacier and the fact that it disintegrated into several separate ice masses as it retreated to its present position. Since a large fraction of the estimated ice loss in this study is due to the retreat of glaciers with multiple tributaries that have become detached over the study period, the possibility of inherent error in these estimates is more problematic than that for very small glaciers.

Certain combinations of c_0 and c_1 consistently result in a significantly different amount of volume loss than that determined through former surface reconstruction. For example, the use of 48.0 and 1.19 for c_0 and c_1 seems to result in a high estimate of glacier volume, and thus volume loss as the difference between two large estimates is greater than that between two small estimates. These parameters are derived from mountain glaciers in Svalbard (Chen and Ohmura, 1990), and are not likely to be representative of glaciers in the Columbia and Rocky Mountains. Similarly, the values of 21.3 and 1.15, which are based on small glaciers in the Cascade Mountains, result in an underestimation of volume loss. Values of c_0 and c_1 such as these are disregarded in the error analysis described in section 3.5 as they do not seem representative of the glaciers in this region. However, some combinations of these parameters produce estimates of volume loss that are in close agreement with the measurements (e.g., 27.6 and 1.36; 30.8 and 1.41; and 24.6 and 1.39). These variations of the volume – area relationship are generally derived from glaciers within the Alps, Cascades, and other regions, which are

likely more similar in nature to those in this region. It is these combinations of values that were used for assessing the uncertainty in the estimates of volume loss in section 3.5. Finally, the combination of c_0 and c_1 of 28.5 and 1.36 that was used for the estimates of volume presented in section 4 agreed closely in most circumstances to the surface reconstruction-based estimates of volume loss.

APPENDIX B

SUMMARY OF MORPHOLOGIC AND GLACIOLOGICAL PARAMETERS

TABLE B.1. Summary of parameters derived for selected glaciers in the southern Rocky Mountains region. Glaciological parameters were derived only for glaciers with an initial area >1 km².

Glacier name	GLIMS ID	Ref #	Initial area (km ²)	Δ area (%)	Initial TA (m)	Elev. range (m)	Mean elev. (m)	Aspct.	Shape	$\bar{\alpha}_t$	ELA (m)	AAR	t_v (yr)	BR	BS
Mangin	G295217E50543[N]	n/a	4.95	-34.1	2325	1050	2749	N	B	0.12	2760	0.49	32.5	0.87	0.58
Petain	G295180E50533[N]	n/a	4.46	-12.8	2415	690	2711	NE	A	0.17	2700	0.55	26.3	1.19	0.37
Haig	G295300E50710[N]	n/a	3.13	-12.9	2385	480	2676	SE	B	0.24	2670	0.69	17.8	1.23	0.92
Abruzzi	G295119E50426[N]	n/a	3.05	-18.8	2445	600	2776	S	A	0.21	2760	0.53	21.9	1.34	0.48
West Haig	G295322E50717[N]	n/a	1.86	-3.3	2475	540	2728	S	B	0.30	2700	0.77	16.5	2.78	0.88
King	G295391E50597[N]	n/a	1.80	-3.9	2355	900	2691	SE	A	0.24	2700	0.47	16.6	0.89	0.59
Robertson	G295333E50731[N]	n/a	1.40	-14.2	2235	750	2615	N	B	0.18	2640	0.45	18.4	0.69	0.51
Smith-Dorrien	G295294E50725[N]	n/a	1.29	0.0	2445	570	2780	SE	B	0.51	2700	0.79	9.9	5.33	0.41
Castelnaud	G295164E50523[N]	n/a	1.15	0.0	2355	600	2690	E	A	0.69	2670	0.56	6.8	1.39	0.51
Elk	G295162E50514[N]	n/a	0.92	1.4	2535	510	2778	E	D	0.41
Northover	G295245E50593[N]	n/a	0.91	-31.4	2205	630	2587	NE	B	0.17
Princess	G295404E50587[N]	n/a	0.70	0.0	2505	870	2771	S	A	0.30
Queen	G295433E50643[N]	n/a	0.63	-1.2	2265	960	2600	E	D	0.47
French	G295317E50732[N]	n/a	0.59	-10.5	2295	480	2552	NE	A	0.22
Beatty	G295285E50673[N]	n/a	0.52	-2.9	2355	420	2586	N	A	0.35
Lyautey	G295231E50609[N]	n/a	0.42	-13.3	2415	480	2644	N	A	0.31
Foch	G295166E50574[N]	n/a	0.36	-7.5	2655	360	2822	NW	A	0.33
Nivelle	G295182E50514[N]	n/a	0.35	-11.3	2505	510	2699	S	A	0.23

Appendix B

TABLE B.2. Summary of parameters derived for selected glaciers in the southern Purcell Mountains region. * denotes unofficial names.

Glacier name	GLIMS ID	Ref #	Initial		Initial TA (m)	Elev. range (m)	Mean elev. (m)	Aspct.	Shape	$\bar{\alpha}_i$	ELA (m)	A.A.R.	t_v (yr)	BR	BS
			area (km ²)	area (%)											
Conrad	G296930E50806[N]	n/a	18.9	-1.8	1720	1490	2564	NW	A	0.23	2460	0.56	11.3	2.66	0.30
Starbird	G296698E50464[N]	n/a	11.7	-14.6	1940	1230	2659	E	B	0.20	2580	0.74	18.5	2.70	0.35
Malloy*	G296866E50781[N]	n/a	10.2	-4.0	1900	1250	2614	N	B	0.15	2540	0.68	21.5	2.05	0.32
Vowell	G296802E50748[N]	n/a	8.41	-11.1	2010	1280	2569	N	B	0.14	2510	0.72	27.3	1.83	0.57
Four Squatters	G296888E50590[N]	n/a	8.39	-0.9	1850	1130	2569	SE	C	0.21	2460	0.75	14.8	3.42	0.27
Toby	G296530E50216[N]	n/a	7.66	-11.1	2140	1000	2576	N	B	0.18	2600	0.47	23.8	0.69	0.73
S. Macbeth	G296787E50403[N]	n/a	6.90	-2.0	2180	770	2642	S	B	0.28	2575	0.75	19.8	2.61	0.21
Catamount	G296565E50634[N]	n/a	6.64	-2.5	2190	890	2590	N	A	0.27	2570	0.59	20.9	1.46	0.60
Stockdale	G296681E50496[N]	n/a	6.31	-12.4	2090	1250	2732	N	B	0.15	2670	0.67	29.6	1.95	0.42
Truce*	G296711E50307[N]	n/a	5.83	-0.1	2100	1090	2793	NW	B	0.40	2620	0.82	12.0	8.62	0.19
MacCarthy	G296944E50738[N]	n/a	5.37	0.0	2060	900	2598	SE	C	0.37	2410	0.90	11.9	.	0.33
Bugaboo	G296780E50722[N]	n/a	5.27	1.4	1760	1310	2671	N	B	0.39	2560	0.76	7.3	2.86	0.18
Kelvin*	G296833E50774[N]	n/a	5.13	-11.2	1900	1070	2493	S	B	0.16	2400	0.71	20.2	2.56	0.23
North Star	G296540E50617[N]	n/a	5.03	-6.9	2280	780	2743	NE	B	0.26	2660	0.65	27.6	3.14	0.36
Commander	G296543E50421[N]	n/a	4.60	1.0	2040	1240	2774	N	B	0.46	2520	0.76	9.6	7.25	0.12
N. Macbeth	G296801E50427[N]	n/a	4.23	-2.0	2290	580	2650	N	A	0.21	2560	0.82	35.1	6.22	0.34
Banquo*	G296828E50409[N]	n/a	4.14	-24.9	2215	695	2533	N	B	0.09	2470	0.60	69.0	2.11	0.23
Delphine	G296434E50460[N]	n/a	3.80	-0.1	2520	750	2833	S	C	0.42	2715	0.94	43.1	.	0.67
Horseshoe	G296703E50327[N]	n/a	3.74	-1.6	2210	870	2718	N	A	0.48	2620	0.74	13.3	3.71	0.37
Cauldron*	G296662E50306[N]	n/a	3.18	0.0	2010	1170	2639	N	A	0.29	2520	0.64	13.6	2.60	0.19
Jumbo	G296682E50518[N]	n/a	3.13	-1.5	2440	630	2722	NE	A	0.21	2630	0.71	58.1	6.20	0.49
Cleaver*	G296572E50421[N]	n/a	2.86	-22.1	2160	1140	2647	NW	A	0.14	2720	0.44	36.8	0.65	0.16
Covenant*	G296521E50421[N]	n/a	1.80	-0.3	2180	970	2709	N	B	0.40	2600	0.70	14.4	3.85	0.34
Findlay	G296486E50086[N]	n/a	1.59	2.3	2200	1010	2810	NE	A	0.54	2750	0.68	11.8	1.69	0.19
			1.45	-0.7	2390	740	2723	NE	C	0.34	2580	0.77	31.2	0.69	0.29

TABLE B.3. Summary of parameters derived for selected glaciers in the southern Selkirk Mountains region.

Glacier name	GLIMS ID	Ref #	Initial area (km ²)	Δ area (%)	Initial TA (m)	Elev. range (m)	Mean elev. (m)	Aspct.	Shape	$\bar{\alpha}_t$	ELA (m)	AAR	t_v (yr)	BR	BS
Nemo	G297311E50388[N]	n/a	4.99	1.78	2020	730	2403	NE	A	0.70	2340	0.66	6.7	3.11	0.31
	G297268E50931[N]	n/a	4.10	-1.52	2260	670	2610	NE	A	0.51	2550	0.69	13.9	3.96	0.82
	G297256E50899[N]	n/a	3.10	0.00	2100	830	2593	E	A	0.78	2550	0.70	7.2	2.27	0.47
Wrong	G297370E50906[N]	n/a	3.06	0.00	2070	750	2424	N	B	0.42	2340	0.64	10.8	4.31	0.29
	G297256E50917[N]	n/a	2.50	0.00	2200	820	2637	E	A	0.79	2550	0.70	8.8	3.29	0.34
Tenderfoot	G297349E50403[N]	n/a	2.21	-44.1	2115	645	2390	NW	B	0.21	2400	0.47	22.1	0.84	0.11
	G297107E50874[N]	n/a	1.90	0.00	2165	625	2376	N	A	0.29	2310	0.61	18.1	3.38	0.04
Spokane	G297194E50186[N]	n/a	1.49	-0.69	1990	1060	2470	NE	A	0.91	2370	0.71	5.4	4.31	0.07
Pequod	G297385E50963[N]	n/a	1.45	0.00	2020	910	2576	NE	A	1.21	2520	0.68	5.0	1.94	0.32
	G297332E50410[N]	n/a	1.41	-11.5	2280	480	2491	NE	C	0.54	2460	0.53	14.1	1.67	0.04
Hatters	G297091E50873[N]	n/a	1.33	0.00	2115	675	2438	N	A	0.36	2370	0.64	13.4	2.42	0.16

TABLE B.4. Summary of parameters derived for selected glaciers in the southern Monashee Mountains region. The reference numbers refer to the figures in section 5.4. * denotes unofficial names.

Glacier name	GLIMS ID	Ref #	Initial area (km ²)	Δ area (%)	Initial TA (m)	Elev. range (m)	Mean elev. (m)	Aspct.	Shape	$\bar{\alpha}_t$	ELA (m)	AAR	t_v (yr)	BR	BS
W. Blanket	G304252E50754[N]	6	4.12	-5.28	2110	580	2432	NW	C	0.28	2380	0.75	27.7	3.64	0.59
E. Blanket	G298229E50765[N]	7	3.61	-19.3	2050	740	2391	N	B	0.20	2330	0.60	32.0	2.41	0.26
Cranberry*	G298200E50708[N]	5	2.51	-21.1	1760	1090	2369	N	B	0.14	2410	0.62	25.5	0.51	0.30
	G298190E50641[N]	8	2.11	-25.7	1940	790	2252	NE	A	0.17	2280	0.44	28.9	0.72	0.22
English*	G298362E50891[N]	n/a	1.83	-7.62	2120	540	2399	N	B	0.23	2370	0.58	34.4	1.70	0.37
	G298161E50554[N]	2	1.79	-39.4	2080	520	2270	NE	C	0.22	2320	0.26	31.7	0.29	0.45
Frigg	G298104E50550[N]	1	1.77	-11.1	2180	650	2511	E	A	0.17	2500	0.70	57.4	1.20	0.39
	G298249E50841[N]	n/a	1.48	-17.2	1950	610	2268	N	B	0.12	2260	0.67	41.5	1.50	0.57
Vanwyk*	G304213E50696[N]	4	1.29	0.00	2410	400	2619	SW	A	0.40	2580	0.72	28.6	3.31	0.33
	G298158E50595[N]	3	1.25	11.4	2050	680	2377	NE	C	0.53	2300	0.66	13.4	4.78	0.30
Kelly*	G298200E50680[N]	n/a	0.97	-37.8	1970	230	2085	NE	A	0.20	2300	0.66	26.3	0.20	0.16
	G298265E50827[N]	n/a	0.80	-60.0	2040	250	2165	E	A	0.12	2300	0.66	26.3	0.20	0.16
	G298197E50693[N]	n/a	0.76	-11.1	1980	340	2150	E	A	0.20	2300	0.66	26.9	0.20	0.16
	G298088E50606[N]	n/a	0.29	0.00	2050	430	2265	N	C	0.56	2300	0.66	12.8	0.20	0.16

Appendix B

TABLE B.5. Summary of parameters derived for the outlet glaciers of the Bridge Icefield in the southern Coast Mountains. The reference numbers refer to the figures in section 5.4. * denotes unofficial names.

Glacier name	GLIMS ID	Ref #	Initial area (km ²)	Δ area (%)	Initial TA (m)	Elev. range (m)	Mean elev. (m)	Aspct.	Shape	$\bar{\alpha}_t$	ELA (m)	AAR	t_r (yr)	BR	BS
Bridge	G30364 E50822[N]	27	89.1	-8.41	1365	1560	2185	E	B	0.06	2160	0.55	47.7	1.17	0.16
Stanley Smith	G303798 E50869[N]	36	83.3	-3.60	1095	1905	2337	W	A	0.12	2235	0.69	17.2	2.00	0.14
Hederson*	G30362 E50872[N]	26	26.3	-6.51	1470	1365	2237	E	B	0.17	2280	0.44	17.5	0.66	0.38
Fowler*	G303795 E50926[N]	12	20.1	-4.48	1500	1390	2417	N	B	0.24	2355	0.69	12.9	1.73	0.24
Frank Smith	G30373 E50909[N]	15	19.8	-7.59	1755	1155	2429	NE	B	0.14	2385	0.63	30.9	1.51	0.27
	G303962 E50938[N]	1	11.7	-2.11	1575	1065	2272	NW	B	0.24	2235	0.66	14.1	1.55	0.31
Lord	G30368 E50899[N]	17	10.8	-3.65	1650	1230	2435	N	B	0.29	2445	0.57	13.3	0.90	0.44
Tait*	G303628 E50910[N]	18	10.6	-7.86	1845	855	2317	N	B	0.19	2280	0.59	27.0	1.73	0.43
Chapman*	G303704 E50991[N]	48	9.85	-9.19	1875	930	2361	E	A	0.12	2430	0.39	46.7	0.42	0.57
Magaera	G303853 E50825[N]	37	8.88	-3.33	1725	1215	2336	SW	B	0.18	2235	0.68	23.6	2.48	0.19
Edmond	G303746 E50970[N]	46	8.59	-4.87	1800	1170	2518	NW	B	0.22	2460	0.69	22.7	1.80	0.31
	G30377 E50246[N]	29	7.88	-9.74	1620	690	2052	E	B	0.23	2085	0.33	16.2	0.59	0.69
Chloe*	G303902 E50844[N]	38	7.36	-2.24	1560	1140	2293	NW	B	0.28	2167	0.78	12.4	3.71	0.22
	G303925 E50951[N]	2	7.27	-3.36	1755	885	2272	N	B	0.18	2272	0.59	24.2	1.01	0.54
Wheatly*	G303588 E50903[N]	25	5.87	-4.29	1890	810	2264	E	B	0.18	2265	0.47	32.5	0.99	0.50
Taylor*	G303704 E50972[N]	47	5.55	-16.1	2010	930	2436	E	A	0.18	2475	0.44	44.8	0.61	0.45
	G303359 E50519[N]	34	5.30	-0.29	1530	1395	2205	SE	B	0.27	2017	0.76	12.3	6.79	0.23
	G303879 E50961[N]	10	5.08	-14.4	1710	1155	2302	N	D	0.17	2340	0.50	23.7	0.68	0.43
	G303170 E50636[N]	35	5.01	-8.51	1620	1245	2259	SE	B	0.17	2160	0.60	21.2	2.35	0.26
	G303574 E50919[N]	24	3.81	-18.9	1965	615	2211	E	A	0.17	2265	0.28	41.4	0.35	0.72
	G303895 E50953[N]	5	3.06	-3.56	1845	1005	2332	NW	D	0.36	2302	0.50	14.9	1.38	0.24
	G303842 E50907[N]	39	2.64	-0.63	2130	705	2573	W	B	0.30	2445	0.76	45.0	5.97	0.26
Perry*	G303598 E50932[N]	19	2.50	-9.27	1965	705	2290	NE	B	0.19	2302	0.40	35.7	0.80	0.62
	G303853 E50917[N]	40	2.49	-2.10	1965	780	2430	W	A	0.35	2362	0.68	21.3	2.87	0.40
	G303953 E50970[N]	3	2.40	-10.4	1830	705	2237	N	B	0.21	2265	0.42	23.9	0.67	0.52
	G303566 E50935[N]	23	2.35	-3.21	1995	570	2284	E	A	0.30	2265	0.50	26.3	1.46	0.60
	G303927 E50927[N]	44	2.07	-7.47	1890	750	2355	SE	B	0.35	2295	0.76	17.6	2.39	0.33
	G303657 E50979[N]	49	1.90	-18.6	1980	795	2335	NE	B	0.17	2445	0.53	44.5	0.23	0.75
	G303579 E50947[N]	20	1.87	-12.7	2040	630	2357	NW	B	0.20	2400	0.41	45.7	0.48	0.64
	G303933 E50917[N]	45	1.81	-2.60	1965	600	2355	SE	B	0.35	2332	0.77	21.3	1.65	0.38
	G303915 E50937[N]	43	1.46	-17.3	2025	630	2361	S	B	0.24	2385	0.39	35.7	0.58	0.82